AMERICAN MUSEUM
Novitates

PUBLISHED BY THE AMERICAN MUSEUM OF NATURAL HISTORY
CENTRAL PARK WEST AT 79TH STREET, NEW YORK, NY 10024
Number 3256, 59 pp., 25 figures, 11 tables March 4, 1999

Amerigo Vespucci and the Rat of Fernando de Noronha: a New Genus and Species of Rodentia (Muridae: Sigmodontinae) from a Volcanic Island Off Brazil's Continental Shelf

MICHAEL D. CARLETON[1] AND STORRS L. OLSON[2]

CONTENTS

[1] Research Associate, Department of Mammalogy, American Museum of Natural History; Curator of Mammals, Department of Vertebrate Zoology, National Museum of Natural History, Smithsonian Institution, Washington, D.C.
[2] Curator of Birds, Department of Vertebrate Zoology, National Museum of Natural History, Smithsonian Institution, Washington, D.C.

ISSN 0003-0082 / Price $7.00

ABSTRACT

Noronhomys vespuccii, a new genus and species (Muridae: Sigmodontinae), is described from Ilha Fernando de Noronha, a small volcanic island located 345 km northeast of Cabo de São Roque, Brazil. The abundant cranial and postcranial material of the fossil rodent was recovered from old beach dunes that are late Quaternary in age (probably late Holocene). *Noronhomys vespuccii* retains incomplete mesolophs on its moderately hypsodont molars and is compared with other tetralophodont oryzomyines (sensu Voss and Carleton, 1993), especially *Lundomys molitor* and species of *Holochilus*. Morphometric analyses conducted separately on craniodental, mandibular, and femoral measurements reveal the sample of *Noronhomys* to be equally differentiated from those of *Lundomys* and *Holochilus*. Based on the criterion of parsimony, phylogenetic analyses of 35 craniodental characters strongly support the recent common ancestry of the new form and *Holochilus*. The clade (*Pseudoryzomys* (*Lundomys* (*Holochilus–Noronhomys*))) appears to represent a lineage of semiaquatic rodents that differentiated from an oryzomyine ancestry in savanna landscapes of southern South America. Morphometric results and anatomical details of the pelvic limb, however, suggest that *Noronhomys* was not a semiaquatic form. It is hypothesized that such aquatic skeletomuscular adaptations were lost (reversed) when the progenitor of *Noronhomys* became stranded on a small oceanic island where palustrine habitats were scarce or absent. The specific patronym of the extinct rodent refers to Amerigo Vespucci's disputed landfall on Fernando de Noronha in 1503 and his possible sighting of "very large rats" on that island. If the species *Noronhomys vespuccii* were alive in 1503, it became extinct shortly thereafter due to the usual anthropogenic causes that have extirpated so many vertebrate species on islands.

INTRODUCTION

On August 10, 1503, during his putative fourth voyage to the New World, Amerigo Vespucci claimed to have landed on a small island just three degrees south of the equator:

> [The] island we found uninhabited, and it contained plenty of trees, and so many birds, both marine and land, that they were without number . . . and we saw no other animals except *very big rats* and lizards with two tails, and some snakes. (Emphasis ours; translation of the original Italian text from Branner [1888: 869].)

Geographers and early naturalists have interpreted the small island mentioned by Vespucci as Ilha Fernando de Noronha (Branner, 1888; Ridley, 1888), an oceanic island located off easternmost Brazil. Although Vespucci's fourth journey to the New World, and by extension his landfall on Fernando de Noronha, has been questioned by some historians (for example, Formisano, 1992), the former presence of "very big rats" on that small island can now be empirically documented. During August 1973, Olson discovered vertebrate fossils in old beach dunes at the eastern corner of Ilha Fernando de Noronha. Among the vertebrate material recovered were abundant, well-preserved bones of a new sigmodontine rodent that was moderately large in size and belongs to the diverse radiation of South American Oryzomyini.

This extinct rodent is diagnosed and described as a new genus and species. In formally recording its scientific name, we also contrast the new form with *Lundomys* and *Holochilus*, its nearest probable relatives on continental South America, evaluate its phylogenetic relationship to those taxa and to other oryzomyine rodents, and discuss its biogeographic origin in the context of other vertebrates indigenous to Ilha Fernando de Noronha. The very recent existence of an endemic rodent on Fernando de Noronha provides corroboration of another biological detail in the account of Vespucci's fourth voyage, which may help in determining its authenticity.

MATERIALS AND METHODS

SPECIMENS AND ANALYTICAL SAMPLES: The fossil sample originated in late Quaternary

beach sands found on Ilha Fernando de Noronha, Brazil. The holotype, along with representative crania, mandibles, and postcranial material, has been deposited in the Museu de Ciències, Pontificia Universidade Catolica da Rio Grande do Sul (MCP-PV), Porto Alegre, Brazil. Comparable series have been retained in the vertebrate paleontological collection, Department of Paleobiology, National Museum of Natural History (USNM).

Museum specimens (skulls, mandibles, and postcranial skeletons) of *Holochilus* and *Lundomys* used for the various statistical tabulations and morphometric analyses are listed below and contained in the following collections of recent mammals: American Museum of Natural History, New York City (AMNH); Field Museum of Natural History, Chicago (FMNH); National Museum of Natural History, Smithsonian Institution, Washington, D.C. (USNM).

Holochilus brasiliensis: Argentina, Buenos Aires, Carhue (USNM 236318-236320). Uruguay, Canelones, Bañado de Tropa Vieja (AMNH 206362); Soriano, 3 km E Cardona (AMNH 206369, 206372, 206374-206379, 206383); Tacuarembo, 16 km NNW San Jorge, Río Negro, Isla Sanchez Chica (AMNH 206390).

Holochilus sciureus: Bolivia, Beni, mouth of Río Baures (AMNH 210218, 210221, 210226, 210228, 210232, 210233, 210235, 210237, 210239, 210241, 210244, 210249, 210255); Mamore, San Joaquin (USNM 364750-364753, 364757-364759, 390248, 461031461035); Río Itenez, Costa Marques (AMNH 210268, 210271); Itenez, Lago Victoria (USNM 390767-390769). Brazil, Pará, Utinga (USNM 394720-394726). Suriname, Commewijne, Mariënburg (USNM 312891-5, 319976-319983). Venezuela, Trujillo, 30 km NW Valera, El Dividive (USNM 372652-372665).

Lundomys molitor: Uruguay, Canelones, Bañado de Tropa Vieja (AMNH 206363-206366); Minas, Pasos de Averías, Río Cebollati (FMNH 29255, 29257, 29258; USNM 259641); Soriano, 3 km E Cardona (AMNH 206368, 206380, 206381); Trienta y Tres, 8 mi E Trienta y Tres (FMNH 29260, 29261, 29263); 25 km WSW Trienta y Tres, Río Olimar Chico (AMNH 206392, 206393).

For summary statistics and multivariate comparisons, the specimens were grouped into seven composite or operational taxonomic units (OTUs) as here defined:

OTU 1, Fernando de Noronha taxon;
OTU 2, all *Lundomys molitor*;
OTU 3, all *Holochilus brasiliensis*;
OTU 4, *H. sciureus* from Bolivia;
OTU 5, *H. sciureus* from Brazil;
OTU 6, *H. sciureus* from Venezuela.

Sample sizes for OTUs are presented in the tables and varied according to the analysis performed and the skeletal element compared. In particular, the relative rarity and fragmentary nature of preserved crania limited sample sizes for morphometric characterization of the Noronha fossil.

Specimens in the USNM of five additional oryzomyine taxa—*Microryzomys minutus*, *Oryzomys palustris*, *O. subflavus*, *Pseudoryzomys simplex*, and *Zygodontomys brevicauda cherrei*—were broadly surveyed to assist evaluation of qualitative character variation and to provide outgroup comparisons in the phylogenetic analyses. Rationale for inclusion of these particular taxa is discussed under Phyletic Inferences.

MEASUREMENTS: Linear measurements were taken from crania, mandibles, and femora as a basis for assessing covariation patterns and taxonomic discrimination. Skulls were viewed under a dissecting microscope when measuring the 13 cranial and 2 dental variables to 0.01 mm by handheld digital calipers accurate to 0.03 mm. Fifteen dimensions of the mandible and its dentition were also quantified in view of its greater abundance among the fossil material. All mandibular measurements were taken to 0.01 mm by use of digital calipers mounted on the movable stage of a binocular microscope set at 45× magnification. Of the postcranial elements recovered for the Noronha fossil, only the femur was preserved intact in sufficient numbers to permit numerical comparisons with living species. Thirteen femoral variables were quantified using handheld calipers. All measurements, their abbreviations, and definitions of landmarks where necessary, are enumerated below.

Cranial variables: Occipitonasal length (ONL); zygomatic breadth (ZB); breadth of braincase (BBC); least interorbital breadth (IOB); length of nasals (LN); postpalatal length (PPL); length of bony palate (BPL); length of upper diastema (LD); length of in-

cisive foramen (LIF); breadth of bony palate across upper first molars (BM1s)—transverse distance between the labial edges of the M1s; posterior breadth of the bony palate (PPB)—taken at the constriction of the maxillary bones immediately posterior to the M3s; breadth of zygomatic plate (BZP); depth of auditory bulla (DAB)—an oblique distance, from the dorsal rim of the auditory meatus to the ventralmost curvature of the bullar capsule; coronal length of maxillary toothrow (CLM); and greatest width of upper first molar (WM1).

Mandibular variables: Depth of mandible below m1 (DMm1)—on the buccal side, from the alveolar rim at the middle of m1 to the ventralmost projection of the symphysis; depth of mandible below m3 (DMm3)—on the lingual side, shortest distance from the shelf behind m3 to the concave ventral margin of the dentary; length of the masseteric crest (LMC)—from the point where the superior and inferior masseteric crests meet to the anterior end of their conjoined ridge; coronal length of mandibular toothrow (CLm); length of m1 (Lm1); length of m2 (Lm2); length of m3 (Lm3); anterior width of m1 (AWm1)—measured across the lateral apices of the anteroconid; posterior width of m1 (PWm1)—between the margins of the hypoconid and entoconid; anterior width of m2 (AWm2)—between the margins of the protoconid and metaconid; posterior width of m2 (PWm2)—between the margins of the hypoconid and entoconid; greatest width of m3 (Wm3)—between the margins of the protoconid and metaconid; height of m1 (Hm1)—on the lingual side, from the enamel-cementum junction at the coronal base to the apex of the metaconid; width of lower incisor (Wi)—at the anterior surface just beyond the emergence of the incisor from the dentary; and depth of lower incisor (Di)—measured at the proximal edge of the wear facet.

Femoral measurements: Femoral length (FL)—dorsal margin of the head to the distalmost curvature of the medial condyle; distal width of the femur (DW)—width across base of the shaft (diaphysis) just above the condyles; middle width of the femur (MW)—narrowest distance across the shaft, measured slightly below the third trochanter; depth of the femur (DF)—anterior-posterior thickness of the shaft taken at the same position as MW; diameter of the head (DH)—width across the articular ball; diameter of the neck (DN)—narrowest constriction, measured along the anterior-posterior axis, below the head; intertrochanteric distance (ITD)—an oblique distance, from the craniodorsal rim of the greater trochanter to the posteromedial projection of the lesser trochanter; breadth across the third trochanter (BTT)—greatest expanse between the lateral margin of the third trochanter (lateral crest) and an opposite point on the medial edge of the shaft; length of the third trochanter (LTT)–distance between the dorsal edge of the greater trochanter to the end of the scar for insertion of the gluteus maximus on the third trochanter; condylar breadth (CB)—transverse distance between the medial and lateral edges of the articular condyles; condylar depth (CD)—anterior-posterior thickness measured from the dorsal lip of the trochlear fossa to the caudal rim of the medial condyle; length of the patellar fossa (LPF)—from the dorsal lip of the patellar fossa to its distal termination medial to the articular condyles; and width of the patellar fossa (WPF)–distance between the lateral and medial edges of the fossa at its midsection.

ANATOMICAL TERMINOLOGY AND MORPHOMETRIC AND PHYLOGENETIC ANALYSES: Descriptive features of the oryzomyine skull are generally those used by Carleton and Musser (1989) and Voss and Carleton (1993). Names for enamel crests and reentrant folds of the molars follow Reig (1977), as adapted and illustrated for the oryzomyine dentition by Carleton and Musser (1989). Positional abbreviations of the molars follow the common alphanumeric convention of using uppercase versus lowercase letters to identify maxillary or mandibular teeth and numbers to indicate their placement in the toothrow (for example, M1 and m1). The myological studies of Howell (1926) and Rinker (1954) are the principal sources for names of muscles and interpretations of their origins and insertions.

Standard descriptive statistics (mean, range, standard deviation, coefficient of variation) were derived for the OTUs. Principal components (PCs) and canonical variates (CVs) were extracted from the variance–covariance or correlation matrix and computed

using natural logarithmic transformations of the craniodental, mandibular, and femoral variables. Loadings are expressed as Pearson product-moment correlation coefficients between the principal components and the original skeletal and dental variables. Mahalanobis distances between OTU centroids were clustered based on the unweighted pair-group method using arithmetic averages (UPGMA). All univariate and multivariate computations were generated using Systat (version 5.0, 1992), a series of statistical routines programmed for microcomputers.

Phylogenetic relationships were explored using PAUP (version 3.1.1; Swofford, 1993) to find trees of minimal length (branch-and-bound option) by the criterion of Wagner parsimony. Both accelerated and delayed transformation routines were used to optimize intermediate character state transformations, but only delayed transformation results are illustrated on trees. Characters were not weighted, and trees were rooted using either a composite hypothetical ancestor (HA) or a designated outgroup OTU. Both bootstrap percentages (1000 iterations, branch-andbound search) and Bremer support indices are provided as measures of cladistic support; for the latter, the congruent cladistic structure in mutually parsimonious trees is summarized by the strict consensus method.

ACKNOWLEDGMENTS

Support for fieldwork by Olson was provided by a grant from the National Geographic Society (number 1105) and supplementary funding from the International Council for Bird Preservation. The Conselho Nacional de Pesquisas of Brazil authorized the expedition to Fernando de Noronha and facilitated various aspects of travel, as did staff members of the American Consulate General in Rio de Janeiro and Recife. Olson was aided in fieldwork and collecting by O. A. Roppa, whose assistance was provided through the Museu Nacional de Rio de Janeiro, I. A. Cruz, and other helpful individuals stationed on the island at the time. For loans of recent specimens, we thank B. D. Patterson (FMNH) and G. G. Musser and R. S. Voss (AMNH). Dra. Maria Claudia L. Malabarba of the Museu de Ciencias in Porto Alegre, Brazil, kindly helped with the cataloging of material to be returned to her institution. Ralph Chapman, Morphometrics Lab, USNM, provided advice on the use of certain Systat routines. Documentation and comparison of the new fossil were made possible through the creative talents of David F. Schmidt, who undertook all specimen photography and most line drawings; Karolyn Darrow, who drew the postcranial figures; and Janine Higgins, who illustrated the cranium and jaw of the holotype. Finally, we appreciate the helpful manuscript reviews offered by Guy G. Musser, Scott J. Steppan, and Robert S. Voss.

GEOLOGY AND PHYSIOGRAPHY OF FERNANDO DE NORONHA

GENERAL: Fernando de Noronha is somewhat generously described as an archipelago because of the 12 smaller islets that extend from the northeast corner of the principal island. It lies just off the rim of the continental shelf (latitude 3°50′S and longitude 32°15′W), 345 km (215 mi) northeast of the nearest Brazilian mainland at Cabo São Roque (fig. 1). The total land area of the archipelago is 18.4 km^2, of which Fernando de Noronha itself, 10 km long by 3.5 km at its greatest width, composes 16.9 km^2 (fig. 2). The highest point is the columnar igneous plug known as Morro do Pico (321 m), but the remainder of the island is, for the most part, considerably lower and less rugged. A rolling plain averaging 45 m elevation dominates the west-central part of the island, and an irregular plateau averaging 70 m the east-central portion. Streams are small and seasonally intermittent, and nowhere have they cut valleys of any significance.

The geology and geochemistry of the small island chain have been treated in detail by Branner (1889, 1890), de Almeida (1958), Mitchell-Thomé (1970), and Gunn and Watkins (1976). Fernando de Noronha is volcanic in origin, formed by a submarine mountain that rises abruptly 4000 m from the ocean's floor as a classical conical seamount, of which only the uppermost tip breaks surface to create the archipelago. Miocene phonolitic monoliths and domes form the high points (160 to 320 m) that rim the main is-

Fig. 1. Position of Fernando de Noronha in relation to South America and its continental shelf (stippled area approximates limit of 100 fathoms [180 m]). Distributional limits of *Holochilus* and *Lundomys* (type locality, Lagoa Santa), rodent genera related to the new genus on Ilha Fernando de Noronha, are also depicted. Numbers designate general areas of analytical samples of *H. brasiliensis* (OTU 3) and *H. sciureus* (OTUs 4–7); see Materials and Methods for precise collecting localities and sample sizes.

land, and Pliocene ankaramite lava flows underlie the central undulating plains. Potassium–argon dating indicates the greatest age of subaerial rocks as 11.8 ± 0.4 million years (Cordani, 1967), and active vulcanism is believed to have ceased by the late Pliocene to very early Pleistocene (de Almeida, 1958). The few sedimentary formations, products of Pleistocene and Recent age, consist of calcareous sandstones of aeolian origin, some marine limestone, and insubstantial alluvial deposits. Old marine terraces record several eustatic oscillations from 40 m above to 6 m below current sea level.

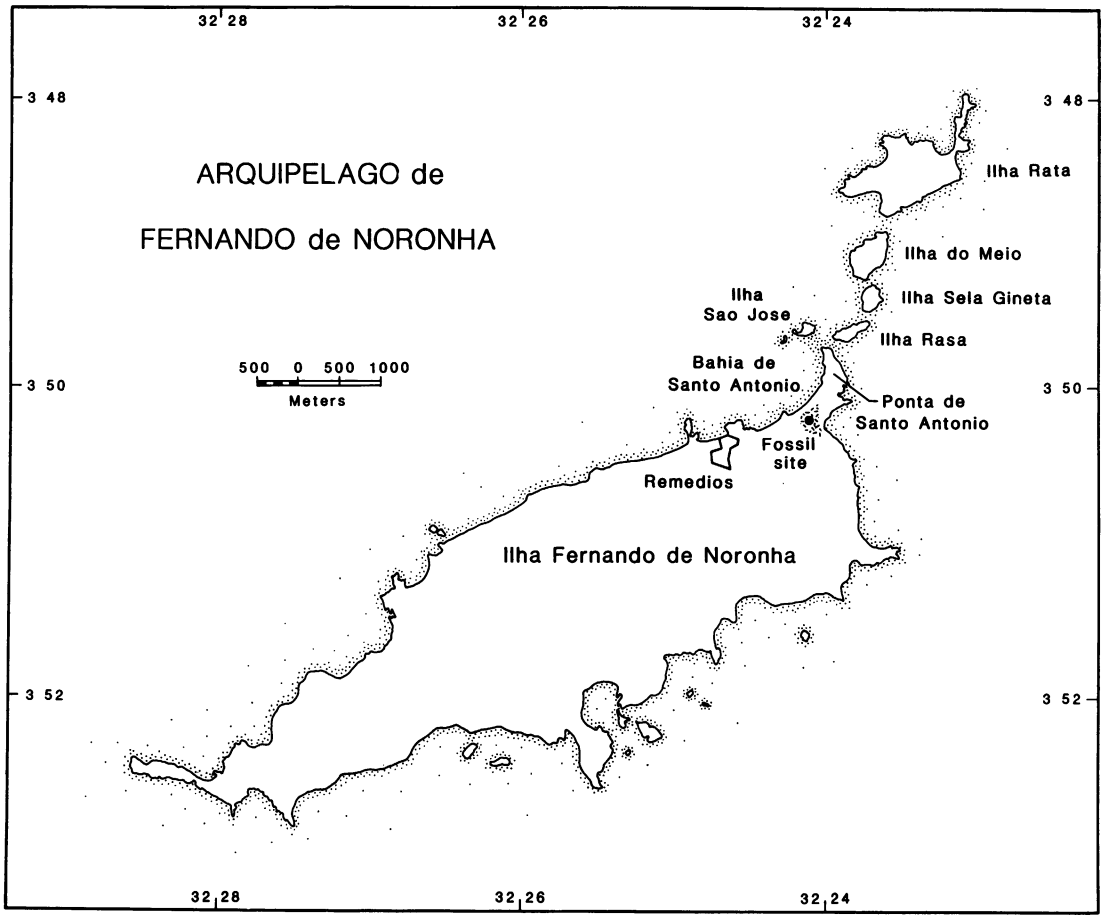

Fig. 2. Islands composing the Arquipelago de Fernando de Noronha, located approximately 345 km east of Cabo de So Rocque, Brazil. Fossil material of the new sigmodontine rodent was recovered from late Quaternary beach dunes situated at the neck of Ponta de Santo Antonio, Ilha Fernando de Noronha.

Fernando de Noronha is actually the outermost of a series of volcanic peaks, all except Atoll das Rocas submerged, that extend between the archipelago and the continental shelf of Brazil. However, no geological evidence suggests that these peaks ever formed continuous land, the depths between them being too great—in some cases over 5000 m.

Mitchell-Thomé (1970) likened the climate of Fernando de Noronha to that of Rio Grande do Norte in easternmost Brazil. The climate is mild and marked by a pronounced dry season (August to January) and distinct rainy period (February to July); October is the driest month and April the wettest. Annual rainfall averages 1318 mm, 60% falling in the three wettest months. The average annual temperature is 25.4°C, the minimum recorded temperature 18°C and the maximum 31°C; August is the coolest month and March the warmest. Yearly relative humidity remains fairly uniform, ranging between an average of 81% in the dry season and 87% in the wet season. Trade winds are strong and constant, generally from the southeast. The southern exposure of the island is thus the weathered side, its shoreline mostly inaccessible and characterized by steep, rugged cliffs; in contrast, the northern side boasts several beaches of unsurpassed beauty and tranquility.

THE FOSSIL LOCALITY: During three weeks of searching in 1973, the only productive fossiliferous site discovered was an area of

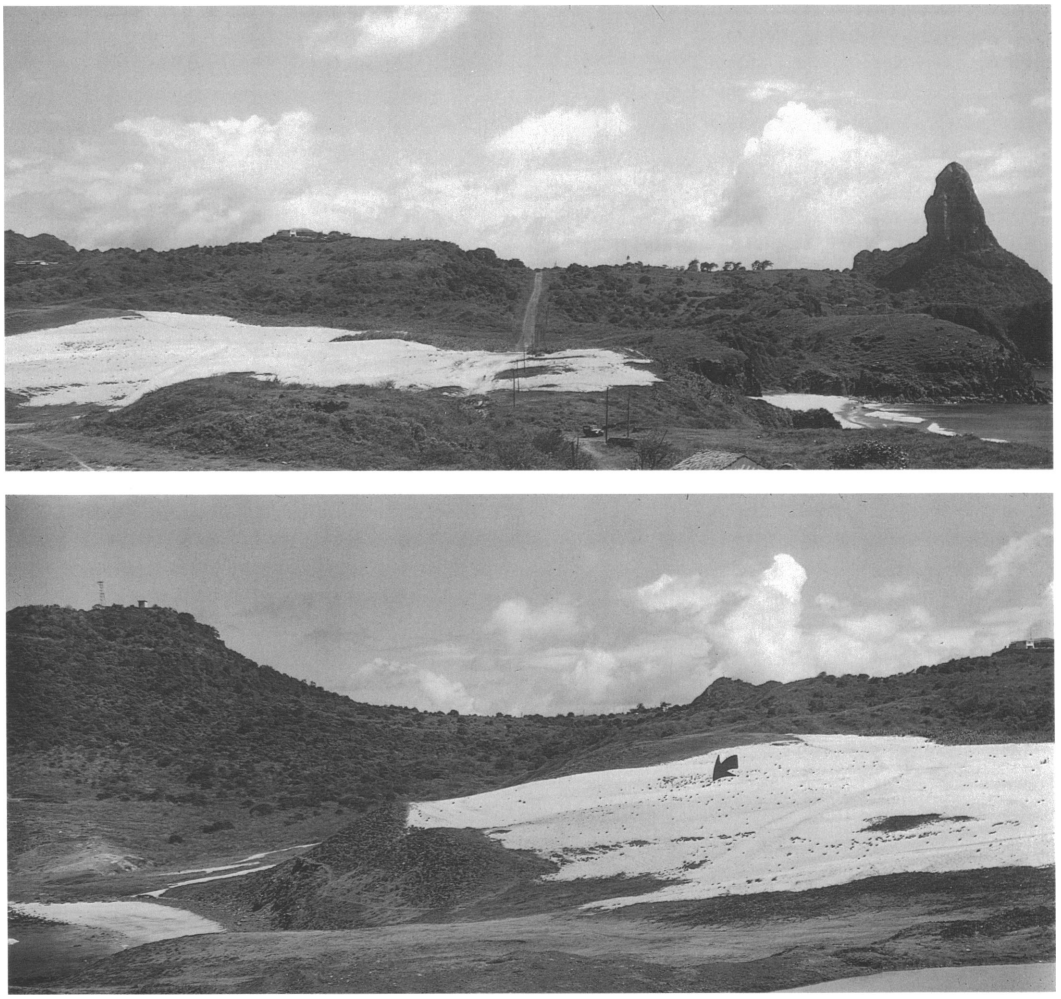

Fig. 3. Two views, looking westward, of the elevated Quaternary beach on Ilha Fernando de Noronha where skeletal remains of *Noronhomys vespuccii* were discovered. **Top:** General overview of beach dunes that straddle the neck of the Ponta de Santo Antonio (also see fig. 2); the phonolitic plug Morro do Pico, "The Peak" (about 2.5 km distant in the right background) forms a conspicuous landmark (321 m) that dominates the otherwise low relief of the island. **Bottom:** Southern portion of beach dunes with arrow indicating the indurated nodular layer around which most surface material was recovered; note the present-day ocean level and active beach in lower left of photo. Photographs by Storrs L. Olson.

dunes that extend nearly across the narrow neck of Ponta de Santo Antonio, which forms the northeastern corner of the island (fig. 2). Here, loose sands reach inland from the southern beach at Bahia de Caleira and extend almost to Bahia de Santo Antonio on the northern side of the peninsula (fig. 3). Just east of the dunes, on the south side of the peninsula, there are also low outcrops of indurated sandstone (calcareous arenites) into which small caves have been weathered. Similar consolidated aeolianites occur elsewhere on the main island and various islets (Branner, 1890; de Almeida, 1958). No vertebrate fossils were found in the indurated sandstone caves except one fragmented bone of a frigate bird (*Fregata*).

Both the unconsolidated and indurated sands are largely calcareous, composed of polished grains representing the comminuted organic remains of corals, nullipores, mollusks, and foraminifera. Analyses of dune

samples have accordingly yielded high percentages, 70 to 97%, of calcium carbonate and small traces of silicon dioxide (Branner, 1890; Mitchell-Thomé, 1970). We lack radiometric or other dates for these dune deposits, but the bulk of the sands may have been blown inland during a glacial period of lower sea level, when more reefs would have been exposed and winds were stronger. Such a taphonomic environment resembles that hypothesized for the fossil-rich sands on St. Helena and the Hawaiian Islands (Olson, 1975; Olson and James, 1982). Of course, vertebrate remains could have been intermixed with the shifting sands at any time afterwards, creating an unstructured stratigraphic context that leaves the age of the fossils as indeterminate. Some bones are obviously much older than others, being heavily encrusted with indurated sand and appearing well mineralized. Others, such as the remains of domestic *Felis*, *Rattus*, and *Mus*, are much more recent and display no signs of mineralization.

Vertebrate fossils recovered from the dunes include various reptiles and seabirds, the dove *Zenaida auriculata,* and an extinct flightless rail (Olson, 1981), as well as the sigmodontine rodent described below. The vertebrate bones occurred mainly in three or four localized patches characterized by an abundance of land snail shells and small white nodules, possibly conglomerates formed from the phosphatic residue of guano. Sand removal from a small quarry had exposed a semiconsolidated layer about 8–12 cm thick that was composed mainly of these nodules; here, the terrestrial snail shells were most prevalent. This layer ranged from 45 cm below the surface of the dunes to much deeper and appeared to be the source of most of the fossils collected. The identifiable land snails, as determined by Joseph Rosewater (late curator of mollusks at USNM), are *Hyperaulax* (*Hyperaulax*) *ridleyi*, *H.* (*Bonnanius*) *ramagei*, *Ridleyi quinquelirata*, and *Lamellaxis micra*. The first three are endemic to the island.

THE EXTINCT SIGMODONTINE RODENT

Olson and assistants collected vertebrate fossils on nine days between 27 July and 16 August 1973. These were found mostly by surface picking, supplemented by sand screening in the more productive areas (see fig. 3). The preserved material of the extinct rodent, rich both in the skeletal parts and number of individuals represented, consists of several crania, many mandibles with intact or partial toothrows, and numerous postcranial elements. Most bones recovered were isolated, but the burial context of some, including the skull with associated mandibles selected as the holotype, suggests that they came from a single individual.

Noronhomys, new genus

TYPE SPECIES: *Noronhomys vespuccii*, new species.

DIAGNOSIS: A genus of sigmodontine rodent, tribe Oryzomyini (sensu Voss and Carleton, 1993), characterized by robust cranial proportions and moderately large size (ONL = 38–40 mm), smaller than *Lundomys molitor* (ONL = 42–46 mm) and *Holochilus brasiliensis* (ONL = 40–44 mm) but equivalent to larger-bodied examples of *H. sciureus* (see tables 1, 2). Interorbital region relatively broad and hourglass shaped without dorsally raised beads (present in mature *Holochilus*), temporal ridging over braincase low in relief (well developed in adult *Holochilus* and *Lundomys*); zygomatic plate comparatively narrow, notch shallow, lacking spine on anterodorsal rim (plate broader, notch well inscribed, and anterodorsal edge produced as moderate to strong spine in *Lundomys* and *Holochilus*); bony palate relatively short, surface broad and flat, mesopterygoid fossa projecting conspicuously between M3s (palate narrower and corrugated, extending even with or beyond the end of M3 in *Lundomys* and *Holochilus*). Molars moderately hypsodont with planar occlusal surface (cuspidate and terraced in *Lundomys*); short mesolophs consistently present on upper M1 and M2 (absent in most *Holochilus*); M1 and M2 posteroloph absent (present on little-worn molars of *Lundomys* and *Holochilus*); m2 posteroflexid and m3 entoflexid closed off as enamel islands, m3 anterolabial cingulum and protoflexid absent (folds confluent with lingual margin, small cingulum

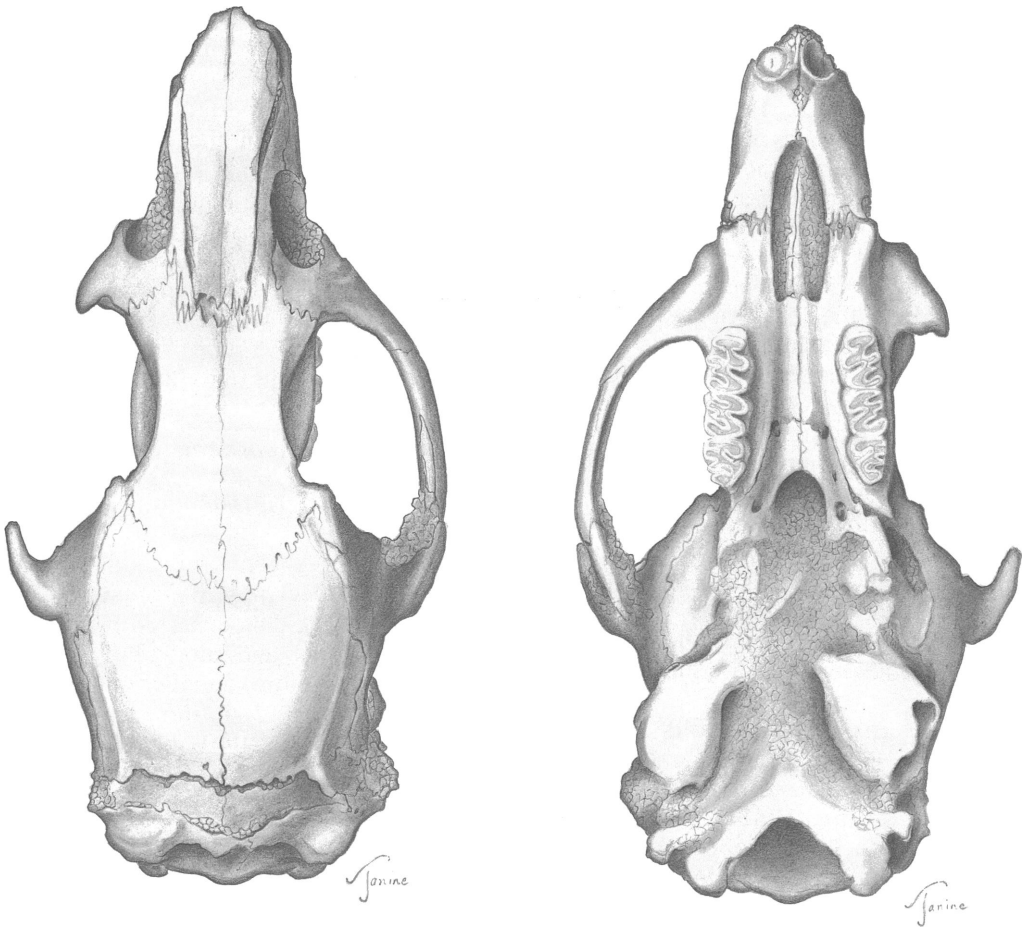

Fig. 4. Dorsal and ventral cranial views of the holotype (MCP 3460-PV) of *Noronhomys vespuccii* (occipitonasal length = 39.2 mm).

and protoflexid present in *Lundomys* and *Holochilus*).

ETYMOLOGY: Named for Ilha Fernando de Noronha, where the extinct fossil species was discovered and to which *Noronhomys* was probably endemic. In Portuguese, the *nh* in "Noro**nh**a" is pronounced like the Spanish *ñ* or the ny in "ca**ny**on."

Noronhomys vespuccii, new species
Figures 4–15; Tables 1–3

HOLOTYPE: MCP 3460-PV, a nearly complete cranium with associated lower jaws, collected by S. L. Olson and O. A. Roppa, on 16 August 1973.

The preservation of the type specimen is remarkably fine, and its moderately worn molars suggest a fully adult animal. The cranium is nearly intact, lacking only the left zygomatic arch and the delicate pterygoid and paroccipital processes (figs. 4–7). There is some breakage of the nasolacrimal capsules, sphenopalatine vacuities, and basal alisphenoid region. Both otic capsules are present though slightly askew from their normal position. Embedding matrix occludes most cranial formina and cements the paired lower jaws found in close physical association; otherwise, the skull is well cleaned and anatomical detail can be readily observed.

Selected dimensions (in mm) of the holotype are ONL, 39.2; ZB. 20.1; BBC, 13.4; IOB, 5.5; PPL, 14.9; BPL, 7.9; LD, 11.2; LIF, 7.1; CLM, 7.28; WM1, 2.24; DMm1,

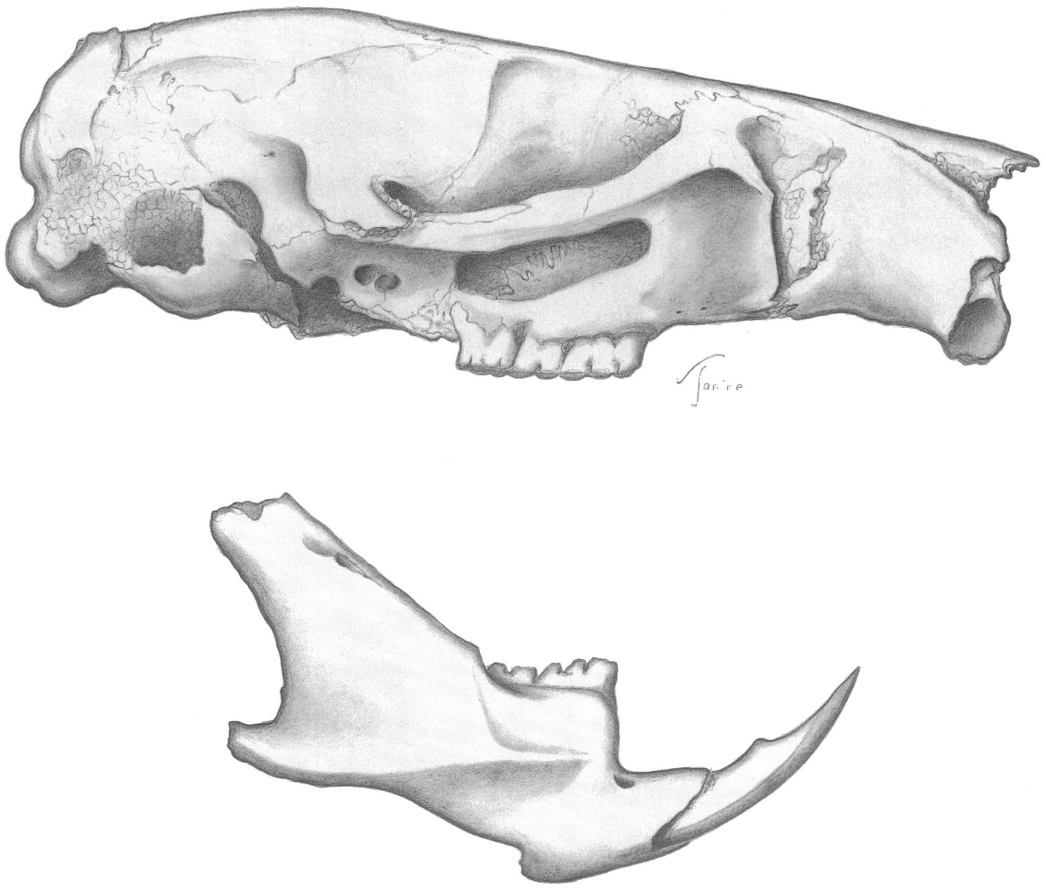

Fig. 5. Lateral view of the cranium and associated left mandible of the holotype (MCP 3460-PV) of *Noronhomys vespuccii*.

7.6; CLm, 8.07; and PWm1, 1.95. See tables 1 and 2 for descriptive cranial and mandibular statistics of the type series and mensural comparisons with samples of *Lundomys* and *Holochilus*.

TYPE LOCALITY: Brazil, Territorio de Fernando de Noronha, Ilha Fernando de Noronha, late Quaternary beach dunes located near Ponta de Santo Antonio (figs. 2, 3); approximately 3°50′S, 32°24′W.

DIAGNOSIS: As for the genus.

REFERRED MATERIAL: Skull, partially invested with matrix, with attached mandibles (USNM 490263); fragmented cranium with mandibles (MCP 3578-PV); cranium with incomplete zygoma (USNM 490264); rostral portion of crania with maxillary toothrows (MCP 3579-PV; USNM 490265); left and right dentaries with intact or partial dentitions (MCP 3580–3610-PV; USNM 490266–490297); maxillaries with intact or partial molar rows (MCP 3611–3613-PV; USNM 490297–490299); left femur (USNM 490300); left tibia (USNM 490301); right ilium (USNM 490302); and miscellaneous uncataloged and mostly fragmentary postcranial elements (MCP-PV, USNM).

ETYMOLOGY: The specific epithet is the Latin genitive singular of the surname of Amerigo Vespucci, Florentine navigator of the late 15th and early 16th centuries. Vespucci may have been one of the few humans to have seen this rodent alive, although his account of landing on Fernando de Noronha in 1503 and there finding "very big rats" has been tainted by controversies surrounding the veracity of his fourth voyage (Pohl, 1944; Formisano, 1992). Whether his observations

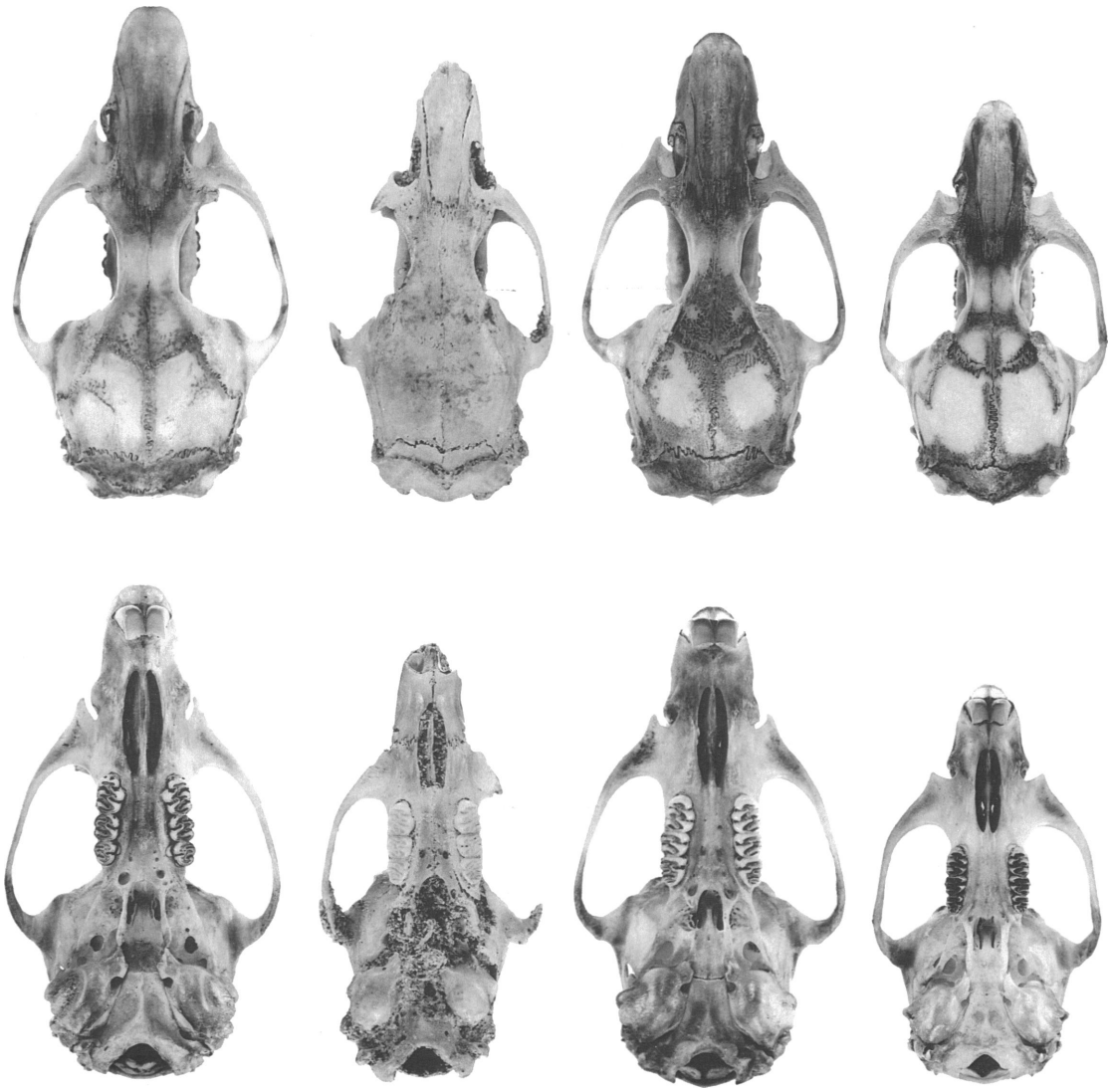

Fig. 6. Dorsal and ventral views of skulls (about 1.5×) of adult *Lundomys*, *Noronhomys*, and *Holochilus*: **A**, *L. molitor* (AMNH 206393); **B**, *N. vespuccii* (MCP 3460-PV); **C**, *H. brasiliensis* (AMNH 206369); and **D**, *H. sciureus* (AMNH 210263).

were personal or purloined from another mariner's log, the 1504 account of four voyages attributed to Vespucci is the first and only reference known that suggests the existence of an indigenous rodent on the island (also see Discussion).

DESCRIPTION: Skull stoutly constructed and moderately large (ONL = 38–40 mm), similar in general size and proportions to large-bodied populations of *H. sciureus* (table 1). Dorsal profile flattened (fig. 5), the highest point of the cranial vault situated near the middle of the parietals and sloping in a nearly straight line from the frontoparietal suture to the nasal tips. Rostrum short and broad; anterior tips of nasals apparently bluntly rounded (edges damaged in all specimens), posterior borders squared off, terminating even with the rostral process of the premaxillary. Interorbital constriction broad relative to expanse of the zygoma; dorsolateral margins of interorbit hourglass shaped, with the

Fig. 7. Lateral view of skulls (about 1.5×) of adult *Lundomys*, *Noronhomys*, and *Holochilus*: **A**, *L. molitor* (AMNH 206393); **B**, *N. vespuccii* (MCP 3460-PV); **C**, *H. brasiliensis* (AMNH 206369); and **D**, *H. sciureus* (AMNH 210263).

frontal edges sharp, not rounded, and produced as a slight supraorbital shelf at the rear of the orbits. Vertical bony ridge present on orbital wall, extending from a point just below the rear of the supraorbital shelf to one just above the zygomatic root of the squamosal, partially obscuring the frontosquamosal suture from lateral view. Shape of braincase somewhat rectangular as seen from above, an effect heightened by the placement of the postorbital vertical ridges (fig. 4); frontoparietal suture defining a broad curve, angle formed at midsagittal junction obtuse; temporal and lambdoidal ridging present but weakly pronounced, even in the oldest specimens available. Interparietal bone short and wide, its lateral apices not reaching the squamosals.

Zygomatic arches heavy and laterally flared, widest across their squamosal roots and gradually convergent toward the zygomatic plates. Jugal very small and the maxillary and squamosal processes of the arch in contact. Anterior rim of zygomatic plate more or less straight, oriented vertically, lacking a spinous process on its free anterodorsal edge; zygomatic notch moderately incised; as seen in lateral view, posterior margin of plate aligned approximately with the anterior root of M1.

Incisive foramina medium in length (LIF about 62% of LD), their posterior ends terminating in front of the molar alveoli (fig. 4); foraminal openings nearly parallel throughout their length, without notable medial expansion, and bluntly tapered at both ends, not sharply pointed. Palatal bridge relatively wide and short, its posterior border positioned about the middle of the third molars (mesopterygoid fossa conspicuously projecting between the M3s); bridge relatively flat, unmarked by well-defined palatal gutters or median longitudinal ridge. Posterior palatine foramina exiting within the maxillary–palatine suture, just medial to the lingual root of the M2s; posterolateral palatal pits not defined as such, but simple unrecessed foramina occurring just in front of the parapterygoid fossae. Anterior margin of mesopterygoid fossa evenly convex, the palatines lacking a posterior extension or spine; walls of mesopterygoid fossa seemingly well ossified but presence or extent of sphenopalatine vacuities indeterminate with available specimens; parapterygoid fossae each about as wide as mesopterygoid fossa and moderately excavated above the level of the bony palate.

Robust strut of the alisphenoid bone dividing the masticatory–buccinator foramen from the foramen ovale accessorius. Stapedial and sphenofrontal foramina absent; no vascular grooves occurring on the inner surface of the

TABLE 1

Selected Cranial Dimensions (in mm) of *Noronhomys vespuccii, Lundomys molitor, Holochilus brasiliensis,* and *H. sciureus*

Species (and OTU[a])	N	Mean	Range	SD
Occipitonasal Length				
N. vespuccii	3	38.5	38.0–39.2	0.6
L. molitor	11	44.3	40.2–48.3	2.6
H. brasiliensis	13	41.8	38.3–45.6	2.3
H. sciureus (OTU 4)	10	35.6	30.0–38.7	3.1
H. sciureus (OTU 7)	14	40.1	34.2–45.6	3.1
Zygomatic Breadth				
N. vespuccii	1	20.1		
L. molitor	10	24.9	22.5–27.0	1.4
H. brasiliensis	14	24.1	22.2–24.1	1.3
H. sciureus (OTU 4)	10	19.3	16.8–21.1	1.5
H. sciureus (OTU 7)	14	21.8	19.4–24.2	1.4
Breadth of Braincase				
N. vespuccii	3	14.1	13.4–14.8	0.7
L. molitor	5	16.7	15.7–17.5	0.6
H. brasiliensis	6	15.5	15.0–15.9	0.4
H. sciureus (OTU 4)	10	13.9	12.8–14.8	0.6
H. sciureus (OTU 7)	9	14.2	13.6–14.9	0.5
Interorbital Breadth				
N. vespuccii	4	5.7	5.4—-6.0	0.3
L. molitor	11	5.1	4.7–5.4	0.2
H. brasiliensis	14	4.7	4.5–5.5	0.3
H. sciureus (OTU 4)	10	4.6	4.3–4.9	0.3
H. sciureus (OTU 7)	14	4.9	4.4–5.5	0.3
Breadth of Zygomatic Plate				
N. vespuccii	5	4.3	4.0–4.5	0.2
L. molitor	5	4.8	4.4–5.1	0.3
H. brasiliensis	5	5.2	4.2–5.7	0.7
H. sciureus (OTU 4)	10	4.3	3.4–4.9	0.5
H. sciureus (OTU 7)	9	4.7	3.8–5.3	0.5
Postpalatal Length				
N. vespuccii	1	14.9		
L. molitor	11	14.3	12.5–16.1	1.2
H. brasiliensis	12	14.2	12.7–16.8	1.3
H. sciureus (OTU 4)	10	11.3	8.9–12.5	1.2
H. sciureus (OTU 7)	14	13.1	11.2–14.4	1.0
Length of Bony Palate				
N. vespuccii	4	8.0	7.7–8.7	0.5
L. molitor	11	10.0	8.4–10.7	0.7
H. brasiliensis	14	9.6	8.7–11.2	0.7
H. sciureus (OTU 4)	10	7.9	6.4–9.2	0.8
H. sciureus (OTU 7)	14	8.9	7.6–10.8	0.8

TABLE 1—(*Continued*)

Species (and OTU[a])	N	Mean	Range	SD
Length of Diastema				
N. vespuccii	5	11.4	11.2–12.2	0.4
L. molitor	8	12.3	10.2–13.4	1.2
H. brasiliensis	9	13.3	11.7–15.0	1.1
H. sciureus (OTU 4)	10	10.4	8.0–11.8	1.3
H. sciureus (OTU 7)	9	12.0	9.3–14.4	1.4
Length of Incisive Foramen				
N. vespuccii	7	7.1	6.7–7.7	0.4
L. molitor	11	8.9	8.1–9.9	0.7
H. brasiliensis	14	8.0	7.0–9.0	0.6
H. sciureus (OTU 4)	10	7.1	6.0–8.3	0.8
H. sciureus (OTU 7)	14	7.9	6.7–8.9	0.6
Palatal Breadth across M1s				
N. vespuccii	4	8.4	8.1–8.9	0.3
L. molitor	8	9.0	7.6–9.7	0.7
H. brasiliensis	9	9.0	8.3–9.6	0.5
H. sciureus (OTU 4)	10	7.0	6.1–7.8	0.5
H. sciureus (OTU 7)	9	7.6	6.8–8.0	0.4
Depth of Auditory Bulla				
N. vespuccii	2	5.2	5.1, 5.3	
L. molitor	11	6.7	6.3–7.1	0.2
H. brasiliensis	13	6.7	6.4–7.0	0.2
H. sciureus (OTU 4)	10	5.5	5.0–5.9	0.3
H. sciureus (OTU 7)	14	6.2	5.7–6.6	0.2
Length of Maxillary Toothrow				
N. vespuccii	3	7.37	7.15–7.60	0.23
L. molitor	15	8.27	7.95–8.75	0.19
H. brasiliensis	14	7.73	7.05–8.15	0.29
H. sciureus (OTU 4)	10	6.61	6.10–7.13	0.27
H. sciureus (OTU 7)	14	7.31	7.00–7.60	0.16
Width of M1				
N. vespuccii	7	2.25	2.16–2.33	0.06
L. molitor	15	2.53	2.4–2.65	0.09
H. brasiliensis	14	2.47	2.30–2.60	0.10
H. sciureus (OTU 4)	10	2.01	1.80–2.24	0.12
H. sciureus (OTU 7)	14	2.24	2.15–2.40	0.07

[a] Operational taxonomic unit (OTU) 4 represents specimens from Bolivia and OTU 7 those from Venezuela.

squamosal and alisphenoid bones or across the posterolateral angle of the parapterygoid fossa (carotid cirulation derived, lacking supraorbital and infraorbital branchs of the stapedial artery). Carotid canal of moderate size, its perimeter delimited by the posteromedial edge of the bony eustachian tube and anterolateral edge of the basioccipital.

TABLE 2

Selected Mandibular Dimensions (in mm) of *Noronhomys vespuccii, Lundomys molitor, Holochilus brasiliensis,* and *H. sciureus*

Species (and OTU[a])	N	Mean	Range	SD
Depth of Ramus below m1				
N. vespuccii	50	7.68	5.65–9.80	0.76
L. molitor	9	7.79	6.95–8.80	0.65
H. brasiliensis	12	8.56	6.90–9.80	0.76
H. sciureus (OTU 4)	16	7.37	5.40–8.40	0.82
H. sciureus (OTU 6)	12	7.22	6.85–7.48	0.20
H. sciureus (OTU 7)	14	7.69	7.52–7.99	0.13
Length of Masseteric Crest				
N. vespuccii	56	3.86	3.04–4.60	0.35
L. molitor	9	2.61	2.12–3.18	0.40
H. brasiliensis	12	4.00	2.79–4.91	0.69
H. sciureus (OTU 4)	16	2.05	1.10–2.71	0.45
H. sciureus (OTU 6)	12	1.84	1.03–2.99	0.66
H. sciureus (OTU 7)	14	2.54	1.46–3.32	0.48
Length of Mandibular Toothrow				
N. vespuccii	39	8.00	7.57–8.29	0.18
L. molitor	9	8.95	8.74–9.14	0.14
H. brasiliensis	12	8.61	8.24–8.99	0.26
H. sciureus (OTU 4)	15	6.93	6.40–7.29	0.22
H. sciureus (OTU 6)	12	7.22	6.85–7.48	0.20
H. sciureus (OTU 7)	14	7.69	7.52–7.99	0.13
Length of m1				
N. vespuccii	53	3.15	2.94–3.32	0.09
L. molitor	9	3.63	3.56–3.82	0.08
H. brasiliensis	12	3.43	3.24–3.73	0.16
H. sciureus (OTU 4)	16	2.75	2.45–3.02	0.13
H. sciureus (OTU 6)	12	2.91	2.70–3.08	0.11
H. sciureus (OTU 7)	14	3.00	2.86–3.18	0.11
Length of m2				
N. vespuccii	44	2.27	2.00–2.42	0.08
L. molitor	9	2.54	2.42–2.78	0.12
H. brasiliensis	12	2.34	2.14–2.43	0.10
H. sciureus (OTU 4)	15	1.92	1.82–1.99	0.05
H. sciureus (OTU 6)	12	2.01	1.91–2.15	0.07
H. sciureus (OTU 7)	14	2.29	2.14–2.73	0.18
Length of m3				
N. vespuccii	38	2.51	2.32–2.75	0.12
L. molitor	9	2.95	2.81–3.20	0.12
H. brasiliensis	12	2.97	2.64–3.21	0.19
H. sciureus (OTU 4)	15	2.38	2.17–2.68	0.14
H. sciureus (OTU 6)	12	2.43	2.23–2.56	0.09
H. sciureus (OTU 7)	14	2.55	2.22–2.80	0.17
Posterior Width of m1				
N. vespuccii	48	1.93	1.80–2.08	0.06
L. molitor	9	2.18	2.04–2.26	0.07
H. brasiliensis	12	2.22	2.12–2.38	0.07
H. sciureus (OTU 4)	16	1.82	1.62–1.92	0.08
H. sciureus (OTU 6)	12	1.93	1.85–2.10	0.07
H. sciureus (OTU 7)	14	2.07	1.96–2.19	0.06
Anterior Width of m2				
N. vespuccii	40	2.00	1.90–2.13	0.06
L. molitor	9	2.29	2.18–2.36	0.05
H. brasiliensis	11	2.28	2.16–2.40	0.08
H. sciureus (OTU 4)	15	1.98	1.84–2.09	0.07
H. sciureus (OTU 6)	12	2.07	1.98–2.23	0.07
H. sciureus (OTU 7)	14	2.28	2.17–2.44	0.08
Width of m3				
N. vespuccii	34	1.88	1.74–2.01	0.07
L. molitor	9	2.12	1.99–2.31	0.10
H. brasiliensis	11	2.17	2.09–2.30	0.05
H. sciureus (OTU 4)	13	1.84	1.68–1.96	0.10
H. sciureus (OTU 6)	12	1.95	1.83–2.07	0.09
H. sciureus (OTU 7)	14	2.18	2.09–2.43	0.09
Width of Incisor				
N. vespuccii	38	1.32	0.88–1.70	0.18
L. molitor	9	1.74	1.28–2.08	0.24
H. brasiliensis	11	1.84	1.53–2.11	0.18
H. sciureus (OTU 4)	16	1.52	1.12–1.81	0.19
H. sciureus (OTU 6)	12	1.63	1.10–1.85	0.14
H. sciureus (OTU 7)	14	1.82	1.37–2.19	0.23
Depth of Incisor				
N. vespuccii	38	2.03	1.48–2.35	0.21
L. molitor	9	2.06	1.69–2.29	0.16
H. brasiliensis	11	2.28	1.88–2.72	0.28
H. sciureus (OTU 4)	16	1.81	1.27–2.06	0.24
H. sciureus (OTU 6)	12	1.79	1.50–2.10	0.18
H. sciureus (OTU 7)	14	1.99	1.56–2.43	0.25
Height of m1 Metaconid				
N. vespuccii	64	0.81	0.31–1.26	0.24
L. molitor	9	1.12	0.74–1.44	0.26
H. brasiliensis	12	0.92	0.41–1.25	0.28
H. sciureus (OTU 4)	16	0.73	0.25–1.04	0.21
H. sciureus (OTU 6)	12	0.81	0.59–1.00	0.13
H. sciureus (OTU 7)	14	0.83	0.58–1.06	0.14

[a] OTU 4 represents specimens from Bolivia, OTU 6 those from Suriname, and OTU 7 those from Venezuela.

Auditory bulla globoid, eustachian tube short and wide, bullar inflation moderate. Terete spine (stapedial process sensu Steppan, 1995) formed on anterolateral wall of bulla, braced against posterolateral margin of the alisphenoid. Tegmen tympani visible within the postglenoid space, apparently not contacting the ventrolateral edge of the squamosal (anatomical orientation uncertain due to investing matrix and probable dislocation of bullae on available crania). Subsquamosal fenestra present as a short, narrow cleft; area of postglenoid foramen greater than subsquamosal fenestra, but not so spacious as observed in *Holochilus*; hamular process of squamosal correspondingly short and stout.

Mandible deep and stocky; ascending ramus broad, its leading edge nearly vertical and terminating dorsad in a sweeping, crescent-shaped coronoid process; dorsalmost extent of the condyloid and coronoid processes equal, the two circumscribing a deep, semioval sigmoid notch; angular process short and bluntly rounded, angular notch a shallow emargination along the posterior edge of ramus; superior masseteric ridge intersects inferior ridge at right angle, the two conjoined as a strong crest that continues anteriad to a point below the anterior root of m1 (fig. 5); terminus of incisor alveolus marked by raised capsular process, situated below the ventral rim of the sigmoid notch; posterior end of symphysis forming rugose, sharply angled projection that accentuates depth of mandible; mental foramen positioned on lateral surface of mandibular diastema, set apart from the end of the masseteric crest.

Upper incisors moderately wide and heavy, asulcate, opisthodont in form; enamel bands pale to deep orange. Lower incisors somewhat narrow relative to the stout appearance of the mandible.

Molar teeth moderately hypsodont, forming planar occlusal surfaces; margin of lingual and labial cusps bluntly rounded (figs. 8, 9); major cusps positioned nearly opposite one another in upper molars, more alternate in lowers. First molars longest of cheek teeth (LM1 about 40% of CLM); upper and lower third molars slightly longer than contiguous second molars (LM3 about 107% of LM2; Lm3 about 110% of Lm2) but narrower. Anterocone of M1 almost as broad as greatest width of tooth, without indication of anteromedian flexus or fossettus for any wear stage of specimens at hand; m1 anteroconid similarly wide, enclosing large enamel pit (anteromedian fossettid?) that persists until late wear stages. Short mesolophs, typically not reaching buccal margin of tooth, uniformly present on M1s and M2s and contributing to planar chewing surface (fig. 8); mesoloph better defined on elongate M3; mesolophids lacking on all lower molars. Anteroloph and anterolophid not developed; protoflexus undefined on M2 and M3; posteroloph of M1 and M2 absent, residual enamel fold or island never observed on the least worn molars. Posteroflexid of m2 and entoflexid of m3 closed off from lingual margin of tooth, represented as fossettids in youngest wear stages in sample; other lingual and labial enamel folds on both upper and lower molars open to basal margins of tooth. Anterolabial cingulum weakly defined on m2, never defined on m3.

M1 with large labial root in addition to usual complement of anterior, posterior, and lingual roots (total of four roots), M2 and M3 with three roots each; m1 with accessory labial root (three roots) and usually with lingual accessory root (four roots), m2 and m3 each with two roots.

Entepicondylar foramen of humerus absent; trochlear process of calcaneum positioned distally relative to posterior articular facet (see character 40 of Carleton, 1980); iliac blade of innominate and limb bones generally stout in proportions (see below for comparisons with *Holochilus*). Meristic traits of vertebral column indeterminate due to disarticulated condition of fossil samples.

COMPARISONS WITH *HOLOCHILUS* AND *LUNDOMYS*

As underscored by our diagnosis, specimens of *Noronhomys* resemble those of *Holochilus* and *Lundomys* in many morphological features. The cranial similarities to *Holochilus* are many and include the comparatively large skulls with stoutly constructed zygomatic arches and reduced jugals; the relatively narrow constriction and amphoral-like shape of the interorbit; the possession of

Fig. 8. Occlusal view of right upper molars (about 12×) of adult *Lundomys*, *Noronhomys*, and *Holochilus*: **A**, *L. molitor* (AMNH 206388); **B**, *N. vespuccii* (MCP 3460-PV); **C**, *H. brasiliensis* (AMNH 206372); and **D**, *H. sciureus* (AMNH 134703).

vertically elongate postorbital ridges; the short, broad interparietal; the relatively short incisive foramina that terminate in front of the molar rows; the deeply recessed parapterygoid fossae; the absence of an alisphenoid strut; a derived carotid circulation and corresponding loss or occlusion of cranial foramina and vascular traces; and the conformation of the mandible and masseteric crests. Dental resemblances between *Noronhomys* and *Holochilus* are equally noteworthy: occlusal surfaces that are planar; pronounced involution of the enamel folds; reduction or absence of the mesoloph and loss of the mesolophid; broad anterocone lacking an anteromedian crease; presence of an internal enamel pit on m1; sigmodont form of the m3s; and presence of satellite roots on the upper and lower first molars.

Considered together, the shared craniodental traits are sufficiently impressive to advance preliminary hypotheses of close phylogenetic relationship between *Noronhomys* and *Holochilus* and the more distant kinship of these two genera to *Lundomys*, hypotheses explored in broader phylogentic context in the next section. The weight of such similarities notwithstanding, substantial differences, both discrete and proportional, exist among these genera and warrant more detailed contrast.

Skeletal and Dental Anatomy

Cranial Vault and Orbital Region: The skull of *Noronhomys*, although as robust as in *Holochilus* and *Lundomys*, has a flatter dorsal profile. The apex of the cranial vault occurs at about the middle of the parietals (with the molar rows positioned horizontally as reference) and slopes gently as a nearly straight line over the interorbit and rostrum. In contrast, the dorsal contour of the latter genera is evenly arched with the apex centered over the interorbital region (figs. 7, 10). The stronger development of the dorsally di-

Fig. 9. Occlusal view of right lower molars (about 12×) of adult *Lundomys*, *Noronhomys*, and *Holochilus*: **A**, *L. molitor* (AMNH 206388); **B**, *N. vespuccii* (USNM 490287); **C**, *H. brasiliensis* (AMNH 206372); and **D**, *H. sciureus* (AMNH 134703).

rected supraorbital ridges of *Holochilus* perhaps exaggerates the dissimilarity in cranial profiles, but the interorbital construction of *Lundomys* more nearly resembles that of *Noronhomys* and still presents the same contrast in shape.

The interorbital contour of all three genera is basically hourglass shaped and appears narrow relative to the expanse of the zygomatic arches (actually more attenuate in *Holochilus* and *Lundomys* than in *Noronhomys*, see below). The dorsolateral margins of the frontals are squarely edged, not rounded, but do not form pronounced supraorbital shelves; slight supraorbital ledges do occur at the rear of the orbits in *Holochilus* and may be found in very old *Lundomys* and *Noronhomys*. Adult and older specimens of *Holochilus* possess a dorsally reflected supraorbital bead along the rear of the frontal, generally continued as a prominent temporal ridge over the squamosal and parietal. Even old adult *Lundomys* and *Noronhomys* lack such a raised bead but may exhibit temporal ridging of low relief.

A rugose vertical crest or ridge, like that seen in *Holochilus* (Voss and Carleton, 1993: fig. 9), marks the rear orbital wall of *Noronhomys*. A postorbital ridge is not developed in *Lundomys*.

ZYGOMATIC REGION: The conformation of the maxillary root of the zygoma sets *Noronhomys* apart from both *Holochilus* and *Lundomys*. No anterodorsal spine is apparent in any of the six fossils that have the zygomatic plate suitably preserved. In each, the zygomatic notch appears relatively shallow, and the rostral border of the plate is nearly straight (figs. 5, 11). Individuals of *Holochilus* and *Lundomys*, on the other hand, typically possess a protuberant anterodorsal spine, a feature that accentuates the depth of the zygomatic notch and the concavity along the forward margin of the plate (fig. 11). The position of the inferior root of the zygomatic arch, as observed relative to the molar rows

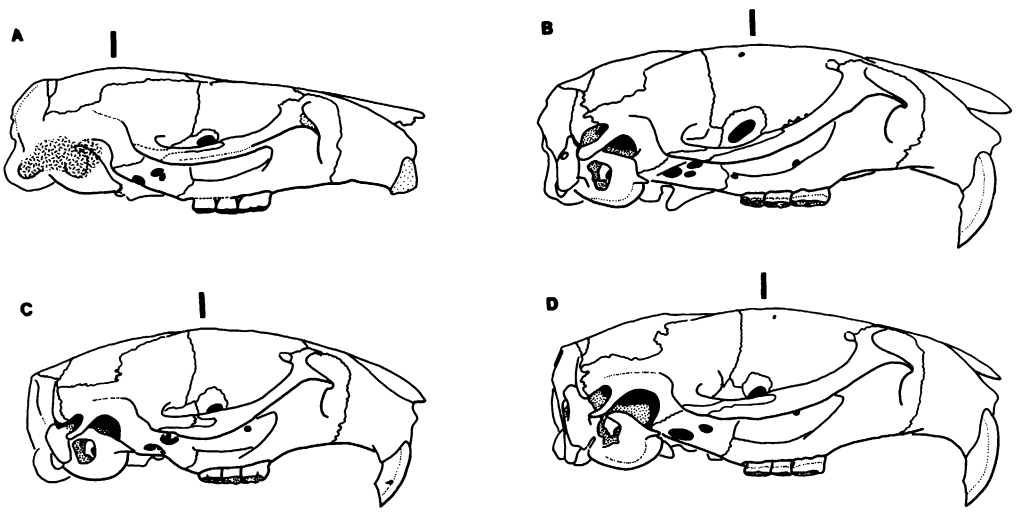

Fig. 10. Lateral cranial profiles of adult representatives of **A**, *Noronhomys vespuccii* (MCP 3460-PV); **B**, *Lundomys molitor* (AMNH 206368); **C**, *Holochilus sciureus* (USNM 394720); and **D**, *H. brasiliensis* (AMNH 206379). The heavy vertical line approximates the position of the apex of the cranial vault when skulls are coaligned on a plane horizontal with their molar occlusal surfaces.

and to the premaxillary–maxillary juncture, also differs. In *Holochilus* and *Lundomys*, the caudal border of the plate is set in front of the anterior root of the M1s, and its rostral border is situated well posterior to the suture of the premaxillary–maxillary bones. In *Noronhomys*, the rearward edge is situated more or less over the anterior root of M1 and the forward edge originates just behind the suture (fig. 11).

As judged by the holotype of *Noronhomys*, which is the only specimen with a nearly complete arch, the jugal is small and irregularly defined, with the maxillary and squamosal processes of the arch being in contact. This condition, if representative of the taxon, agrees with that of *Holochilus* and departs from the consistently formed, larger jugal observed in *Lundomys*.

BONY PALATE AND PALATAL FORAMINA: The construction of the bony palate of *Lundomys* conforms to the long type (sensu Hershkovitz, 1962), in which the posterior margin clearly extends behind the M3s. The long palate also characterizes adult specimens of *H. brasiliensis*, but in those of *H. sciureus*, it terminates more or less equal with the posterior margin of the M3s (Voss and Carleton, 1993). In those examples of *Noronhomys* that have the palatal region intact, the hard palate reaches to only the middle of the M3s, and the mesopterygoid fossa correspondingly protrudes between them (figs. 4, 6). Furthermore, the intermolar area of *Noronhomys* is relatively broad, without notable palatal gutters or a median longitudinal ridge as observed in mature examples of *Lundomys* and *Holochilus*.

Variation in development of the posterolateral palatal pits may correlate with the posterior extent of the hard palate. These vascular foramina occur as highly perforated palatal recesses in both *Holochilus* and *Lundomys*; in *Noronhomys*, apparently homologous foramina penetrate the anterolateral walls of the mesopterygoid fossa but are not set within a conspicuous depression.

ALISPHENOID REGION, OTIC CAPSULES, AND CRANIAL FORAMINA: A sturdy alisphenoid strut, separating the masticatory–buccinator and accessory oval foramina, can be verifed on several crania of *Noronhomys*. The strut is likewise present in members of *Holochilus* but is uniformly lacking in *Lundomys* (Voss and Carleton, 1993: fig. 10).

The auditory bullae of *Noronhomys* are moderately bulbous, shaped like those of *Holochilus* and *Lundomys* but less inflated. Their ectotympanic volume approximates

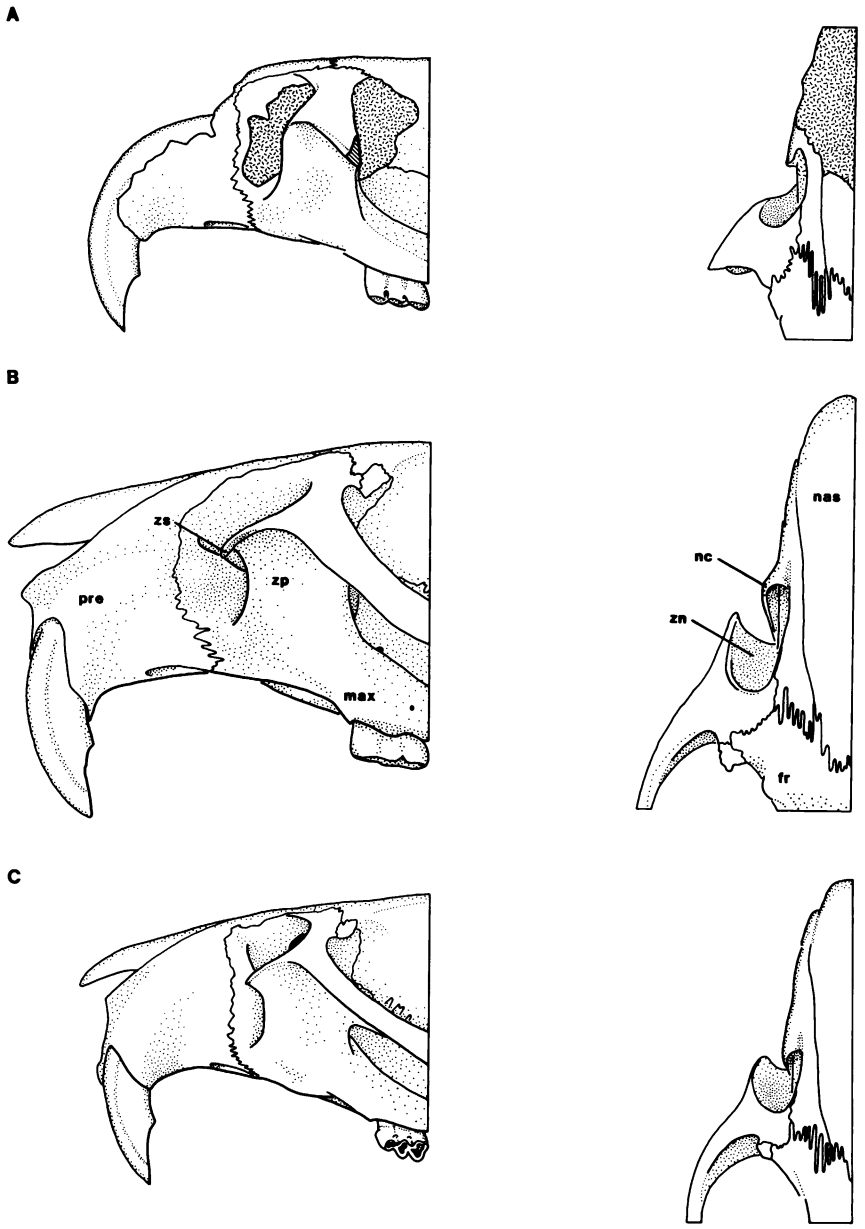

Fig. 11. Architecture of the anterior zygomatic region (left, lateral view, and right, dorsal view) in adult representatives of **A**, *Noronhomys vespuccii* (USNM 490265); **B**, *Lundomys molitor* (AMNH 206368); and **C**, *Holochilus sciureus* (USNM 394724). Abbreviations are **fr**, frontal; **max**, maxillary; **nc**, nasolacrimal capsule; **nas**, nasal; **pre**, premaxillary; **zn**, zygomatic notch; **zp**, zygomatic plate; and **zs**, zygomatic spine.

certain *Oryzomys* sensu stricto, such as *O. palustris* and *O. subflavus*.

The apparently unequal size of the postglenoid foramen and subsquamosal fenestra and the short thick hamular process in *Noronhomys* recall the condition in *Holochilus*. In *Lundomys*, equally large temporal openings perforate the lateral wall of the braincase and define a thin, elongate hamular process (Voss and Carleton, 1993: fig. 4). The

damaged or partially concealed condition of the temporal region in the available fossil sample advises some caution in accepting these contrasts as typical of *Noronhomys*. In like manner, the slight dislocation of the bullae and their retention in so few specimens obscure the configuration of the tegmen tympani. The unmodified posteroventral edge of the squamosal nonetheless intimates that overlap and fitted contact are absent in *Noronhomys*, as has been described for other oryzomyines including *Holochilus* and *Lundomys* (Voss, 1993; Voss and Carleton, 1993).

Several fossil specimens with undamaged otic capsules have a pinhole-sized stapedial foramen that pierces the petrotympanic fissure. The reduced size of the stapedial foramen, together with the lack of a sphenofrontal foramen and squamosal–alisphenoid vascular groove and occlusion of the posterior opening to the alisphenoid canal, suggest that the orbitofacial circulation of *Noronhomys* originates mainly from the internal carotid instead of the stapedial artery (Bugge, 1970; Carleton, 1980; Voss, 1988; Carleton and Musser, 1989). Such a tiny stapedial aperture occurs irregularly in individuals of *Holochilus* and *Lundomys*, genera that also have derived cephalic circulatory patterns (Voss and Carleton, 1993).

POSTCRANIAL SKELETON: Comparisons here emphasize aspects of the pelvic girdle, both because hind-limb bones were more frequently recovered as nearly intact or whole elements and because their morphology significantly relates to locomotory adaptations considered below. Although *Noronhomys* is contrasted with only *H. brasiliensis* in the illustrations (the two average nearly the same in femoral length), the differences noted are more exaggerated in the larger-bodied *Lundomys* and are generally less conspicuous in the smaller-bodied *H. sciureus*.

The pelvis of *Noronhomys* is heavily constructed with a broad neck between the acetabulum and iliac blade. The greater circumference of its acetabulum (fig. 12, top), relative to those of *Holochilus* and *Lundomys*, is immediately obvious and predictably conforms to the wider diameter of the articular head of the femur (table 3). In *Noronhomys*, the femoral tubercle, a rugosity near the anterior lip of the acetabulum that provides origin for the rectus femoris muscle, is a small irregular mound; in both *Holochilus* and *Lundomys*, the tubercle forms a well-defined, conical eminence positioned farther craniad from the acetabulum (fig. 12, bottom). The lateral ridge in *Noronhomys* is gently rounded, the superior gluteal fossa broad and flat; the inferior gluteal fossa appears much smaller in area and faces more ventrad. In contrast, the innominates of *Holochilus* and *Lundomys* possess a more acute lateral ridge that scallops the lateral surface of the ilium, clearly demarcating the superior and inferior gluteal fossae; the inferior gluteal fossa is oriented more ventrolaterally, and its area is only slightly smaller than that of the superior fossa (fig. 12, bottom). The iliac crest in *Holochilus* and *Lundomys* also bends more conspicuously laterad and accentuates the curvature of the iliac blade.

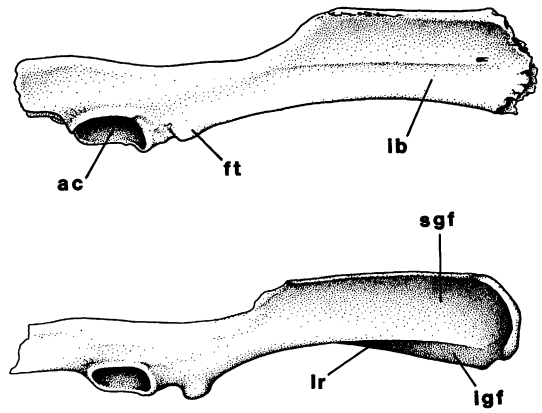

Fig. 12. Dorsolateral views of anterior portion of the right innominate of **top**, *Noronhomys vespuccii* (USNM 490302) and **(bottom)**, *Holochilus brasiliensis* (AMNH 206383). Note the wider diameter of the acetabulum of *Noronhomys* and conspicuous projection of the femoral tubercle in *Holochilus*. Abbreviations are **ac**, acetabulum; **ft**, femoral tubercle; **ib**, blade of ilium; **igf**, inferior gluteal fossa; **lr**, lateral ridge; and **sgf**, superior gluteal fossa.

In general aspect, the long limb bones of *Noronhomys* are robust compared with the appendicular skeletons of *Holochilus* and *Lundomys*. This contrast is best conveyed by dimensions of the femur, the most abundant long bone recovered as intact fossils. Measurements of the head, neck, and shaft of the

TABLE 3

Selected Femoral Dimensions (in mm)of *Noronhomys vespuccii, Lundomys molitor, Holochilus brasiliensis,* and *H. sciureus*

Species (and OTU[a])	N	Mean	Range	SD
Length of Femur				
N. vespuccii	9	36.5	32.5–41.0	3.23
L. molitor	6	38.8	30.3–44.5	5.44
H. brasiliensis	6	37.6	33.8–41.0	2.66
H. sciureus (OTU 4)	15	30.8	25.2–35.8	3.22
Distal Width of Shaft				
N. vespuccii	9	6.68	5.17–7.77	0.92
L. molitor	6	5.91	5.31–6.40	0.39
H. brasiliensis	6	5.71	5.22–6.19	0.34
H. sciureus (OTU 4)	15	5.01	4.10–5.92	0.57
Middle Width of Shaft				
N. vespuccii	9	4.39	3.01–5.72	1.01
L. molitor	6	4.09	3.17–4.84	0.63
H. brasiliensis	6	3.66	3.47–3.96	0.17
H. sciureus (OTU 4)	15	3.26	2.69–3.96	0.45
Depth of Shaft at Middle				
N. vespuccii	9	3.20	2.55–3.83	0.45
L. molitor	6	3.33	2.81–3.57	0.33
H. brasiliensis	6	3.15	2.82–3.32	0.20
H. sciureus (OTU 4)	15	2.70	2.23–3.17	0.28
Diameter of Head				
N. vespuccii	9	3.99	3.53–4.59	0.37
L. molitor	6	3.90	3.61–4.07	0.20
H. brasiliensis	6	3.56	3.30–3.86	0.20
H. sciureus (OTU 4)	15	3.13	2.60–3.46	0.27
Diameter of Neck				
N. vespuccii	9	2.28	1.78–2.71	0.33
L. molitor	6	1.94	1.74–2.10	0.13
H. brasiliensis	6	1.79	1.67–1.87	0.07
H. sciureus (OTU 4)	15	1.57	1.33–1.85	0.17
Condylar Breadth				
N. vespuccii	9	7.02	6.30–7.75	0.54
L. molitor	6	7.70	7.11–8.14	0.37
H. brasiliensis	6	6.71	6.34–7.12	0.26
H. sciureus (OTU 4)	15	5.81	5.35–6.22	0.30
Condylar Depth				
N. vespuccii	9	7.75	6.92–8.49	0.59
L. molitor	6	8.95	7.90–9.50	0.59
H. brasiliensis	6	8.54	8.18–8.89	0.24
H. sciureus (OTU 4)	15	6.94	6.10–7.80	0.49
Length of Patellar Fossa				
N. vespuccii	9	6.15	5.44–6.68	0.45
L. molitor	6	7.30	6.01–8.17	0.76
H. brasiliensis	6	7.05	6.71–7.55	0.29
H. sciureus (OTU 4)	15	5.80	5.08–6.51	0.46
Width of Patellar Fossa				
N. vespuccii	9	2.99	2.35–3.50	0.42
L. molitor	6	2.96	2.68–3.22	0.20
H. brasiliensis	6	2.72	2.52–2.91	0.13
H. sciureus (OTU 4)	15	2.30	2.05–2.58	0.19

[a] OTU 4 represents specimens from Bolivia.

femur of *Noronhomys* typically exceed even those of *H. brasiliensis* or *L. molitor* (table 3), species that are considerably larger based on average femur length and craniodental size (table 1). The patellar fossa (or trochlea), the trough in which the patella slides, is shallow, short, and wide in *Noronhomys* but deeper, longer, and relatively narrow in *Holochilus* and *Lundomys* (fig. 13). The greater and lesser trochanters are developed similarly in all three genera; however, the lateral femoral crest (third trochanter) of *Noronhomys* is scored by a shallow flute along its free edge, a feature not observed in *Holochilus* or *Lundomys*. The distal articular condyles are less rounded in *Noronhomys*, the breadth across their lateralmost edges being about equal to their anterior–posterior depth; the condyles of *Holochilus* and *Lundomys* are more bulbous and pulleylike in contour, their depth greater than the greatest width and the intercondyloid notch correspondingly deeper. The shape discrimination offered by these and other univariate differences are more readily appreciated in the multivariate analyses reported in the following section.

In *Noronhomys*, the tibial crest forms a low, curved ridge that approximately bisects the anterior face of the upper tibia; the lateral tibial fossa is nearly flat and fully exposed in frontal view; and the crest is marked by a raised scar (insertion of the semitendinosus?) at its distal end where it merges with the shaft (fig. 14A). In *Holochilus* and *Lundomys*, the tibial crest is straighter and displaced laterally, its anteromedial surface thus broad and smoothly convex; the lateral fossa is deeply concave and hence largely obscured in frontal view (fig. 14B); and no rugosity marks the distal end of the anterior crest. The medial and lateral ridges of *No-*

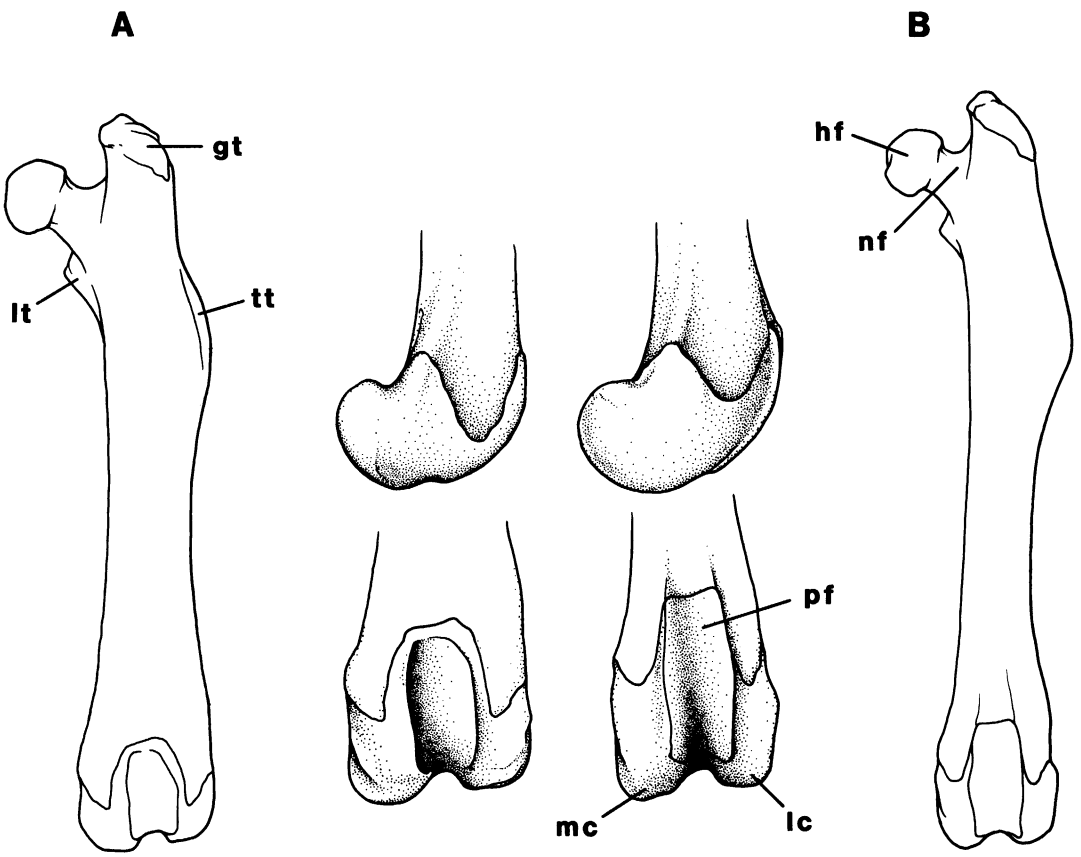

Fig. 13. Full frontal comparisons of the left femur of **A**, *Noronhomys vespuccii* (USNM 490300, femoral length = 37.4 mm) and **B**, *Holochilus brasiliensis* (AMNH 206362, femoral length = 38.4 mm). Middle views portray medial (top) and frontal (bottom) enlargements of the distal articular condyles of *N. vespuccii* (left pair) and *H. brasiliensis* (right pair). Note the greater circumference of the medial articular condyle and longer patellar fossa that characterize *H. brasiliensis* as well as *Lundomys molitor*. Abbreviations are **gt**, greater trochanter; **hf**, head of femur; **lc**, lateral condyle; **lt**, lesser trochanter; **mc**, medial condyle; **nf**, neck of femur; **pf**, patellar fossa; and **tt**, third trochanter.

ronhomys are short and low, defining a shallow posterior tibial fossa; in contrast, the posterior ridges of *Holochilus* and *Lundomys* are longer and project above the rear tibial surface, enfolding a cavernous caudal fossa (fig. 14C). The proximal articular facets appear more convex on the tibiae of *Holochilus* and *Lundomys*, especially as observed in the posterior overhang of the lateral tuberosity.

DENTITION: Voss and Carleton (1993: fig. 12) drew attention to the beveled edge and angular surface that mark the enamel face of the upper incisors in species of *Holochilus*. This faceted condition is more distinct in *H. sciureus* than in *H. brasiliensis* or *Noronhomys*. Moreover, the lower incisors in *H. sciureus* exhibit complementary development of an enamel facet and possess a wide, flattened lateral edge set off from a narrower medial bevel. Examples of *H. brasiliensis* and *Noronhomys* possess evenly curved enamel bands on the lower incisors, in contrast to the angularization that characterizes those of *H. sciureus*. Description of this subtle enamel variation and delineation of character states would profit from careful scanning electron microscopy and histological examination.

The cuspidate molars of *Lundomys* differ strikingly from those of *Noronhomys*, in basically the same ways as it does from *Holochilus* (Voss and Carleton, 1993: 19–20).

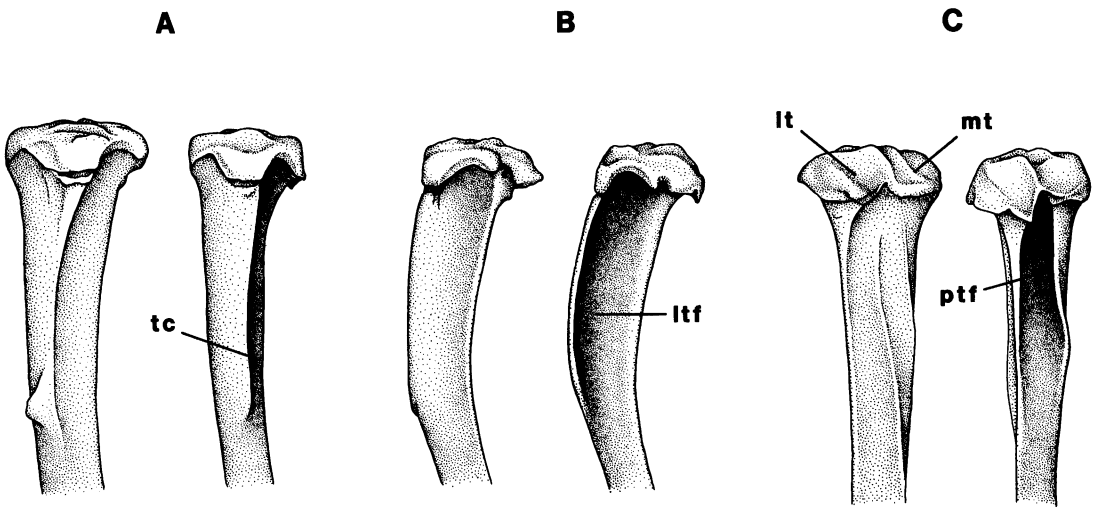

Fig. 14. Frontal (**A**), lateral (**B**), and caudal (**C**) views of the proximal half of the left tibia of *Noronhomys vespuccii* (USNM 490301, left member in each pair) and *Holochilus brasiliensis* (AMNH 206362, right member). Note the pronounced excavation of the lateral and posterior tibial fossae in *H. brasiliensis* and the presence of the rugosity on the tibial crest of *N. vespuccii*. Abbreviations are **lt**, lateral tuberosity; **ltf**, lateral tibial fossa; **mt**, medial tuberosity; **ptf**, posterior tibial fossa; and **tc**, tibial crest.

The moderately hypsodont, planar molars of *Noronhomys* and *Holochilus* are generally similar but contrast subtly in formation of certain enamel folds and their corresponding ridges. All preserved M1 and M2s of *Noronhomys* have truncated but well-formed mesolophs that contribute to the planar occlusal surface (fig. 8). The short mesolophs, in lateralmost projection like those found in *Lundomys*, are consistently defined, unlike the

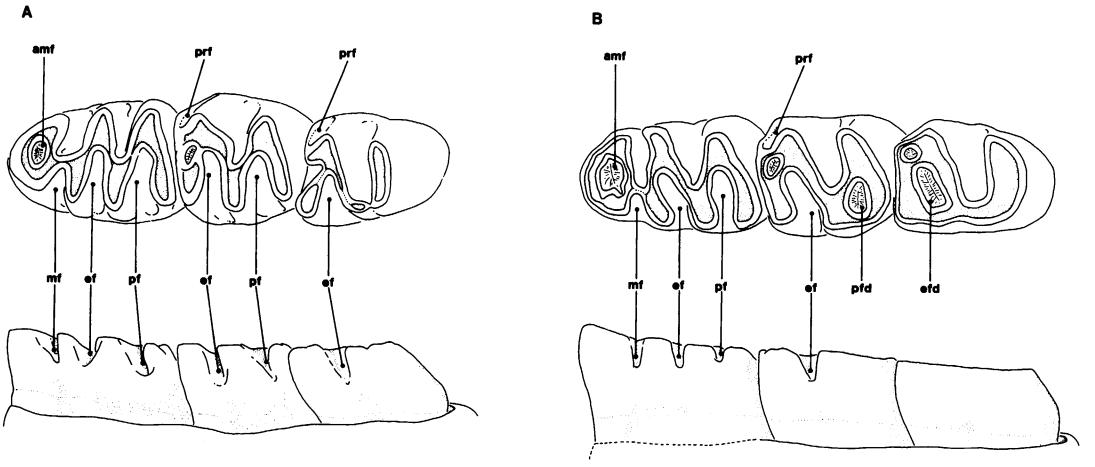

Fig. 15. Dorsal (occlusal) and medial (lingual) views of the lower right toothrow of **A**, *Holochilus sciureus* (USNM 390249) and **B**, *Noronhomys vespuccii* (USNM 490287). Abbreviations are **amf**, anteromedian fossettid; **ef**, entoflexid; **efd**, entofossettid; **mf**, metaflexid; **pf**, posteroflexid; **pfd**, posterofossettid; and **prf**, protoflexid. Note the isolation of certain medial folds as enamel islands (fossettids) on the second and third molars of *Noronhomys* as compared with *Holochilus*, as well as the lack of an anterolabial cingulum and protoflexid on the third molar of *Noronhomys*.

occasional spur that arises from the central mure of some *H. brasiliensis*. Moreover, in such instances in the latter species, the tip of the mesoloph recedes into the metaflexus and does not form part of the triturative surface as in *Noronhomys*. Upper first and second molars of *H. sciureus* uniformly lack a mesoloph. In both species of *Holochilus*, a remnant of the posteroflexus persists as an enamel island (posterofossetus) at the posterior rim of the M1 and M2s until moderately worn. This fold and the adjoining posteroloph are not evident on any molars of *Noronhomys*, apparently being wholly lost or undefinably incorporated into the laminated union of the hypocone and metacone across the rear of the tooth.

Lingual and labial folds of the lower molars of *Holochilus* broadly coalesce with the basal margins of the crown. On the lowers of *Noronhomys*, the posteroflexid of m2 and entoflexid of m3 are sequestered as enamel pits (fig. 15). Accordingly, the medial borders of the m2 and m3 are not dissected by emergent valleys corresponding to those visible on molars of *Holochilus*. Incipient isolation of the m1 posteroflexus in *Noronhomys* is also suggested by its relatively shallow indentation along the medial wall. These contrasts hold even on the youngest, least abraded specimens of *Noronhomys* in our sample, which compare favorably in wear stage to young adult *Holochilus*. The dissimilarity in closure of the lingual folds may relate to the greater coronal hypsodonty seemingly characteristic of *Noronhomys*, an impression that we cannot easily quantify, however. The m3 of *Noronhomys* lacks a cingulum and enamel crease (protoflexid) on its anterolabial corner (fig. 15); however, both features are typically present on m3s of *Holochilus* and *Lundomys*, although small and weakly defined on some individuals.

Examples of *Noronhomys* possess stout labial roots on the upper and lower first molars, like those found in *Holochilus* (Voss and Carleton, 1993: fig. 13). Also like *Holochilus* and *Lundomys*, a smaller lingual root usually anchors the middle of m1 of *Noronhomys*—among 44 specimens in which the crown base is suitably exposed, a lingual root is present and well developed on 9, present but weakly to moderately defined on 25, and apparently not formed on 10.

Morphometric Analyses

The five population samples of *Holochilus* used in the numerical analyses are geographically scattered but fairly circumscribe the range of craniodental divergence in this widely distributed sigmodontine (fig. 1). Although usage of the nominal epithets *H. brasiliensis* and *H. sciureus* conforms to recent classifications of Sigmodontinae (Massoia, 1981; Musser and Carleton, 1993), we must emphasize the inadequate comprehension of specific limits among populations of *Holochilus*, in particular those now grouped under *H. sciureus*. Although insufficient to clarify the alpha taxonomy of *Holochilus*,[3] the coarse sampling design does furnish an adequate backdrop to interpret variational patterns within our sample of *N. vespuccii* and to gauge its level of differentiation from continental forms. The fossil sample, given the disassociation of skeletal parts and their usually broken condition, constrained the analytical design and scope of multivariate analyses performed. Consequently, the following morphometric comparisons with living species were computed separately for mensural data obtained from crania, mandibles, and femora.

Sample Variation and Univariate Statistics: Of the skeletal elements recovered for *Noronhomys*, only the mandibles, in view of their abundance, offer a suitable sample to assess population variation and homogeneity. Among the 15 measurements obtained from the mandible and its dentition, two subsets of highly intercorrelated variables are apparent—those representing the molars, which once erupted do not change in size, and those representing the dentary bone, which exhibits some age-related increase in size. Molar

[3] Although sample sizes are small, we draw attention to the consistent separation in our multivariate results of the sample (OTU 7) drawn from the rim of the Maracaibo Basin, Venezuela. Northernmost populations, as *H. venezuelae*, have been argued as specifically distinct from *H. sciureus* based on chromosomal data (Aguilera and Pérez-Zapata, 1989). These suggestive lines of evidence should be integrated in order to illuminate fully the taxonomic status and distributions of *Holochilus* populations in Venezuela.

TABLE 4

Matrices of Pairwise Pearson Correlation Coefficients among Dental and Mandibular Measurements of *Noronhomys vespuccii* and *Holochilus sciureus* from Bolivia (OTU 4)

	CLm	Lm1	Lm2	Lm3	AWm1	PWm1	AWm2
			Noronhomys vespuccii				
X			(N = 20–64)[a]				
Lm1	0.65***						
Lm2	0.67***	0.47***					
Lm3	0.55***	−0.06	0.19				
AWm1	0.44**	0.44**	0.31*	0.33			
PWm1	0.46**	0.29*	0.28	0.45**	0.57***		
AWm2	0.62***	0.29	0.34*	0.46**	0.38*	0.76***	
PWm2	0.62***	0.34*	0.42**	0.32	0.43**	0.71***	0.81***
Wm3	0.55***	0.06	0.24	0.72***	0.15	0.40*	0.58***
Wi	−0.43*	0.16	−0.26	−0.17	0.19	0.01	0.11
Di	−0.14	0.17	−0.11	−0.05	0.13	0.03	0.14
Hm1	0.13	−0.37*	−0.25	0.37*	−0.15	−0.03	0.19
LMC	0.02	0.12	−0.16	0.16	−0.07	0.15	−0.03
DMm1	−0.22	0.18	−0.13	−0.11	0.19	0.13	0.07
DMm3	0.02	0.22	0.05	0.02	0.25	0.27	0.23
			Holochilus sciureus				
			(N = 16)				
Lm1	0.72**						
Lm2	0.70**	0.43					
Lm3	0.65**	0.01	0.44				
AWm1	0.77***	0.52*	0.65**	0.43			
PWm1	0.72**	0.55*	0.61*	0.43	0.81***		
AWm2	0.26	0.36	0.08	0.04	0.45	0.55*	
PWm2	0.41	0.19	0.35	0.34	0.60*	0.66**	0.81***
Wm3	0.65*	0.11	0.18	0.73**	0.28	0.48	0.48
Wi	0.11	0.17	−0.15	−0.09	0.08	0.23	0.37
Di	0.01	0.09	−0.21	−0.16	−0.02	0.16	0.24
Hm1	0.02	−0.11	0.53*	0.28	0.05	0.11	−0.24
LMC	0.07	−0.29	−0.04	0.58*	−0.02	0.07	−0.26
DMm1	0.33	0.20	−0.13	0.05	0.17	0.27	0.30
DMm3	−0.27	−0.24	−0.61*	−0.20	−0.21	−0.23	0.10

[a] Due to the variable preservation of recovered dentaries, not all measurements could be recorded for all specimens.

* $P \leq 0.05$; ** $P \leq 0.01$; *** $P \leq 0.001$.

dimensions are, in general, positively and strongly correlated (table 4); correlation values of length and width measurements of an individual tooth typically surpass those recorded between different teeth. The other consistent association involves dimensions measured on the mandible (LMC, DMm1, DMm3) and lower incisor (Wi, Di), most of which also correlate positively with one another (table 4). The height of the m1, which incidentally decreases with advancing age, is inversely associated with this dentary subset, and significantly so except for length of the masseteric crest. Although correlation coefficients tend to be large and positive among variables within each subset, they are smaller, commonly negative, and usually insignificant between the two. The same two suites of intercorrelated mandibular variables also characterize the series of *H. sciureus* from Bolivia (OTU 4), although coefficients tend to be smaller than those computed for the larger sample of *Noronhomys* (table 4).

Coefficients of variation (CV) impart a similar contrast among variables recorded from the mandible and lower dentition. Values of sample variation are typically small (CV = 2.3–4.6) for all molar dimensions of

TABLE 4—(*Extended*)

PWm2	Wm3	Wi	Di	Hm1	LMC	DMm1
		Noronhomys vespuccii (extended) (N = 20–64)[a]				
0.48**						
−0.13	−0.14					
−0.08	0.08	0.91***				
0.13	0.37*	−0.45**	−0.41**			
−0.19	−0.05	0.53**	0.57***	−0.02		
−0.10	−0.07	0.89***	0.92***	−0.42**	0.53***	
0.08	0.02	0.84***	0.87***	−0.22	0.50***	0.91***
		Holochilus sciureus (extended) (N = 16)				
0.43						
0.00	0.21					
−0.15	0.18	0.95***				
0.11	−0.12	−0.70**	−0.67**			
0.02	0.10	0.07	0.08	0.16		
0.01	0.38	0.87***	0.91***	−0.75***	0.07	
−0.22	0.13	0.75**	0.79***	−0.78***	0.11	0.78***

Noronhomys (except height of m1 metaconid), whereas they are considerably larger (CV = 9.2–13.5) for those dimensions measured on the dentary and its incisor (table 5). Moreover, the magnitudes and patterns of measurement variability closely parallel that observed in population samples of *H. brasiliensis* and *H. sciureus*; these exhibit comparably small coefficients for molar size, intermediate values for incisor and mandibular dimensions, and greatest variation for the contingently age-related crown height (fig. 16).

That postweaning growth, or lack thereof, explains some of the covariation among these measurements is suggested by sample means and analyses of variance derived from qualitatively defined tooth wear classes, which roughly approximate relative age of specimens. The dentary and lower incisor of *Noronhomys* exhibit relatively large, incremental increases in mean size from young to old-adult age classes; however, mean dimensions of the molar teeth vary little and erratically with respect to age. Correspondingly, *f*-values for age-related effects are much greater and significant for the incisive and mandibular measurements (except LMC) but small and negligible for all molar dimensions (table 5). Again, metaconid height of the first lower molar (Hm1) is inversely related to age, as indexed by tooth wear class, a factor

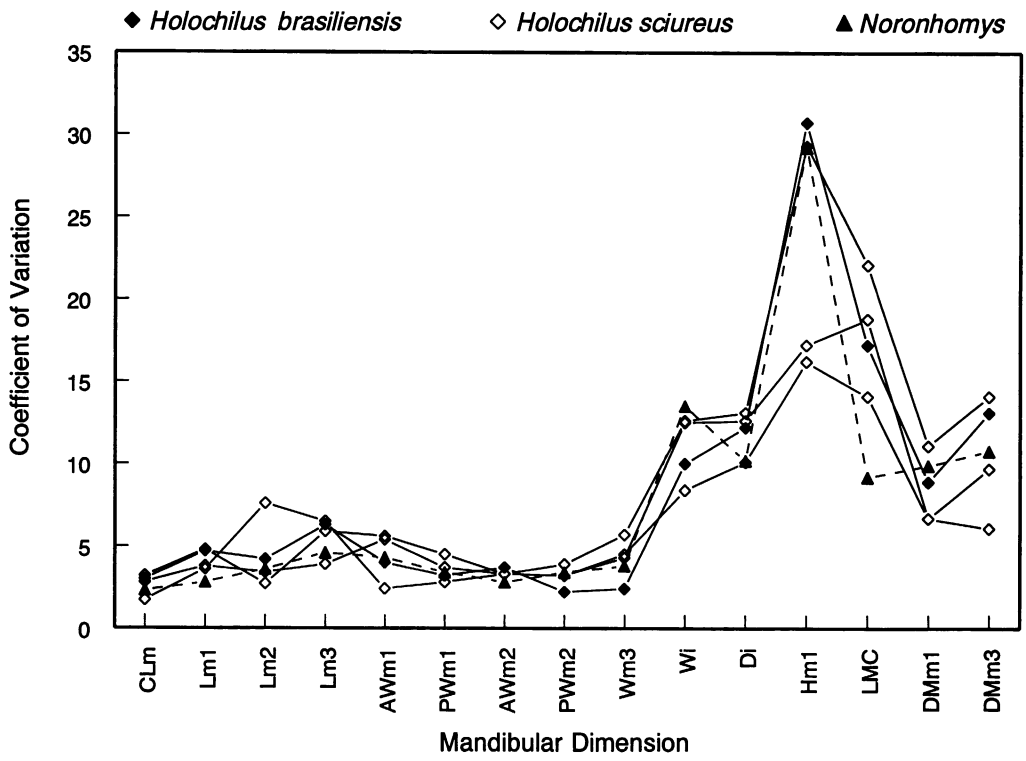

Fig. 16. Profiles of coefficients of variation (sample mean divided by sample standard deviation × 100) for dental and mandibular variables of *Noronhomys vespuccii* (N = 34–64), *Holochilus brasiliensis* (N = 12), and three samples of *H. sciureus* (OTU 4, N = 16; OTU 6, N = 12; and OTU 7, N = 14). See Materials and Methods for explanation of OTUs and variable abbreviations.

which logically accounts for most of its extensive variation.

Univariate ranges, correlation coefficients, and measures of dispersion among mandibular and lower molar dimensions of *Noronhomys* are unremarkable in comparison with those derived from population samples of extant *Holochilus*. Further, the intensity, direction, and pattern of these numerical associations conform to those reported for other muroid species, particularly in regard to age-related size increase of the mandible and incisor and to age-invariance of fully erupted molars (for example, see Carleton and Eshelman, 1979; Voss, 1988, 1991). Aside from the clearly recent admixture of commensal *Rattus rattus* and *Mus musculus*, these statistics support the specific homogeneity of the fossil sample and supply no evidence for the presence of some cryptic, morphologically similar species within our sample of *N. vespuccii*.[4]

MULTIVARIATE COMPARISONS: Results from both discriminant function and principal component analyses reveal the cranial geometry of the island form to be distinctive. The dispersion of individual specimens and distances between centroids among OTUs of

[4] Although sex cannot be determined in the fossil sample, no bimodal patterns are apparent in any of the measurements of *N. vespuccii* with sufficient sample size, nor do probablility plots or goodness-of-fit tests supply persuasive evidence for departure from a log-normal distribution for most variables. Although slight sexual dimporphism in size is demonstrable in balanced series of known-aged muroid rodents (Voss et al., 1990), such divergence is minor relative to that attributed to age and geographic effects within sigmodontine species and wholly negligible compared with taxonomic differences between them (for example, Carleton and Eshelman, 1979; Voss, 1988, 1991; Carleton and Musser, 1989, 1995).

TABLE 5

Mean Values of Dental and Mandibular Variables for Age Cohorts of *Noronhomys*

(Given are the mean values by age class, coefficients of variation [CV], and *f* values from one-way ANOVAs for age effects. Age classes are Y, young adult [N = 3–6]; A, full adult [N = 19–33]; and O, old adult [N = 14–25].)

Variable	Age class			CV	ANOVAs *f* (Age)
	Y	A	O		
CLm	7.96	8.06	7.93	2.3	2.9
Lm1	3.08	3.15	3.15	2.8	1.1
Lm2	2.24	2.27	2.27	3.6	0.2
Lm3	2.55	2.54	2.45	4.6	3.1
AWm1	1.51	1.54	1.51	4.3	1.3
PWm1	1.91	1.95	1.91	3.4	1.5
AWm2	2.01	2.01	1.99	2.8	0.7
PWm2	2.04	2.08	2.03	3.4	2.1
Wm3	1.86	1.91	1.86	3.8	1.6
Wi	1.10	1.30	1.39	13.5	5.9**
Di	1.76	2.00	2.12	10.2	6.9**
Hm1	1.18	0.91	0.60	29.2	48.8***
LMC	3.58	3.91	3.85	9.2	1.9
DMm1	6.52	7.56	8.02	9.9	7.4**
DMm3	4.36	4.92	4.92	10.8	3.3*

* $P \leq 0.05$; ** $P \leq 0.01$; *** $P \leq 0.001$.

Lundomys and *Holochilus* are consistent with our current understanding of their generic and specific classification (fig. 17). The skull of the holotype of *N. vespuccii* stands apart from the samples of both *Lundomys* and *Holochilus*. The extremal position of *Noronhomys* on canonical variate II reflects certain breadth measurements (IOB, BM1s, PPB) and the long basicranium (PPL) and toothrow (CLM) relative to size of skull (fig. 17A; table 1). On canonical variate III, the relatively short zygomatic plate (BZP), small ectotympanic bulla (DAB), and narrower molars (WM1) similarly influence the high score of *Noronhomys* on this factor.

Based upon log-transformed means of OTUs, the first two principal components extracted summarize most intersample variation (93.4%). The large, positive correlations of most dimensions with the first component implicate general size as a primary explanation for the array of OTU scores (table 6). Along this component, the type specimen of *N. vespuccii* compares favorably with a large example of *H. sciureus*, a numerical finding which corroborates one's visual impression when laying out skulls for comparison. As in the canonical variate scatter plots, proportional contrasts in three variables (DAB, IOB, PPL) largely account for the segregation of *Noronhomys* from examples of *Lundomys* and *Holochilus* on the second principal component (fig. 18; table 7).

Several of the mensural variables that contribute to the consistent morphometric separation of *Noronhomys* lend objectivity to qualitative differences noted in the anatomical comparisons. For example, the narrower constriction of the interorbit and broader zygomatic plates of *Holochilus* and *Lundomys* agree with the patterns of variable loading uncovered and their influence on the ordinal segregation of *Noronhomys*, whether seen in discriminant function or principal component analysis (figs. 17, 18). However, the large effect divulged for postpalatal length was unexpected with regard to the divergence of *Noronhomys*. The comparatively greater postpalatal length, and by extrapolation the basicranial segment this linear dimension spans, conceivably relates to the flat cranial profile characteristic of *Noronhomys* and certainly correlates inversely with the shortness of its hard palate. In summary, while we acknowledge the minimal sample size of one intact skull, the covariation patterns among the 15 craniodental variables depict the fossil form as something other than an insular variant of either *Holochilus* or *Lundomys*.

In view of the ample number of mandibles recovered for *Noronhomys*, small sample size cannot be advanced to qualify interpretation of multivariate analyses based on measurements of the dentary and lower dentition. Thirty-eight of the 64 mandibles analyzed possess complete molar rows, and 18 of those are sufficiently intact to permit measurement of all 15 variables defined for the lower jaw. Compared with the topographically complex, three-dimensional conformation of the rodent cranium, a lower discriminatory potential might be anticipated for linear variables obtained from the flat, basically two-dimensional dentary.

Nevertheless, principal component analysis of these dimensions, as extracted from the correlation matrix, still conveys the singular morphology of *Noronhomys* (fig. 19, table

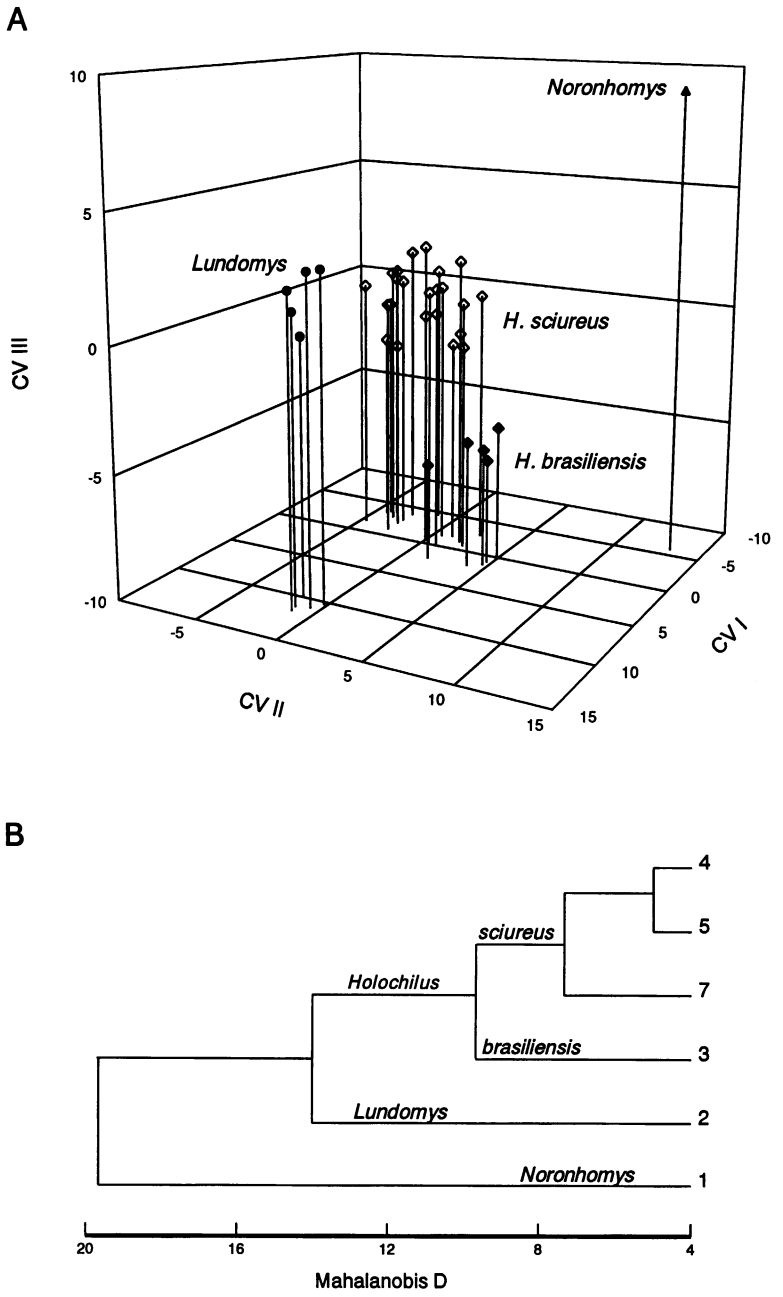

Fig. 17. Results of discriminant function analysis performed on 15 log-transformed craniodental variables as measured on 35 intact specimens representing samples of *Holochilus* (OTUs 3–5, 7), *Lundomys*, and *Noronhomys* (see table 6). **A**, Projection of specimen scores on first three canonical variates (CVs) extracted. **B**, UPGMA phenogram based on Mahalanobis distances (D) between the six OTU centroids. See Materials and Methods for explanation of OTUs.

TABLE 6

Discriminant Function Analysis and One-Way ANOVAs Based on Craniodental Variables

(Analyses performed on intact specimens [N = 35] representing six OTUs: *Holochilus* [Nos. 3–5, 7][a], *Lundomys,* and *Noronhomys*; see fig. 17.)

Variable	Correlations CV[b] I	CV II	CV III	ANOVAs *f* (OTU)
ONL	0.71	0.37	−0.11	10.4***
ZB	0.76	0.36	−0.26	16.7***
BBC	0.89	0.12	−0.17	25.9***
IOB	0.41	0.48	0.27	5.9**
LN	0.72	0.17	0.00	9.2***
BZP	0.34	0.40	−0.32	3.4*
PPL	0.60	0.54	−0.02	10.3***
BPL	0.74	0.31	−0.27	12.6***
LD	0.48	0.37	−0.23	4.5**
LIF	0.71	0.51	−0.21	6.2**
BM1s	0.71	0.51	−0.21	21.3***
PPB	0.83	0.42	0.00	44.9***
CAB	0.76	0.32	−0.43	27.8***
DLM	0.83	0.49	−0.10	60.5***
WM1	0.81	0.42	−0.29	39.1***
Canonical correlation	0.98	0.97	0.95	

[a] OTU 3 represents all *H. brasiliensis*; OTU 4 represents *H. sciureus* from Bolivia, OTU 5 those from Brazil, and OTU 7 those from Venezuela.

[b] Canonical variate.

* $P \leq 0.05$; ** $P \leq 0.01$; *** $P \leq 0.001$.

TABLE 7

Principal Component Analysis Based on Craniodental Variables

(Analysis performed on log-transformed means representing six OTUs: *Holochilus* [OTUs 3–5, and 7, as in table 6], *Lundomys,* and *Noronhomys*; see fig. 18.)

Variable	Correlations PC I	PC II
ONL	0.99	0.04
ZB	0.98	0.21
BBC	0.93	0.16
IOB	0.40	−0.84
LN	0.85	0.30
BZP	0.86	0.25
PPL	0.80	−0.59
BPL	0.96	0.27
LD	0.92	0.01
LIF	0.90	0.32
BM1s	0.93	−0.31
PPB	0.89	−0.38
DAB	0.82	0.52
CLM	0.98	−0.15
WM1	0.99	−0.06
Eigenvalue	0.12	0.02
Percent variance	79.1	14.3

8). Most variables, but especially molar lengths and widths, contribute strongly to variance of the first principal component, an association that is consistent with the separation of the two largest species, *L. molitor* and *H. brasiliensis*, from all others on this axis. No discrimination among taxa is apparent along the second component, which atypically emerged as an age factor as indicated by the large positive coefficient for crown height of m1 and by the strong negative correlations disclosed for incisor girth and mandibular depth (table 8). The third factor extracted suggests the distinctiveness of examples of *Noronhomys* from those of *Holochilus* and *Lundomys*, an isolation influenced by certain molar dimensions, the narrow width of the incisor, and the long masseteric crest. The somewhat disharmonious combination of these variable covariations portrays *Noronhomys* as a rodent having a robust mandible, a long toothrow consisting of relatively narrow molars, and decidedly thin yet deep incisors. This shape syndrome contrasts with that observed in members of *Holochilus*, which also possess a robust dentary and long toothrow but have wider molars and notably broader lower incisors (see table 2 for mensural comparisons).

We necessarily limited morphometric analyses of the hind limb to the femur because of its greater occurrence as an intact bone within *Noronhomys* material. Discriminant function analysis, using log-transformed values of the 13 femoral measurements, consistently isolated *Noronhomys* from the three living taxa on the second canonical variate extracted (fig. 20). Dimensions that influence the *Noronhomys* separation include those that reflect the greater girth of its femoral shaft (MW, DW), its stout neck and articular ball (DH, DN), and the area of the patellar fossa (LPF, WPF). All hind-limb variables are significantly and positively associated with the first canonical variate (table 9), which predictably sorts the specimens from smallest (*H. sciureus*) to largest (*Lundomys*); on this

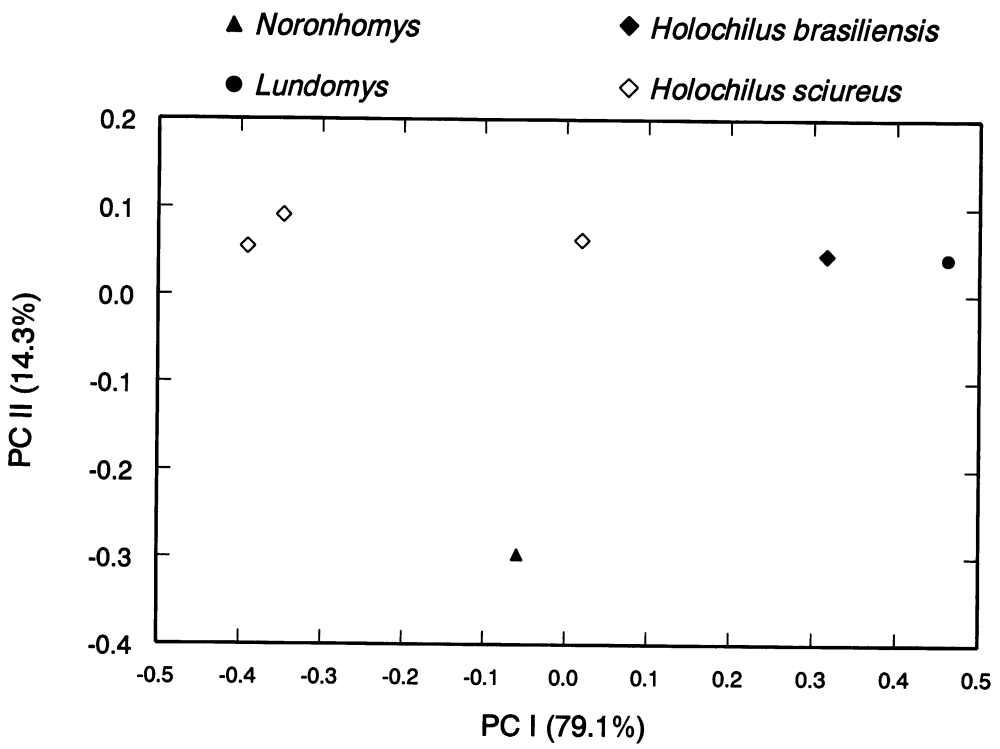

Fig. 18. Projection of sample scores on first two principal components (PCs) extracted from analysis of log-transformed means of 15 craniodental variables representing six OTUs of *Holochilus* (OTUs 3–5, 7), *Lundomys*, and *Noronhomys* (see table 7).

axis, examples of *Noronhomys* are inseparable from those of *H. brasiliensis*. These results underscore the long, slim appearance of the femora possessed by *Holochilus* and *Lundomys* relative to the stocky conformation characteristic of *Noronhomys* (fig. 13).

In order to better grasp shape differences with respect to age influences and possible allometric effects, ordination of the femoral data was repeated for the three largest species (omitting *H. sciureus*), and individual scores were plotted against actual femur length (excluding FL from principal components analysis). Variable coefficients for the first principal component extracted from the covariance matrix again reveal the large positive correlation of this axis of variation with most measurements. For a long limb bone like the femur, much of its variation in greatest length plausibly represents growth-related age differences, expressed as simultaneous increases in the girth of its shaft, the size of its articular condyles, and the size of processes for muscle attachment (table 10). Taxonomic separation is more clearly evident in the dispersion of scores along the second component, which instead suggests certain proportional contrasts in development of the distal articular condyles and associated patellar fossa and in thickness of the neck (fig. 21).

PHYLETIC INFERENCES

In assessing the phylogenetic relationships of *Noronhomys*, we a priori accept the monophyly of the tribe Oryzomyini (Muridae: Sigmodontinae) and its generic contents as recently argued by Voss and Carleton (1993). This hypothesis has been generally borne out by subsequent cladistic studies surveying more sigmodontine taxa and additional morphological characters (Steppan, 1995) and by studies based on other kinds of data, such as karyology (Baker et al., 1983, as reanalyzed by Voss and Carleton, 1993) and DNA se-

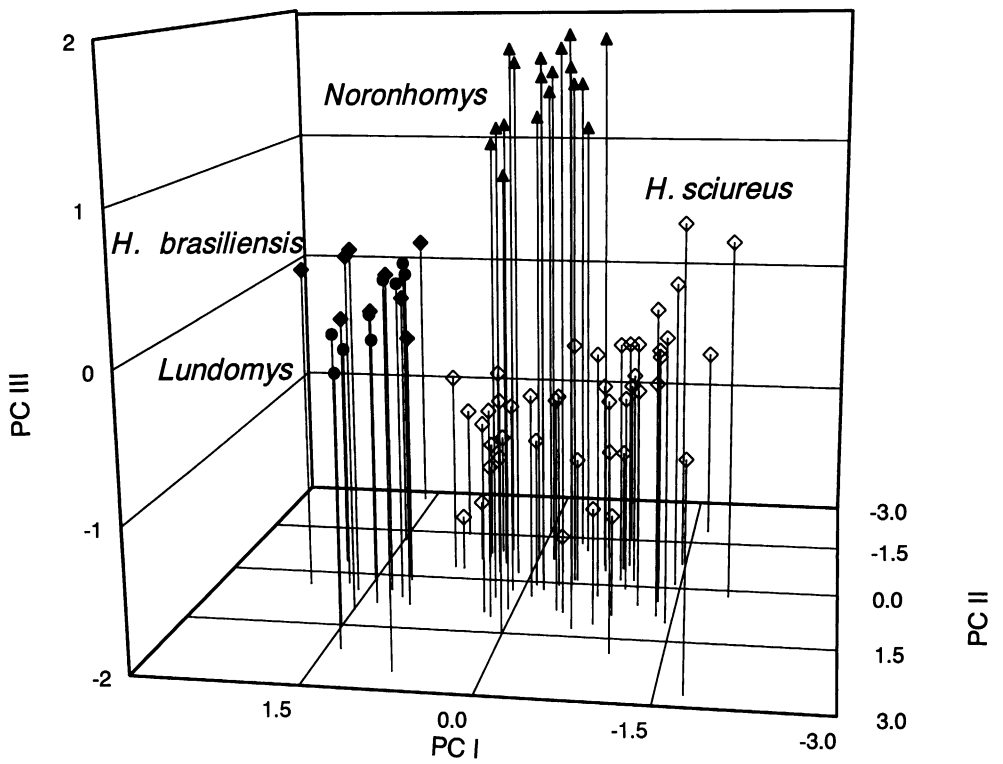

Fig. 19. Projection of individual scores on first three principal components (PCs) extracted from analysis of 15 log-transformed mandibular variables as measured on 80 intact specimens representing *Holochilus* (OTUs 3–7), *Lundomys*, and *Noronhomys* (see table 8). See Materials and Methods for explanation of OTUs.

quencing (Myers et al., 1995; Patton and da Silva, 1995). These tribal limits thus exclude the short palate, pentalophodont thomasomyines, contra Reig (1980), but accord closely with the narrower definition of oryzomyines as first outlined by Thomas (1906, 1917) and reiterated by Hershkovitz (1944, 1960) and Carleton and Musser (1989). However, membership of Oryzomyini sensu stricto does embrace certain tetralophodont genera (namely *Holochilus*, *Pseudoryzomys*, and *Zygodontomys*) that were formerly allocated to other tribes. Voss (1991), Voss and Carleton (1993), and Steppan (1995) review the taxonomic history of the Oryzomyini and discuss the morphological evidence for these generic reassociations.

Diagnosis of *Noronhomys* necessarily required comparisons with *Holochilus* and *Lundomys*, but other oryzomyine genera were examined to provide a broader phylogenetic context. Prior studies have implicated a close kinship among *Holochilus*, *Pseudoryzomys*, and *Zygodontomys* (Voss, 1991; Voss and Carleton, 1993; Steppan, 1995), genera that also need to be considered in illuminating the relationships of *Noronhomys*. In addition, we included *Oryzomys palustris*, the type species of the genus, *O. subflavus*, a South American relative of *O. palustris*, and *Microryzomys*, a genus which is endemic to Andean wet montane forests and which possesses many plesiomorphic traits within the Oryzomyini (Carleton and Musser, 1989).

Character Definitions

In total, 40 ordered characters, most restricted to cranial and dental features for comparability with available material of the extinct *Noronhomys*, are described below for nine species of Oryzomyini and a hypothetical sigmodontine ancestor (table 11). Char-

TABLE 8

Principal Component Analysis Based on Mandibular Variables

(Analysis performed on intact specimens of *H. brasiliensis* [N = 9], *H. sciureus* [N = 44], *Lundomys* [N = 9], and *Noronhomys* [N = 18]; see fig. 19.)

Variable	Correlations		
	PC I	PC II	PC III
CLm	0.88	0.19	0.36
Lm1	0.84	0.15	0.31
Lm2	0.80	0.23	0.26
Lm3	0.81	0.29	0.09
AWm1	0.86	0.18	−0.13
PWm1	0.89	0.21	−0.21
AWm2	0.82	0.09	−0.49
PWm2	0.91	0.09	−0.08
Wm3	0.78	0.10	−0.49
Wi	0.51	−0.53	−0.58
Di	0.57	−0.68	0.31
Hm1	0.34	0.76	0.05
LMC	0.40	−0.18	0.71
DMm1	0.56	−0.73	−0.16
DMm3	0.70	−0.60	0.27
Eigenvalue	8.1	2.5	1.9
Percent variance	54.0	17.0	12.4

acter definitions and rationale for the polarities adopted draw upon a now substantive body of phylogenetic investigations on neotropical muroid rodents—for example, Hershkovitz (1962), Carleton (1980), Voss (1988, 1991, 1993), Carleton and Musser (1989), Braun (1993), and Steppan (1995). In their study of *Lundomys* and *Holochilus*, Voss and Carleton (1993) elaborated upon and figured many of the characters listed below, so their polarity arguments are not repeated here. Remarks are given where our character-state treatment contradicts or clarifies aspects of the ongoing dialogue about muroid character analysis. The alphabetic order of states within most characters represents the hypothesized linear sequence of primitive to derived changes; the ancestral state of several characters is acknowledged as unknown and the condition of the five external variables (36–40) for *Noronhomys* as missing.

Character 1. Development of zygomatic plate and notch:

(a) plate narrow, notch indistinct;

(b) plate broader with moderately deep notch, anterodorsal margin smoothly rounded, without a sharp corner or spinous process;

(c) plate broad and notch conspicuous, anterodorsal margin produced as a sharp corner or spinous process.

Character 2. Posterior margin of zygomatic plate:

(a) situated noticeably anterior to the alveolus of M1, as observed in ventral view;

(b) approximately even with the alveolus of M1.

Remarks: Among the oryzomyines included, a more rostral placement of the zygomatic plate, as judged by the position of its rear edge relative to the molar row, is the usual condition (table 11). Steppan (1995) provisionally interpreted the relatively forward orientation as plesiomorphic in view of its slightly broader occurrence among his outgroup taxa; on the other hand, some paleontologists (for example, Lavocat, 1973) have considered the posterior disposition of the zygomatic plate in certain Miocene cricetids as ancestral to later forms that have the zygomatic plate produced forward. The state of this character in the hypothetical outgroup is recorded as unknown.

Character 3. Size of jugal:

(a) small but consistently formed, zygomatic processes of maxillary and squamosal never in contact;

(b) tiny and irregularly formed, zygomatic processes of maxillary and squamosal typically in contact.

Character 4. Interorbital shape and supraorbital ridging:

(a) hourglass shaped over midsection (amphoral), supraorbital edges rounded in cross section, temporal ridging absent even in oldest adults;

(b) hourglass shaped over midsection, supraorbital edges squared, temporal ridging weakly pronounced except in old adults;

(c) hourglass shaped over midsection, supraorbital edges squared, slight shelf at postorbital margins with dorsally projecting bead, temporal ridging strongly expressed except in young animals;

(d) strongly convergent at midsection (cuneate), supraorbital ledges pronounced with dorsolaterally projecting ridge, temporal

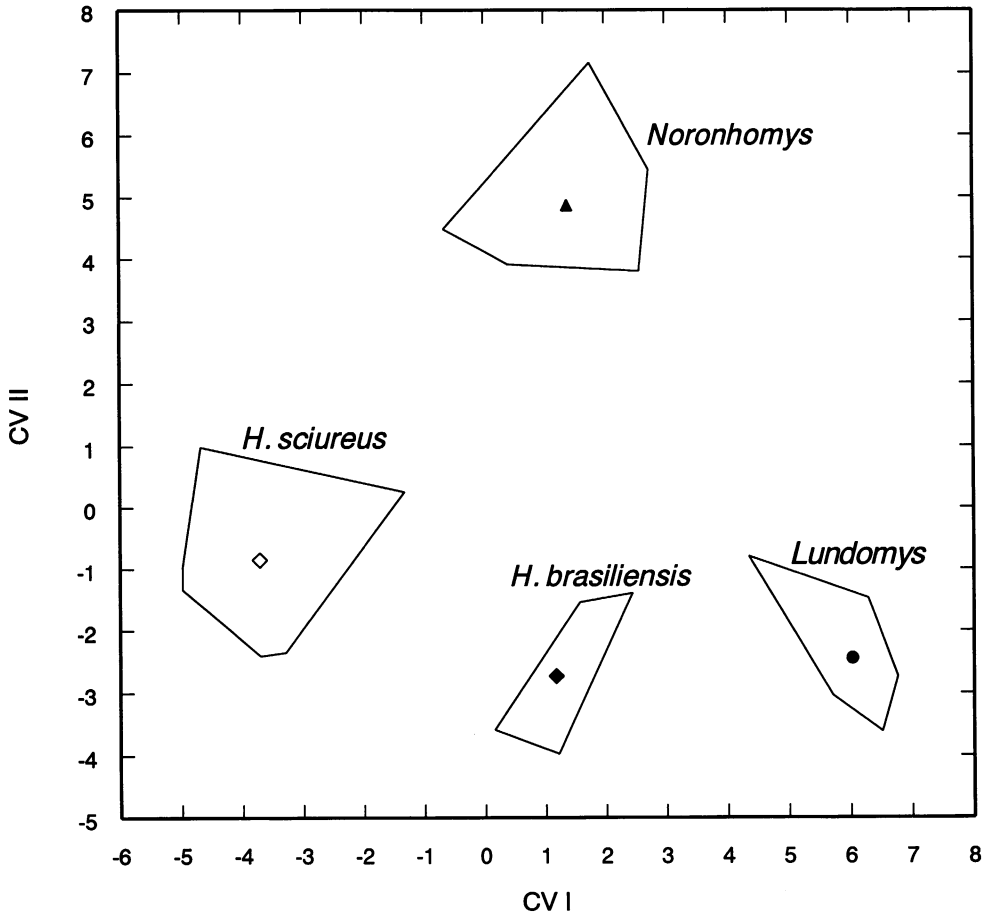

Fig. 20. Plot of first two canonical variates (CVs) extracted from discriminant function analysis performed on 13 log-transformed femoral variables as measured on 36 specimens representing *Holochilus brasiliensis*, *H. sciureus* (OTU 4, specimens from Bolivia), *Lundomys*, and *Noronhomys* (see table 9). Polygons enclose maximal dispersion of individual specimen scores around a group's centroid.

ridging strongly expressed except in young animals (derived from state b).

Remarks: Throughout the superfamily, the interorbital region of the muroid skull exhibits various and complex modifications that have spawned their own special terminology and comparative context. The shape of the interorbit (amphoral, cuneate) and the elaboration of its dorsal rim (ledges, shelves, ridges, beads) figured prominently in the early alpha-level taxonomy of muroids and logically acquired significance as cladistic characters in estimates of higher-level systematic relationships. In recent attempts at phylogenetic reconstruction, some investigators have represented this variation as a single complex character (Carleton, 1980), whereas others have separately emphasized features of interorbital shape from those of supraorbital ornamentation (Braun, 1993; Steppan, 1995). The two aspects of interorbital configuration, as well as their relation to temporal ridging, are so strongly interrelated that the former treatment is adopted here: modifications of the supraorbital rim (states c and d) are coded as independently derived from state b. For the cladograms produced, the different coding approaches are inconsequential with regard to tree length or structure.

Character 5. Postorbital ridge:

(a) absent, posterior orbital wall without conspicuous relief;

TABLE 9

Discriminant Function Analysis and One-Way ANOVAs Based on Femoral Variables

(Analysis performed on 13 log-transformed measurements for all intact specimens [N = 36] of *H. brasiliensis, H. sciureus* [OTU 4], *Lundomys,* and *Noronhomys*; see fig. 20.)

Variable	Correlations		ANOVAs
	CV[a] I	CV II	*f* (OTU)
FL	0.68	0.06	10.4***
DW	0.56	0.51	13.4***
MW	0.53	0.37	6.9**
DF	0.64	0.12	7.5**
DH	0.74	0.40	20.7***
DN	0.59	0.61	23.4***
ITD	0.77	0.37	24.6***
BTT	0.39	0.12	2.0
LTT	0.69	0.09	9.3***
CB	0.91	0.14	42.4***
CD	0.82	−0.20	27.1***
LPF	0.71	−0.33	16.4***
WPF	0.73	0.34	17.0***
Canonical Correlation	0.97	0.95	

[a] Canonical variate.

* $P \leq 0.05$; ** $P \leq 0.01$; *** $P \leq 0.001$.

TABLE 10

Principal Component Analysis Based on Femoral Variables

(Analysis performed on 12 log-transformed measurements [excluding length] for intact specimens of *H. brasiliensis* [N = 6], *Lundomys* [N = 6], and *Noronhomys* [N = 9]; see fig. 21.)

Variable	Correlations	
	PC I	PC II
DW	0.87	−0.40
MW	0.97	−0.13
DF	0.87	0.34
DH	0.82	−0.27
DN	0.76	−0.63
ITD	0.89	−0.13
BTT	0.95	0.15
LTT	0.83	0.41
CB	0.77	0.30
CD	0.47	0.82
LPF	0.44	0.86
WPF	0.92	−0.05
Eigenvalue	0.14	0.03
Percent variance	73.8	16.3

(b) present, concealing frontal–squamosal suture in adult specimens.

Character 6. Breadth of interparietal:

(a) broad, strap shaped, nearly as wide as caudal border of parietals;

(b) narrow, wedge shaped, about half as wide as caudal border of parietals.

Character 7. Extent of incisive foramina:

(a) short, not extending posteriorly to or between molar alveoli except in juvenile specimens;

(b) long, extending to or between molar alveoli in all or most adult specimens.

Remarks: The ancestral state was treated as unknown in the hypothetical ancestor.

Character 8. Configuration of palatal bridge:

(a) relatively broad and flat;

(b) narrower and moderately corrugated;

(c) narrower anteriorly, deeply furrowed with median ridge and occasionally with palatal excrescences formed at posterior end.

Character 9. Posterior extent of bony palate:

(a) terminates noticeably short of posterior margin of M3s;

(b) extends even with or slightly behind M3s;

(c) extends conspicuously beyond M3s.

Remarks: The development of the bony palate, particularly its production caudad beyond the molar rows, is a trait that was advanced first by Thomas (1906, 1917) to separate oryzomyine from thomasomyine rodents and that has gained importance in phylogenetic diagnosis of the tribe Oryzomyini (Voss and Carleton, 1993; Steppan, 1995). Whereas most thomasomyines do possess an unambiguously short palate (Voss, 1993), a long palate, although typical, is by no means ubiquitous within Oryzomyini. Among the taxa we consider, the bony palate terminates only slightly beyond or nearly even with the end of the third molars in examples of *Microryzomys*, *Holochilus*, and *O. subflavus*; the palate is by operational definition "short" in specimens of *Noronhomys*.

Character 10. Development of posterolateral palatal pits:

(a) usually a single nutrient foramen at posterolateral margin of bony palate;

(b) multiple foramina occurring at posterolateral margin, often recessed within oval pit;

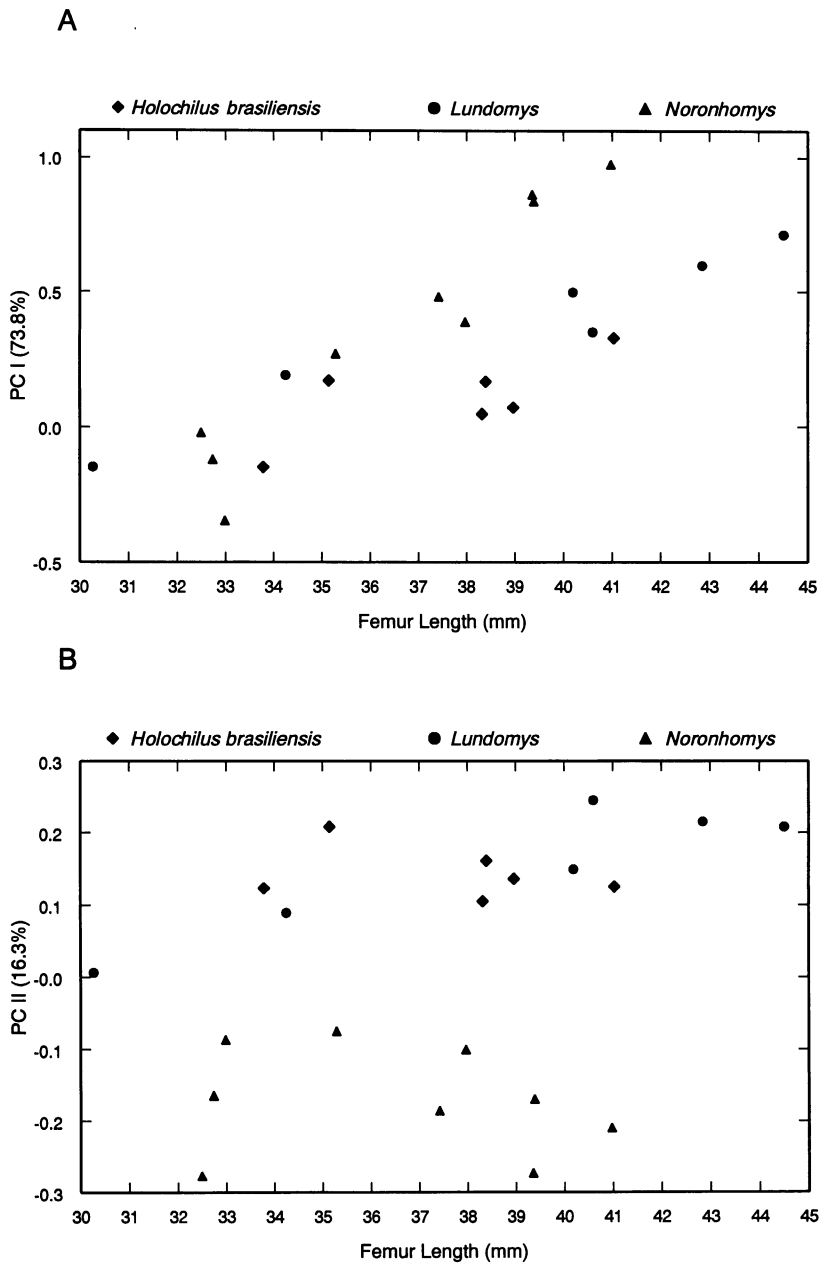

Fig. 21. Plots of femur length against the first two principal components (PCs) extracted from analysis of 12 log-transformed femoral variables (femur length excluded) measured on 19 intact specimens representing *Holochilus brasiliensis*, *Lundomys*, and *Noronhomys* (see table 10).

(c) multiple foramina present in similar position but not set within oval pit.

Remarks: Pronounced palatal pits characterize most oryzomyine species in our study. In *Noronhomys*, clearly circumscribed pits are lacking, but seemingly homologous foramina, as judged by their anatomical location, perforate the anterolateral wall of the mesopterygoid fossa; this character is conceivably associated with the unusually short

TABLE 11

Morphological Character States (See Text) for Nine Oryzomyine Species

(Taxa abbreviations: HA, hypothetical ancestor; Hb, *Holochilus brasiliensis*; Hs, *Holochilus sciureus*; Lm, *Lundomys molitor*; Mm *Microryzomys minutus*; Nv, *Noronhomys vespuccii*; Op, *Oryzomys palustris*; Os, *Oryzomys subflavus*; Ps, *Pseudoryzomys simplex*; and Zb, *Zygodontomys brevicauda.*)

Character	Character states									
	HA	Mm	Zb	Op	Os	Ps	Lm	Hb	Hs	Nv
1. Zygomatic plate	a	a	b	b	b	c	c	c	c	b
2. Position of plate	?	a	b	a	a	a	a	a	a	b
3. Size of jugal	a	b	a	a	a	a	a	b	b	b?
4. Interorbital shape	a	a	d	d	d	b	b	c	c	b
5. Postorbital ridge	a	a	a	a	a	a	a	b	b	b
6. Interparietal	a	a	a	b	b	a	a	a	a	a
7. Incisive foramina	?	a	b	b	b	b	b	a	a	a
8. Palatal bridge	a	a	a	b	b	a	c	c	c	b
9. Extent of bony palate	a	b	c	c	b	c	c	b	b	a
10. Palatal pits	a	a	b	b	b	b	b	b	b	c
11. Parapterygoid fossa	a	a	b	a	a	b	b	c	c	c?
12. Ectotympanic bullae	a	a	b	b	b	b	c	c	c	b
13. Alisphenoid strut	a	b	b	b	b	b	b	a	a	a
14. Carotid circulation	a	a	a	b	b	b	b	b	b	b
15. Masseteric ridges	a	a	a	a	a	b	a	b	b	b
16. Mandibular ramus	a	a	a	a	a	a	a	b	b	b
17. Incisor facets	a	a	a	a	a	a	a	b	c	b
18. Molar topography	a	a	b	b	b	b	b	c	c	c
19. Occlusal design	a	a	a	a	a	a	a	b	c	b
20. Procingulum M1	a	a	b	b	b	b	a	c	c	c
21. Mesoloph M1 and M2		a	a	c	a	a	b	b	c	c
22. Mesoloph M3	a	a	b	a	a	b	b	a	a	a
23. Anteroloph M1	a	a	c	a	a	c	b	c	c	c
24. Posteroloph M1 and M2		a	a	a	a	a	a	a	b	b
25. Protoflexus M2	a	a	a	a	a	a	a	b	b	b
26. Procingulum m1	a	a	b	b	b	c	c	c	c	c
27. Mesolophid m1 and m2		a	a	c	a	a	c	b	c	c
28. Posterolophid m1	a	a	a	a	a	a	a	b	b	b
29. Protoflexid m3	a	a	b	a	a	a	a	a	a	b
30. Posteroflexid m3	a	a	a	a	a	a	b	b	b	b
31. Lingual folds m2 and m3	a	a	a	a	a	a	a	a	a	b
32. Labial root M1	a	a	a	b	b	b	a	b	b	b
33. Accessory roots m1	a	a	a	b	c	c	c	c	c	c
34. Relative size of M3	?	b	b	b	b	b	b	a	a	a
35. Relative size of m3	?	b	a	a	a	a	c	c	c	c
36. Ungual tufts	a	a	a	b	a	b	b	b	b	?
37. Natatory fringe	a	a	a	a	a	a	b	b	b	?
38. Plantar pads	a	a	b	c	b	b	c	c	c	?
39. Interdigital webbing	a	a	a	b	a	b	c	c	c	?
40. Hind-foot conformation	a	a	b	b	b	b	b	b	b	?

bony palate of this taxon. Whether entered as an ordered or unordered character type in PAUP, the lack of well-defined pits was parsimoniously depicted as a character reversal on the branch leading to *Noronhomys*.

Character 11. Conformation of the parapterygoid fossae:

(a) fossae relatively broad (greater than width of mesopterygoid fossa at the palatine–pterygoid suture), approximately level with plane of the bony palate;

(b) fossae narrower (about equal to width of mesopterygoid fossa), moderately excavated above bony palate;

(c) fossae narrow and short, cavernous, with anterior margins undercut.

Character 12. Size of ectotympanic bullae:

(a) relatively small, exposed flange of periotic bone extends to internal carotid canal;

(b) intermediate, exposed portion of periotic bone smaller and not contributing to wall of carotid canal;

(c) relatively large, periotic bone mostly masked in ventral view.

Character 13. Alisphenoid strut:

(a) present, buccinator–masticatory and accessory oval foramina separate;

(b) absent, buccinator–masticatory and accessory oval foramina confluent.

Remarks: The consensus of outgroup comparisons conducted for phylogenetic studies of Muroidea has favored the presence of an alisphenoid strut as primitive (Carleton, 1980; Musser and Newcomb, 1983; Voss, 1993). Steppan (1995) viewed the possession of a well-formed alisphenoid strut as derived for certain phyllotine species. Although many muroids, including most oryzomyine taxa, uniformly lack the strut, its presence varies within species of *Oligoryzomys* (Olds and Anderson, 1987; Carleton and Musser, 1989), *Pseudoryzomys* (Voss and Myers, 1991), *Oecomys*, and the *Oryzomys nitidus* complex (Musser et al., 1998). Such population-level polymorphisms lend plausibility to the independent fixation of this trait as present or absent in various descendent lineages.

Character 14. Cranial foramina and carotid circulation:

(a) stapedial and sphenofrontal foramina present, vascular groove crosses the inner surface of the squamosal and alisphenoid bones, posterior opening to alisphenoid canal large (stapedial artery, via the supraorbital and infraorbital branches, forms major supply to orbitofacial region);

(b) sphenofrontal foramen and internal vascular groove absent, stapedial foramen absent or minute, posterior opening to alisphenoid canal irregularly formed or occluded (distal segments of supraorbital and infraorbital arteries arise from secondary anastomoses to internal carotid).

Character 15. Configuration of masseteric ridges:

(a) superior and inferior masseteric ridges converge anteriorly as an open chevron;

(b) anterior portion of ridges variably conjoined as single crest that extends nearly to the mental foramen.

Character 16. Conformation of mandibular ramus:

(a) shallow, leading edge of ascending ramus oriented more obliquely, coronoid process placed lower than condyloid process, posterior margin of angular process about equal to that of condyloid process;

(b) deep, leading edge of ascending ramus oriented more vertically, coronoid process arches level with or above the condyloid process, angular process produced behind the condyloid process.

Character 17. Enamel facets on incisors:

(a) upper and lower incisors smoothly rounded or flattened, without labial bevel;

(b) upper incisors somewhat flattened medially, with presumptive labial bevel, lowers unmodified;

(c) upper incisors flattened laterally, with distinct labial bevel, lowers flattened laterally with lingual bevel.

Character 18. Molar coronal topography:

(a) brachyodont, cusps tuberculate with lingual and labial rows crested;

(b) higher crowned, cusps bunodont with lingual and labial rows unevenly terraced;

(c) moderately hypsodont, occlusal surface planar.

Character 19. Molar occlusal design:

(a) cusps essentially opposite with rounded outer margins (not prismatic), lingual and labial folds not interpenetrating;

(b) cusps slightly alternating with rounded outer margins, some lingual and labial folds moderately interpenetrating;

(c) cusps conspicuously alternate with acute outer margins (prismatic), some lingual and labial folds deeply interpenetrating.

Character 20. Development of M1 procingulum:

(a) anteromedian flexus clearly inscribed on younger specimens, anterocone bilobate as lingual and labial conules;

(b) anteromedian flexus absent, anterocone broader with separate conules variably evident on only unworn teeth;

(c) anterocone wide, lacking any suggestion of a flexus or constituent conules.

Remarks: Reconstructing the homology of enamel structures and contiguous hollows that attended the elaboration of the wide, entire procingula found in the upper and lower first molars of *Holochilus* poses uncertainties. For the M1s, the above transformation hypothesis acknowledges the coalescence of formerly independent lingual and labial conules and sequestration of the remnant flexus as an internal depression, as was interpreted for *O. palustris* (Carleton and Musser, 1989). Such a modification is suggested by the occasional presence in some juvenile *Oryzomys* and *Pseudoryzomys* of bilobate anterocones, a condition that is coded as an intermediate character state. On such specimens, a medial enamel border segregates the dentinal cores of the apparently conjoined lingual and labial conules. See Reig (1977), Voss (1993), and Steppan (1995) for further discussion and cladistic treatment of the procingulum complex in other sigmodontine rodents.

Character 21. Mesolophs on M1 and M2:

(a) mesolophs present and long, typically extending from median mure to labial cingulum;

(b) mesolophs present and short, not reaching the labial cingulum;

(c) mesolophs absent or minimally suggested in unworn molars as an enamel deflection of the median mure.

Character 22. Mesoloph on M3:

(a) usually present and well developed;

(b) absent or vestigial.

Character 23. Anteroloph on M1:

(a) present and well developed, extending to labial cingulum;

(b) present and short, not extending to cingulum;

(c) absent.

Character 24. Posteroloph on M1 and M2:

(a) present, moderately long and persisting until later wear stages;

(b) present, short and disappearing after little to moderate wear;

(c) absent.

Character 25. Protoflexus of M2:

(a) present as a shallow indentation, at least in unworn dentitions;

(b) absent.

Character 26. Development of procingulum on m1:

(a) anteromedian flexid present, defining anterolabial and anterolingual conulids and communicating with anteromedian fossettid;

(b) anteromedian flexid absent, anteroconid a single wider cusp, and anteromedian fossettid, anterolophid, and protolophid variously defined;

(c) anteroconid broad, enclosing an internal enamel pit, other procingular elements indiscernable.

Remarks: Like its occlusal counterpart on the upper first molar (see character 20), the formation of the m1 procingulum, particularly the derivation of the so-called internal enameled pit of certain oryzomyines (Voss and Carleton, 1993), remains obscure. The morphology of the enamel pit appears similar among the genera *Pseudoryzomys*, *Holochilus*, *Lundomys*, and *Noronhomys*. This procingular basin may represent a phylogenetic remnant of the anteromedian fold that became enclosed: anteriorly by fusion and broadening of the lingual and labial conulids along their forward rim; and posteriorly by retention and hypertrophy of the medial segments of the anterolophid, protolophid, and possibly the contiguous portion of the murid. All of these elements are irregularly defined in species of *Oryzomys*, in which the size of an m1 pit is neither so large nor its boundaries, especially at the posterior border, so completely formed. This procingular condition is coded as intermediate to those observed in *Microryzomys* and the four genera mentioned above.

Character 27. Mesolophids on lower molars:

(a) consistently present and well-developed, extending to lingual cingulum;

(b) present and short, not meeting the lingual cingulum;

(c) absent.

Character 28. Definition of the m1 posterolophid:

(a) clearly defined as a discrete entity from the hypoconid;

(b) boundaries of the posterolophid and hypoconid indistinct, the two continuous as a broad loph across the rear margin of the tooth.

Character 29. Protoflexid of m3:

(a) present, short anterolabial cingulum well defined, at least in unworn teeth;

(b) absent, anterolabial margin of m3 smoothly rounded.

Character 30. Posteroflexid of m3:

(a) present;

(b) absent.

Remarks: The posteroflexid in examples of *Z. brevicauda* is observable in only very young specimens (juvenile and subadult) with scant wear on the m3; those of *Z. brunneus* possess a larger fold that generally persists until later wear stages (young adults). The obliteration of the posteroflexid, together with other coronal rearrangements—loss of the mesolophid, suppression of the entoconid, and coalescence of the hypoconid-posterolophid—yield the "s-shaped" third molar central to Hershkovitz's (1955) classical definition of the sigmodont group.

Character 31. Lingual folds on m2 and m3:

(a) m2 posteroflexid and m3 entoflexid open to lingual margin of tooth;

(b) lingual folds isolated as enamel islands on m2 (posterofossettid) and m3 (entofossettid), respectively.

Character 32. Labial root of M1:

(a) absent;

(b) present.

Character 33. Accessory roots of m1:

(a) absent, m1 with two roots;

(b) labial accessory root present, lingual root smaller and variable, three or four roots total;

(c) labial and lingual accessory roots present and typically well developed, four roots total.

Character 34. Relative size of M3:

(a) longer than second molars, principal coronal features of posterior half of third molars recognizable;

(b) distinctly shorter than second molars, posterior half noticeably reduced and serial enamel homologies obscured or distorted.

Character 35. Relative size of m3:

(a) shorter than second molars, reduction principally evident in posterior half such that serial enamel homologies may be obscured;

(b) subequal in size to second molars, principal coronal features of posterior half of third molars recognizable;

(c) longer than second molars.

Remarks: The character state for both upper and lower third molars was recorded as unknown in the composite ancestor. Within Muroidea, the contribution of the last-erupted molars to overall toothrow length and occlusal area is not necessarily positively correlated in the upper and lower dentitions of the same species. Commonly, the M3 is noticeably smaller relative to M2, its occlusal details distorted, while the m3 approximates the size of the m2, its enamel landmarks clearly discernable. Systematists have rendered differing polarity interpretations for departures from this prevalent plan (see Hershkovitz, 1962; Carleton, 1980; Voss, 1988; Steppan, 1995).

Character 36. Ungual tufts on hind foot:

(a) present;

(b) absent.

Character 37. Natatory fringe on hind foot:

(a) absent;

(b) present.

Character 38. Plantar pads on hind foot:

(a) pads large and fleshy, interdigitals 1–4 set close together, hypothenar conspicuous;

(b) pads smaller, interdigitals 1 and 4 displaced proximally relative to 2 and 3, hypothenar present but small;

(c) pads distributed as in state (b) but tiny and of low relief, hypothenar pad absent or minute.

Character 39. Interdigital webbing on hind foot:

(a) absent;

(b) present but small, not extending to first interphalangeal joint of any digits;

(c) present and large, extending to or beyond first interphalangeal joints of digits II, III, and IV.

Character 40. Conformation of hind feet:

(a) digits II–IV slightly longer than I and

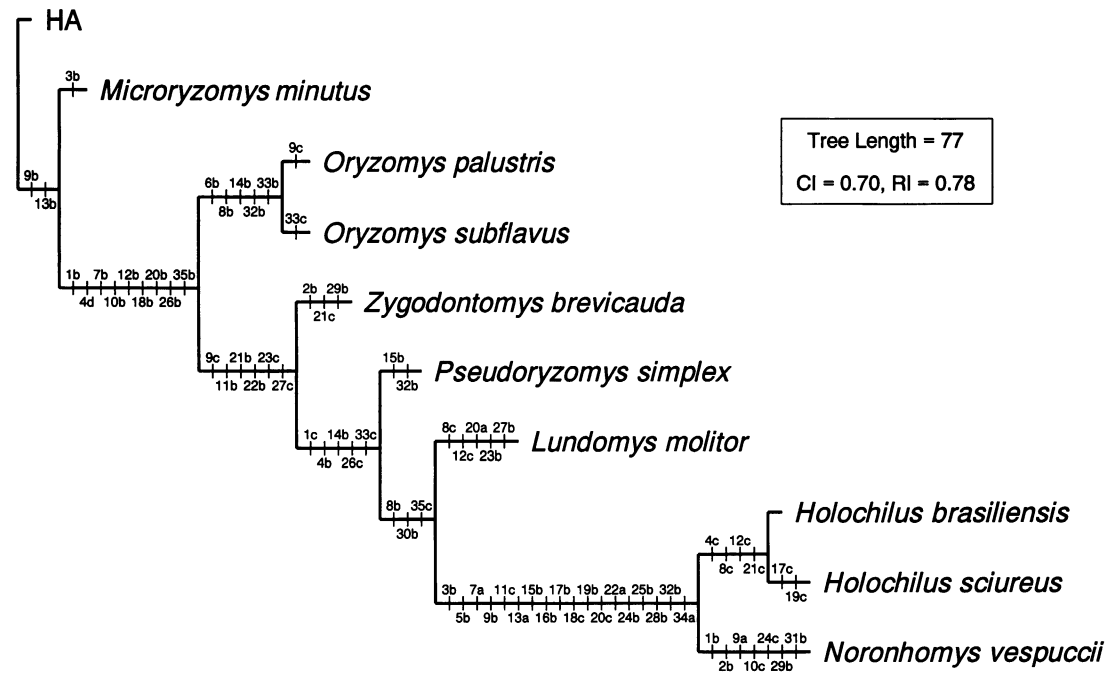

Fig. 22. Hypothesis of relationship among nine oryzomyine taxa based on 35 craniodental characters (see text and table 11). Derived character-state changes are portrayed according to delayed transformation optimization of intermediate taxonomic units.

V; nail of digit V extends to terminal phalanx of digit IV;

(b) digits II–IV conspicuously longer than I and V; nail of digit V extends to second phalanx of digit IV.

Phylogenetic reconstructions based on PAUP were conducted first for the 35 craniodental characters and then for the entire data set, including the 5 external traits.

Results

The minimum number of changes represented by the craniodental data (characters 1–35, table 11), absent any homoplastic conversions, is 54 steps. However, for the ancestral states and polarity sequences argued above, maximum parsimony yielded just one shortest tree of 77 steps (fig. 22; consistency index [CI] = 0.70, retention index [RI] = 0.78). Elimination of three unique states (17c, 19c, 24c) and one cladistically uninformative character (31) reduced the tree length to 73 steps (CI = 0.69, RI = 0.78). The same cladistic topology among the terminal taxa was preserved in additional parsimony analyses, whether treating all multistate characters as unordered (length [L] = 71, CI = 0.76) or designating extant *Microryzomys* as the default outgroup (L = 75, CI = 0.72), although tree lengths and hypothesized character state changes perforce differed slightly (trees not illustrated).

Noronhomys vespuccii is hypothesized to share closest common ancestry with species of *Holochilus*, a relationship sustained by 18 apomorphic changes. Of these, 10 character-state transitions are unique and unreversed, including some traits of the cranium (5b, 11c, 16b) and many of the dentition (17b, 18c, 19b, 24b, 25b, 28b, 34a). The branch leading to *Noronhomys* contains seven derived states, only three of them autapomorphies; the seven involve loss or occlusion of minor enamel features (24c, 29b, 31b), shortening of the bony palate (9a) and the possibly correlated reduction of palatal pits (10c), and formation of the zygomatic plate (1b, 2b). Under the accelerated transformation option of PAUP, the length of the stem uniting the two species of *Holochilus* is correspondingly shortened

and two additional reversals contribute to the branch of *Noronhomys*—a flatter palatal bridge (8b) and diminution of the auditory bulla (12b).

The remainder of our tree (fig. 22) conforms to the cladograms generated by Voss and Carleton (1993) and Steppan (1996) for those taxa common to all three studies. Areas of agreement include the earlier differentiation of *Oryzomys* sensu stricto and the monophyletic grouping of *Pseudoryzomys*, *Lundomys*, and *Holochilus*. For the characters defined here, the recognition of the last three genera (plus *Noronhomys*) as a clade results from unique changes in supraorbital design (4b) and the m1 procingulum (26c) and from homoplastic transformations that involve formation of a zygomatic spine (1c, reversed in *Noronhomys*), modification of carotid circulation (14b, also shared with *Oryzomys*), and proliferation of accessory roots on m1 (33c, independently derived in *O. subflavus*). The cognate affinity of *Zygodontomys* and (*Pseudoryzomys–Lundomys-Holochilus–Noronhomys*) is due mostly to the loss of the anteroloph and mesoloph(id) (21b, 22b, 23c, 27c), enamel structures that characterize the more complex, pentalophodont molars found in *Microryzomys* and *Oryzomys*. Finally, the retention of so many primitive states by the Andean genus *Microryzomys* assures its basalmost origin relative to the other oryzomyine rodents included (table 11).

Two clades were invariantly recovered in bootstrap iterations for the 35 craniodental transformations defined (fig. 23A)—one consisting of all taxa that form a sister-group to basal *Microryzomys* and the other containing *Noronhomys* and *Holochilus*. Other moderately to strongly supported internal nodes, as indicated by bootstrapping values and Bremer indices, include the cognate affinity of *Pseudoryzomys* and (*Lundomys–Holochilus–Noronhomys*) and the monophyly of *Holochilus*.

Predictably, the two weaker clades uncovered through bootstrap resampling subtend those taxa for which alternative phylogenies are found in the two next-shortest trees generated (L = 78, CI = 0.69, RI = 0.77). In one tree of 78 steps, *Pseudoryzomys*, instead of *Lundomys*, is arranged as the sistergroup to *Holochilus* and *Noronhomys* (fig. 24A); in the other, the genus *Oryzomys* is depicted as paraphyletic, with *O. subflavus* and *O. palustris* forming successive outgroups to the remaining taxa (fig. 24B). The closer kinship between *Pseudoryzomys* and (*Holochilus–Noronhomys*) emphasizes parsimony for derivation of the conjoined masseteric ridge (15b), gain of the labial root on M1 (32b), and losses of the anteroloph (23c) and mesolophid (27c); in this tree (fig. 24A), the genus *Pseudoryzomys* is undifferentiated from the node that subtends it and (*Holochilus–Noronhomys*). In the shortest tree of 77 steps (fig. 22), these changes are reconstructed as parallelisms (15b, 32b) between *Pseudoryzomys* and the (*Holochilus–Noronhomys*) lineage and as reversals (23c to b, 27c to b) defining the *Lundomys* branch. The placement of *O. subflavus* as a clade apart from *O. palustris* (fig. 24B) stems from parsimonious rearrangements that involve character differences between these species—extent of the hard palate (shorter in *O. subflavus*) and m1 root development (both lingual and labial satellite rootlets present in *O. subflavus*). Further, those shared character states in the most parsimonious tree are instead depicted as parallelisms (6b, 8b) within each species branch.

A single shortest tree was again generated when using all 40 characters (fig. 25). Compared with the phylogeny estimated with only the 35 craniodental attributes, tree length is concomitantly longer (L = 89 steps), yet branching structure is entirely congruent and measures of character homoplasy are nearly alike (CI = 0.69, RI = 0.78). In effect, addition of the five external characters (characters 36–40) for the eight extant taxa bolstered the stems subtending *Pseudoryzomys* and kin and the (*Lundomys–Holochilus–Noronhomys*) clade, resulting in higher bootstrap percentages and Bremer indices (fig. 23B). These character-state transitions involve hind-foot adaptions for a semiaquatic lifestyle, including reduction of the ungual tufts (36b), acquisition of stiff fringing hairs (37b), diminution of the plantar pads and loss of the hypothenar (38c), and elaboration of interdigital webbing (39b, c). Parallel changes of several of these (36b, 38c, 39b) are foreshadowed within the line leading to *O. palustris*.

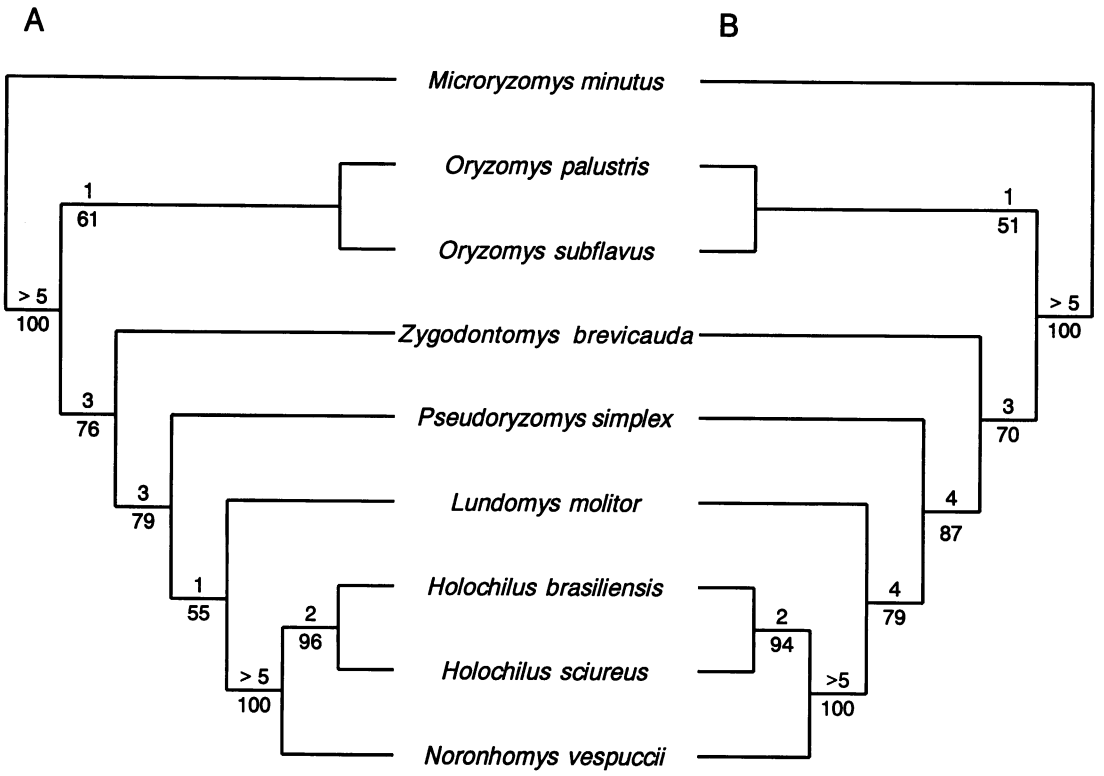

Fig. 23. Support measures for most parsimonious trees of nine oryzomyine species, with Bremer indices indicated above internal stems and bootstrapping percentages (1000 replicates using branch-and-bound search) below. **A**, Cladogram obtained from 35 craniodental characters (see fig. 22). **B**, Cladogram obtained from 35 craniodental and 5 external characters.

None of the alternative choices of outgroup, character-type assumptions, character sets, or next-shortest trees discussed above disturbs the sister-group stature of *Noronhomys* and *Holochilus*. Nor was *Noronhomys* ever associated with another genus in any partition of greater than 5% frequency generated through bootstrap replicates. The robustness of the inferred relationship is anticipated by the comparatively large number of apomorphies that accrue along their nodal branch (fig. 22). However, one of three trees recovered with 79 steps (CI = 0.68, RI = 0.76) represented the relationship of *H. brasiliensis*, *H. sciureus*, and *Noronhomys* as an unresolved trichotomy. Of the four characters that defined a monophyletic genus *Holochilus* in the shortest tree, two are instead represented as parallel changes (4c, 21c) within each species of *Holochilus* and two are redistributed as reversals (8b, 12b) in the line leading to *Noronhomys*. Notwithstanding the cladistic uncertainty conveyed by this longer tree, the brunt of the character information and parsimony analyses persuasively implicates mainland *Holochilus* as genealogically closest to the island fossil.

DISCUSSION

Amerigo Vespucci and the Rat of Fernando de Noronha

Prior to Olson's discovery in 1973, the only recorded historical sighting that conceivably pertains to a native rodent on the island of Fernando de Noronha comes from the account of the Fourth Voyage of Amerigo Vespucci—the Florentine adventurer after whom the New World is named. This reference appears in the *Lettera di Amerigo Vespucci delle Isole Nuovamente in Quattro Suoi Viaggi*, in which his putative exploits in

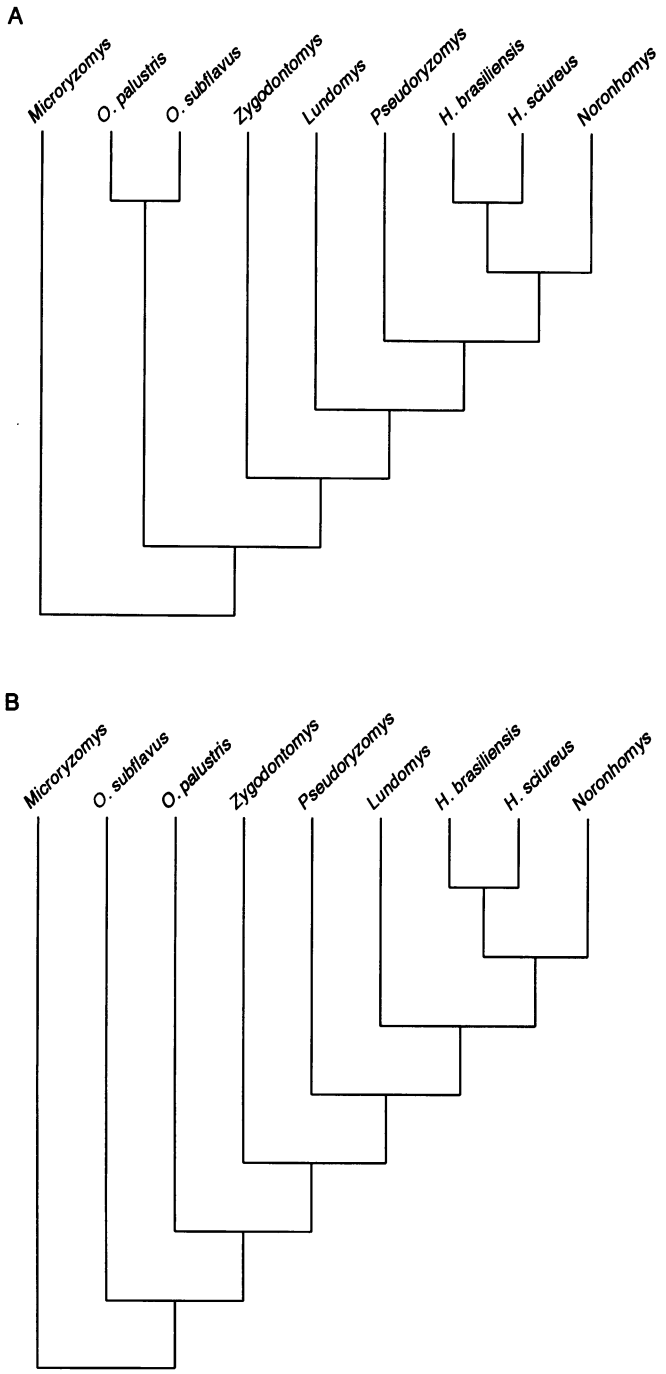

Fig. 24. The next two most parsimonious trees derived from the 35 craniodental characters presented in table 11 (L = 78, CI = 0.69, and RI = 0.77 for both). Compare with the shortest tree illustrated in figure 22. **A**, Tranposition of *Pseudoryzomys* and *Lundomys* as sister-group to *Holochilus* and *Noronhomys*; **B**, Paraphyly of *Oryzomys*.

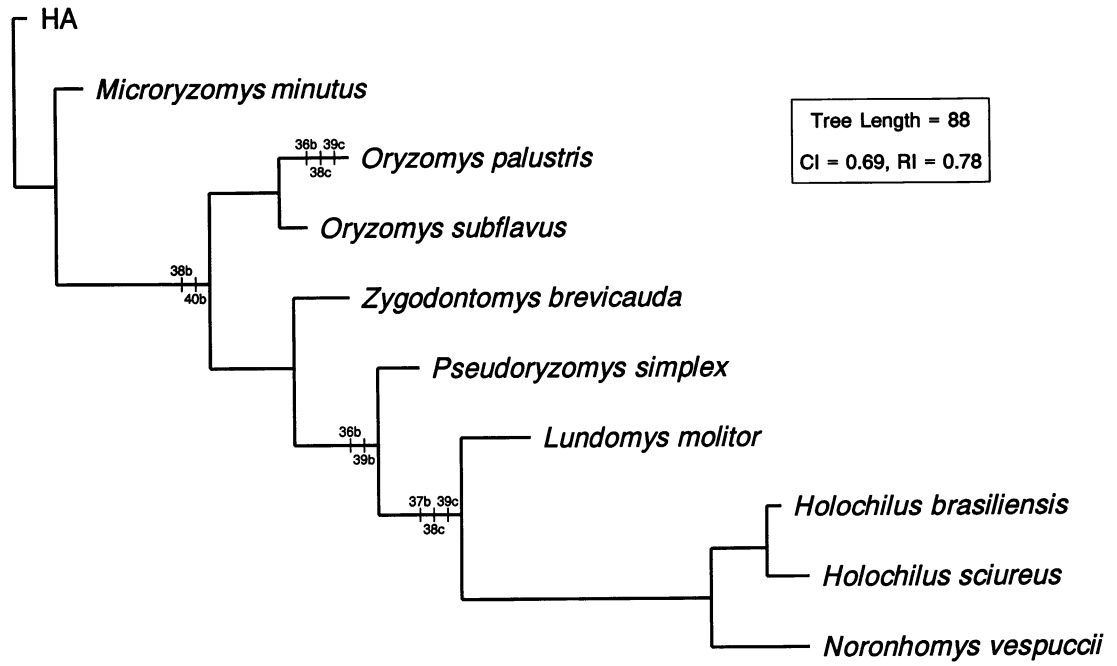

Fig. 25. Hypothesis of relationship among nine oryzomyine taxa based on 35 craniodental and 5 external characters (see text and table 11). The branch lengths are proportional to the number of character state-changes along them, but only transformations of the five external characters are portrayed (optimized by delayed transformation).

the New World are recounted as four voyages made between 1497 and 1504 (see Formisano, 1992). Addressed to Piero di Soderini, gonfalonier of the Florentine Republic, the *Lettera* was published in Florence in September 1504 and was being widely reproduced and circulated by 1505. In 1507, a popular Latin translation was included in Martin Waldseemüller's *Cosmographiae Introductio*, the first work in which the name "America" appeared on a map of the newly found lands in the west. Historians and linguistic scholars, however, strongly doubt that Vespucci was directly responsible for the *Lettera*, and the earlier printed *Mundus Novus*, or that he sanctioned their dissemination (see Pohl, 1944, and Formisano, 1992, and references cited by each).

The *Lettera* and *Mundus Novus* were manifestly designed for popular consumption to celebrate the achievements of a Florentine native son, expressly as counterpoint to the transatlantic explorations of Columbus, a Genoese, and were printed during a time of intense patriotic and political rivalries. The two public documents contain many internal contradictions and inconsistencies of chronology and geography, and so contrast with the style and tone of Vespucci's so-called "familiar letters," sent to Lorenzo de Medici, his longtime patron. Historians have accepted the personal correspondences, which originally circulated in only manuscript form, as proof that Vespucci did undertake some voyages to the New World, namely those traditionally numbered as the second and third (Pohl, 1944; Formisano, 1992). With regard to these navigations, one for Spain (1499–1500) and one for Portugal (1501–1502), the familiar and public documents retain much general and specific agreement. This complementarity has led historians to suspect that composite accounts were forged by persons unknown, who drew extensively upon information contained in the familiar letters and other Vespuccian manuscripts now lost, and embellished other details of destination and chronology to emulate a Colombian four-act drama. Formisano (1992: xxxv) thus characterized the *Mundus*

Novus and *Lettera* "as texts that might best be labelled not pseudo- but rather para-Vespuccian."

As relayed in the *Lettera*, the fourth voyage was hardly a shining success. According to Formisano (1992: xxiii), it was "traditionally identified with the expedition of Gonçalo Coelho, which has no parallel in the corpus of the familiar letters, and above all is incompatible with the news of Amerigo's reentry into Spain from October 1502." In 1503, the fleet of six caravels sailed to the Cape Verde Islands, attempted unsuccessfully to land at Sierra Leone, West Africa, and then crossed the Atlantic to the vicinity of a small island, presumably Fernando de Noronha, where the flagship ran aground and the fleet was scattered. Vespucci reported that he continued to Brazil where he and his men spent five months, built a fort, and returned to Lisbon with a cargo of brazilwood. With no new lands discovered, no extravagant riches acquired, nor glorious exploits achieved to enhance the navigator's reputation, there would seem little reason for Vespucci, or others, to set forth this account had it not contained some truth.

Whatever the actual historical circumstances, the chronicle of the fourth voyage and the island now known as Fernando de Noronha so accurately captures certain geographical and biological details that it cannot be casually dismissed as imaginary. More than a century ago, Branner (1888: 869) intelligently framed the problem.

> I am aware that historians question whether this voyage was ever really made by Americus Vespucius, but judging from the description given by him it must be confessed that if that navigator did not himself see this island, he obtained his information concerning it from some one who did visit it, and for our purposes this serves the same end. If his informant was a member of Fernando de Noronha's party, it is only the more valuable in the present connection.

The island is said to have appeared on a map as early as 1500, but it "is generally stated that Gonçalo Coelho was the real discoverer in the year 1503" (Mitchell-Thomé, 1970: 13), bits of information which are consistent with the *Lettera*'s passage on the fourth voyage. Branner (1888) cited Portuguese archives that report the specific date of discovery as 24 June 1503. The present name for the tiny archipelago originates in a rich nobleman and shipowner, Fernão de Loronha, who was a concessionaire of the Portuguese brazilwood monopoly (de Almeida, 1958) and who received the land in deed from the king of Portugal in 1504 (Branner, 1888). According to the *Lettera*, Vespucci landed on the island on 10 August 1503. Whether the observations reported therein are Vespucci's own or were appropriated from some record of the Coelho expedition, they would seemingly date from 1503 and were certainly obtained prior to September 1504, when the *Lettera* was first printed. Regardless of who made them, these very first descriptions of the natural history of the island, however scant, were made at a time when the island was undoubtedly pristine.

The island Vespucci described stood 3° south of the equator, which accords with Fernando de Noronha's position at approximately 3°50′ south latitude, and was high. The terrain is dominated by a conspicuous peak, Morro do Pico, that signaled landfall to early sailors and that Branner (1889: 152) called "the most striking landmark in the South Atlantic" (see fig. 3). Vespucci described the island as "no more than two leagues long and one wide" (Formisano, 1992: 94). At its extremes, the island is about 10 km long by 3.5 km wide (about 2.1 by 0.7 standard English leagues of the Middle Ages—see, for example, Darton and Clark, 1994). Thus, the physical features, size, and geographic position of Fernando de Noronha agree remarkably well with Vespucci's description, there being no other island in the Atlantic at this latitude. Vespucci, according to the *Lettera*, continued as follows (Formisano, 1992: 95).

> We returned to the island and used the auxiliary boat in my convoy to supply ourselves with water and firewood. We found this island to be uninhabited, with many sources of fresh water and countless delightful trees, full of so many sea and land birds that they were without number, and were so guileless that they let themselves be taken in hand; and we took so many of them that we loaded a boat full of them. We did not see any animals, except for very large rats, green lizards with two tails, and some snakes." (The last sentence in the original Italian reads "*nessuno non vedemmo, salvo topi molto grandi, e ramarri con due code, e alcuna serpe*" [Bandini, 1745: 60].)

The island of Fernando de Noronha, even in its present highly disturbed state, remains

one of the major breeding grounds for seabirds in the western South Atlantic. Landbirds such as a species of dove (*Zenaida auriculata*) and a now-extinct flightless rail (Olson, 1981) would also have been abundant at the time of first contact, so filling a boat with birds in 1503 is easily imagined.

The report of snakes may be readily explained by the endemic *Amphisbaena ridleyi*, a limbless worm-lizard whose serpentine appearance would suggest a snake to anyone save an experienced herpetologist. In 1973, Olson found this reptile to be quite common in suitable habitat; sailors gathering firewood in 1503 could scarcely have failed to encounter it.

Lizards, in the form of the endemic skink *Mabuya maculata*, are still ubiquitous and incredibly abundant. Although these skinks are not green, the translation of *rammari* as green lizards is a strictly literal dictionary definition. In Italy, *ramarro* applies to the common European species *Lacerta viridis*, which is green, so Vespucci's account is best translated to mean only lizards, as was concluded by the early naturalists Branner (1888) and Ridley (1888) in their translations of this passage. With regard to these lizards having two tails, both Branner (1888) and Ridley (1890a, 1890b) independently offered the same plausible explanation (quotation from Branner, 1888: 867).

> I was told by the inhabitants that there was another kind of lizard on the island which had two tails. I found, however, that the so-called fork-tailed lizard was the same as the above mentioned one [that is, *Mabuya maculata*]. The tail of this species is long and slender, and is so easily broken that it was quite difficult to catch one without breaking off a portion of its tail. If the piece broken does not fall off entirely, the break may heal over sufficiently to hold it securely, while the growing out of the new tail gives the lizard a forked or double one.

This leaves only the very large rats (*topi molto grandi*) as unaccounted. Branner (1888: 871) attempted to explain the presence of Vespucci's rats through introduction of *Rattus*, presumably *R. rattus*, from some derelict vessel. However, the elapse of two months between the island's discovery and Vespucci's landing, as relayed in the *Lettera*, seems too brief for even the prolific *Rattus* to overpopulate the island and attract comment (or there may have been no lapse if Vespucci's account comes from that of Coelho). Moreover, it is curious that Vespucci would have remarked upon black rats, vermin already familiar to and despised by any sailor of wooden ships, when the remainder of his narrative pertains to only the native animals. The size of *R. rattus*, the common ship rat of early overseas travel, merits consideration as well in view of Vespucci's emphasis on the island's very big rats. *Noronhomys vespuccii* would have been similar in size to Venezuelan *Holochilus sciureus*, which are heavy-bodied rodents, 200 to 250 grams in average weight. Such animals would indeed have impressed Vespucci as very large compared with the slender physique and smaller body of *R. rattus*, which typically weigh about 150 grams. Ridley (1888: 8), too, discounted so early an introduction of black rats, declaring that: "It is impossible that the animals seen by Vespucci could have been this species, which could not at that time [in 1503] have been introduced. Is it not probable that there was *formerly an indigenous rat-like mammal*, exterminated by the introduction of the black rat?" (emphasis ours).

We salute Ridley's prescient insight. As documented herein, an endemic sigmodontine rodent, *Noronhomys vespuccii*, once inhabited the island, evidence of which renders ad hoc explanations involving commensal rats as irrelevant. Because so many particulars of Vespucci's description of the small island 3° south of the equator fit closely with what is now known about Fernando de Noronha, we believe that the discovery of bones of this large rodent further upholds the account of 1503. Perhaps historians should consider the biological evidence in support of the veracity of the *Lettera*, especially when assessing the passage concerning Vespucci's fourth voyage.

In all likelihood, the species *N. vespuccii* was thriving in 1503 and became extinct thereafter due to the usual anthropogenic causes that have befallen so many vertebrate species on islands. No proper biological reconnaissance of Fernando de Noronha was conducted until the visits of Branner in 1876 and Ridley in 1887 (Branner, 1888; Ridley, 1888, 1890a&b). *Rattus rattus* still occurs on the island and was probably introduced some

time during the 16th century when transatlantic voyages began to flourish. The domestic mouse, *Mus musculus*, is also found, and both species[5] are mentioned in many accounts of the island as being present in extraordinary numbers (for example, Pereira da Costa, 1887; Branner, 1888: 862; Ridley, 1888: 46). The overwhelming presence of *Rattus* may have adversely affected populations of *Noronhomys* through direct predation on young, competition for food, or inoculation with pathogens such as the plague bacillus, which can decimate native rodent populations. Disease transmission from introduced *Mus musculus*, for instance, is postulated to have contributed to the late Holocene extinction of the endemic lava mouse (*Malpaisomys insularis*) of the Canary Islands (Boye et al., 1992). Any of these pressures, alone or in combination, could prove lethal for an indigenous rodent, especially one restricted to an island setting and having a relatively small population size. Habitat alteration, introduction of terrestrial predators (*Felis*), and direct predation by early sailors or settlers for food are additional factors that may have hastened the extinction of *N. vespuccii*.

Phylogenetic Relationships

Evidence derived from evaluation of discrete character data strongly supports the recent common ancestry of Vespucci's now extinct rat from Fernando de Noronha and species of *Holochilus* found today on the South American continent. The catalog of their cranial and dental synapomorphies is impressive and accounts for a more distant relationship to *L. molitor*. The genealogical nearness of *Holochilus* and *Noronhomys* contrasts with their considerable phenetic divergence, whether evidenced by morphometric analyses of cranial, mandibular, or femoral measurements. Based on these results, *Noronhomys* appears as much differentiated from *Holochilus* as from *Lundomys* and cannot be simply construed as an insular variant of mainland populations of either. Moreover, other qualitative characters not coded for phylogenetic analysis, such as the arch of the cranium and features of the hind limb, set *Noronhomys* apart from *Holochilus* (and *Lundomys*) and reinforce its recognition as a separate genus.

General patterns of oryzomyine phylogenetic affinity revealed here agree closely with results presented by Voss and Carleton (1993) and Steppan (1996). Of the several traits that unite *Pseudoryzomys*, *Lundomys*, *Holochilus*, and *Noronhomys*, the singular formation of an internal enamel pit on the lower first molar is especially noteworthy among sigmodontine rodents. Voss and Carleton (1993) obtained equally parsimonious alternatives for the closest generic relative of *Holochilus* (exclusive of *Noronhomys*, of course), their two shortest trees disclosing either *Pseudoryzomys* or *Lundomys* as the sister-group. The same ambiguity is evident in our next-shortest trees, but the most parsimonious solution based on craniodental traits uniformly depicted the cladistic pattern as (*Pseudoryzomys*–(*Lundomys*–(*Holochilus*–*Noronhomys*))) (compare figs. 22 and 24A). Inclusion of the hind-foot modifications (characters 36–40) provides additional weight for close relationship among the three living genera (fig. 25), all of which are moderately to highly semiaquatic in habit and habitat, in apparent contrast to *Noronhomys* (see discussion below).

The tetralophodont genera *Pseudoryzomys*, *Lundomys*, *Holochilus*, and *Noronhomys* compose a small clade that may have originated in riverine and palustrine habitats found within savanna enclaves of southern South America. Hershkovitz (1993) has highlighted such environments and the rodents that inhabit them as "fringe zone faunas," and emphasized the possible role of such ecotonal zones as evolutionary staging areas for differentiation of pastoral species that subsequently lost the mesoloph. The distributions of *Pseudoryzomys* and *Lundomys* are today confined to habitats within southern South America—the former in xerophytic formations from northern Argentina and southeastern Bolivia to Pernambuco, Brazil (Voss and Myers, 1991), and the latter in

[5] The only identifiable *Rattus* recovered from the beach sands is *R. rattus*, as is the one recent specimen (USNM 397324) collected near Olson's field camp. The occurrence of the Norway or brown rat, *R. norvegicus*, on Ilha Fernando de Noronha has not been documented and seems doubtful.

subtropical pampas of Uruguay and Rio Grande do Sul, Brazil (Voss and Carleton, 1993). Fossils of both genera have been recovered from the Lagoa Santa caves in Brazil, demonstrating their broader geographic occurrence in the recent past. Populations of *Holochilus* range over a far greater area, approximately coincident with the boundaries of Amazonia and the Atlantic Forest (Hershkovitz, 1955). A southern area of origin for this clade would presume the northward dispersion and differentiation of *Holochilus* populations and the dispersal of the progenitor of *Noronhomys* onto Fernando de Noronha (see below). Such an interpretation is not implausible for *Holochilus*, because the species *H. brasiliensis*, compared with its more widely distributed congenor *H. sciureus*, is confined to nonforested habitats in southernmost Brazil, Uruguay, and neighboring Argentina. The former species retains more plesiomorphic features of the dentition (17b, 19b), including the infrequent presence of vestigial mesolophs; with regard to these traits, *H. brasiliensis* resembles *N. vespuccii* (table 11).

Steppan (1996) recently described a fossil oryzomyine recovered from the Tarija Basin, Bolivia, in alluvial sediments assigned to the middle Pleistocene (Ensenadan Land Mammal Age). The hypodigm consists mainly of dentaries and associated teeth, as well as some partial maxillae and isolated molars. As evidenced by its scientific name, *Holochilus primigenus*, the species displays some characters, such as molars transitional between pentalophodonty and tetralophodonty, that suggest its early genesis in the clade leading to the living species of *Holochilus*. The cuspidate molars and short mesolophs(ids) of *H. primigenus* also bear considerable resemblance to *Lundomys*. Indeed, Steppan (1996: 524) cautioned that "It is important to note that *primigenus* would be likely classified in *Lundomys*, and possibly not even recognized as distinct from *L. molitor*, if the only material available were isolated teeth." He elected to allocate the new species to *Holochilus* based on the influence of certain traits (lengths of incisive foramina and bony palate) that cladistically affiliated *primigenus* with *Holochilus* in his parsimony analysis (15 of 27 characters employed were necessarily coded as unknown for *primigenus*). Based on the evidence so far available, we view this generic assignment as tenuous. Instead, the weight of molar features surveyed herein suggests placement of the Bolivian species outside the (*Holochilus–Noronhomys*) clade, perhaps nearer to the separation of *Lundomys* or even *Pseudoryzomys*, a possibility anticipated by Steppan (1996: 528).

The tribal-level affinity of *Zygodontomys* has remained obscure since the taxon's description (see review by Voss, 1991). Recent systematic studies, however, have illuminated its morphological similarity to certain oryzomyines, in particular *Pseudoryzomys* (Voss, 1991), and mustered phylogenetic support for its membership in Oryzomyini (Voss and Carleton, 1993; Steppan, 1995). The association of *Zygodontomys* with the (*Pseudoryzomys–Lundomys–Holochilus–Noronhomys*) clade is dominated by dental transformations that mark the transition from pentalophodont to tetralophodont molars (namely the loss of mesolophs and mesolophids), a thesis central to Hershkovitz's (1962) scenario of the evolutionary and ecological diversification of Neotropical muroids. Nevertheless, those oryzomyine genera with pentalophodont dentitions are underrepresented in our analytical samples, an inadequacy that weakens our confidence in the posited relationship of *Zygodontomys*. Whether molar simplification occurred only once within the oryzomyine radiation, as suggested here, or whether *Zygodontomys* evolved in northern savannas independent of *Pseudoryzomys* and kin in southern savannas, are matters for future studies that draw upon broader taxonomic sampling and other kinds of data.

The cladistic separation of *O. palustris* and *O. subflavus* in the next-shortest tree (fig. 24B) underscores the tenuous evidence for generic monophyly as nominally listed (for example, Musser and Carleton, 1993). Leaving aside the unresolved status of other *Oryzomys* species complexes (*albigularis*, *alfaroi*, *megacephalus*, and *nitidus*), none of which we considered, the congeneric union of North and Middle American *Oryzomys*, including the type species of the genus, *Mus palustris* (Baird, 1858), with such disparate South American forms as *subflavus* is in need

of corroboration. *Oryzomys palustris* and *O. subflavus* do share certain derived traits, such as a pronounced supraorbital shelf and cuneate interorbit, a narrow interparietal, the lack of a stapedial branch to the orbitofacial circulation, and a proliferation of satellite rootlets. Other traits held in commmon are plausibly interpreted as primitive for the tribe, such as the pentalophodont molars, cuspidate occlusal design, and long palate with conspicuous posterolateral palatal pits. Yet North American *O. palustris* (as well as Middle American *couesi*, *gorgasi*, and *nelsoni*) displays certain modifications of the hind foot—namely, reduction of the ungual tufts and plantar pads and presence of interdigital webbing—not characteristic of South American *O. subflavus* (or *buccinatus*, *galapagoensis*, *polius*, *ratticeps*, and *xantheolus*). The significance of such differences bears on an unambiguous diagnosis of *Oryzomys* and attendant decisions regarding the rank of allied forms.

The Andean genus *Microryzomys*, an inhabitant of montane and upper-montane wet forests, retains many primitive conditions and may have originated early relative to the radiation of other Oryzomyini (Carleton and Musser, 1989). It is clearly distantly related to the oryzomyine exemplars we included. Although Carleton and Musser (1989) identified another genus of pygmy rice rat, *Oligoryzomys*, as a close relative of *Microryzomys*, subsequent studies employing allozyme or sequence data have disclosed its sister-group relationship either to a clade composed of *Neacomys* and *Oligoryzomys* (Dickerman and Yates, 1995) or to *Neacomys* alone (Myers et al., 1995; Patton and da Silva, 1995).

Certain traits of soft anatomy recently set forth to diagnose the Tribe Oryzomyini (Voss and Carleton, 1993) are obviously impossible to determine in *N. vespuccii*. Derived attributes such as the presence of pectoral mammae and lack of gall bladder are verifiable on fluid-preserved specimens of *Pseudoryzomys* and *Holochilus* and sustain the allocation of these tetralophodont genera to the otherwise pentalophodont oryzomyines (see Voss, 1991; Voss and Carleton, 1993).

In addition to lacking such pivotal evidence for *Noronhomys*, two hypothesized changes that characterize the (*Holochilus–Noronhomys*) clade, namely the reacquistion of an alisphenoid strut (13a) and the reduction in palatal length (9b to a), are noteworthy for their retrograde evolution from traits proposed as diagnostic of Oryzomyini (alisphenoid strut absent and palate long with prominent posterolateral pits; see Voss and Carleton, 1993: 31). These two features are plausibly considered instances of evolutionary character reversal in the *Noronhomys* lineage. If not, the genesis of *Noronhomys* must be assumed to have occurred prior to the divergence of most oryzomyines, an unlikely chronology in view of origination times (5 to 7 mya) of genera estimated from molecular data (Patton and da Silva, 1995). Furthermore, an extraordinary degree of parallelism must be invoked to explain the fineness of morphological resemblance between *Holochilus* and *Noronhomys* in features such as the unique construction of the postorbital ridge, internal enamel island on m1, and planar occlusal pattern. At this stage of understanding of Neotropical rodent evolution and biogeography, these alternatives are less persuasive reconstructions of phylogenetic history; certainly they are less parsimonious based on the character information at hand.

Ecological and Functional Considerations

The ecology and behavior of *Holochilus* and *Lundomys* are here summarized to frame questions both on the trophic niche and hindlimb morphology of *N. vespuccii* and on the origin and evolution of the island fossil from a continental ancestor.

Ecological and Behavioral Background: The ecology and habits of *Holochilus* and *Lundomys*, insofar as known, befit their vernacular name, marsh rats. The distribution of *Holochilus* is actually more localized than can be indicated on a generalized range map (fig. 1). Wherever collected, these rodents are associated with mesic microenvironments and are found in habitats that are either permanently aquatic or seasonally inundated–such as sites in moist lowland, usually near streams coursing through grasslands, croplands, or evergreen forest (Venezuela–Handley, 1976); grass-covered

savanna, usually swampy and often flooded during rainy months (Guyana—Twigg, 1965); grassy marsh, margins of grassy ponds, and riparian forest amidst cerrado brush and shrub (Brazil—Redford and Fonseca, 1986; Mares et al., 1989); and gallery forest along shallow watercourses through rolling, grassy plains (Uruguay—Barlow, 1969). *Lundomys molitor* has been trapped in similar circumstances and may occur syntopically with *H. brasiliensis* where their ranges overlap (M. L. Tuttle in Voss and Carleton, 1993).

Species of *Holochilus* are large, nocturnal rats, semiaquatic in habit, and principally herbivorous in diet. They feed mainly on the succulent parts of aquatic and riparian plants, stems and seeds of savanna grasses, and, in agricultural fields, the young shoots of cane and rice (Twigg, 1965; Barlow, 1969; Martino and Aguilera M., 1989). *Holochilus* and *Lundomys* swim expertly and retreat to water when pursued; M. L. Tuttle shot rats of both genera that were swimming in streams whose banks were densely shaded by trees and overhanging ferns and grasses (field notes, cited in Voss and Carleton, 1993). They apparently do not burrow but can climb surprisingly well. Females of *Holochilus* and *Lundomys* construct ovoid nests about 2–3 m above ground, affixing them to intertwined tall grasses and reeds near the water's edge or onto the low branches of trees and bushes growing close to streams (Twigg, 1965; Sierra de Soriano, 1969). A mother and her older nestlings may climb higher when the nest is disturbed. In view of their preference for wet habitats and aquatic plant foods, *Holochilus* adapts readily to certain human cultivation practices, invading rice and sugarcane fields and periodically attaining plaguelike population outbreaks (Twigg, 1965; Massoia, 1974).

CRANIODENTAL MORPHOLOGY AND DIET: The presence of a longitudinal ridge on the rear orbital wall of the cranium in *Holochilus* and *Noronhomys* is unique within Sigmodontinae. The position and configuration of such a ridge recall the postorbital process of arvicoline rodents (Repenning, 1968; Kesner, 1980), a rugose crest that provides origin for a hypertrophied internal tendon of the medial temporalis muscle. Kesner (1980) highlighted the role of the postorbital process and attached tendon as a suspensory sling to enhance mandibular motion and longitudinal grinding by the molar rows. Within Arvicolinae, development of the postorbital process is reasonably interpreted as a neomorphic structure, elaborated in conjunction with the striking hypselodonty and other derived dental features that characterize members of the subfamily and reflect their exploitation of a graminivorous trophic niche (Kesner, 1980; Koenigswald, 1980).

In their moderately developed hypsodonty, planar occusal design, and involution of enamel folds, the molars of *Holochilus* and *Noronhomys* indeed resemble the incipient dental modifications found in Miocene and early Pliocene arvicolines. In cranial traits such as the recessed parapterygoid fossae where the internal pterygoid muscles originate, the vertical orientation of the ascending ramus, and the conjoined masseteric ridges, the morphology of the sigmodontine genera also suggests adaptation to propalinal mastication and a predominantly herbivorous diet, as has been well documented for extant *Holochilus* (Twigg, 1965; Massoia, 1974; Martino and Aguilera M., 1989).

HIND-LIMB STRUCTURE AND LOCOMOTION: The aquatic habits of *Holochilus* and *Lundomys* are readily conveyed by their large hind feet equipped with hairy fringes and expansive interdigital membranes (Hershkovitz, 1955; Sierra de Soriano, 1965). This correspondence of form and function conforms to a pattern that has been robustly demonstrated for a variety of semiaquatic marsupials, insectivores, and rodents, in comparison with their terrestrial kin (Stein, 1981, 1988; Voss, 1988). That is, the degree of hind-foot modification and proportional development of the hind-limb skeleton and muscles are logically correlated with increasing adaptation to semiaquatic environments and swimming ability. More generally, insights to the functional significance of hind-limb differences between *Noronhomys*, *Holochilus*, and *Lundomys* may be drawn from a substantial primatological literature that integrates biomechanical design, locomotory classes, and animal lifestyle (Oxnard et al., 1990; Gebo, 1993).

The webbed hind feet and pelvic limb

structure of *Holochilus* or *Lundomys* are typical of mammals that swim by oscillatory propulsion, a mode of aquatic locomotion commonly evolved among secondary swimmers such as the muskrat, *Ondatra zibethica* (in contrast to undulatory propulsion by most primary swimmers such as fish). In this swimming style, the alternating motion of the paired hind limbs and their paddlelike extensions propels the animal through the water (Fish, 1984; Webb and Blake, 1985). During the power stroke, the fully spread hind foot is drawn through the water at right angles to the direction of movement; while so engaged, the angle between the limb sections (femur and tibia, tibia and pes) is varied to maintain hydrodynamic angles of attack of the pes that are close to 90° and thereby to protract the power phase. The recovery phase involves flexion and supination of the hind foot, coupled with plantar flexion of the digits, to minimize drag while the thigh is protracted and the leg extended preparatory to the next propulsive stroke (Fish, 1984).

Aside from the obvious importance of large hind feet and interdigital webbing for effective paddling, other skeletal and muscular proportions of more subtle biomechanical advantage have been described for semiaquatic rodents. Proximal limb elements tend to be shorter relative to distal limb bones in more specialized swimmers (Stein, 1988; Voss, 1988). Stein (1988) found that several hind limb muscles of semiaquatic rodents are relatively larger, namely the gluteus medius, rectus femoris, and vastus lateralis (contrasted to the terrestrial forms *Sigmodon* and *Neotoma*). She further noted that the trend of size increase among these muscles mirrors the degree of external specialization of each taxon for an amphibious existence in aquatic environments—from least specialization (*Oryzomys palustris*), thru intermediate (*Nectomys squamipes*), to most (*Ondatra zibethica*). Species of *Holochilus* possess a hind foot whose natatory development approximates that of *Nectomys*, another oryzomyine; the hind foot of *Lundomys* is even more highly modified for paddling (Sierra de Soriano, 1965), though not so extremely as that of *Ondatra*.

These functional observations can be meaningfully related to aspects of the pelvic limb anatomy in *Holochilus* and *Lundomys*. The scalloped surface and pronounced curvature of the iliac blade amplify the area of origin of the gluteus medius (superior gluteal fossa) and gluteus minimus (inferior gluteal fossa). These major thigh extensors insert on the greater trochanter, and their expansion would serve to accentuate the power and perhaps initial velocity of femoral extension and to elongate the arc through which the distal end of the femur moves. The well-developed femoral tubercle and its forward position imply enlargement of the rectus femoris in these genera comparable to other semiaquatic muroids (Stein, 1988). This long and thick muscle inserts with the vastus lateralis on the dorsolateral border of the patella and extends the leg (tibia–fibula). Its increase in size may generate greater force while paddling. Moreover, because the rectus femoris spans both the hip and knee joint, its hypertrophy may simultaneously assist quick repositioning of the extended femur during the recovery stroke. The tibialis anterior and flexor digitorum fibularis originate principally from the concave lateral and caudal tibial fossae, respectively. Whether the deepened fossae of *Holochilus* and *Lundomys* augment the size or action vectors of these major plantar extensors and flexors is uncertain, but their enlargement would be consistent with modulating the webbed hind feet during hind limb paddling.

Studies of semiaquatic rodents have not addressed the morphology of the distal femur, but primatologists have given much attention to variation in this region. The bulbous articular condyles and elongate patellar fossa of *Holochilus* and *Lundomys* (fig. 13) recall the condition found in small, arboreally nimble primates described as vertical clingers and leapers (Anemone, 1993). Anemone (1993) has hypothesized that the deep pulleylike configuration of such condyles improves the mechanical leverage of knee extension by the quadriceps femoris (which includes the rectus femoris and vastus lateralis, whose size increase in semiaquatic rodents was noted by Stein, 1988). Expansion of the condyles, coupled with a longer arc of curvature of the patellar groove, extends the distance from the quadriceps tendon to the center of rotation of the knee joint,

increasing the moment arm and power of this important leg extensor. To be sure, marsh rats do not progress by clinging and leaping, but the significance of such an articular construction relates to flexibility and motion around the knee joint. Amply rounded condyles and a long patellar fossa for enhancing flexion and extension at the knee would be advantageous in a semiaquatic rodent that swims by alternate propulsive strokes of the hind limbs. In fact, the condylar index (ratio of anterior–posterior depth to the transverse width of the femoral condyles) for *Holochilus* and *Lundomys* ranges from 1.16 to 1.27 (compared with 1.10 in *Noronhomys*) and conforms well to the larger values derived for vertical clingers and leapers among primates (Anemone, 1993: table 6.3).

With this background on function and biomechanical design, we now turn to the many differences between the pelvic skeletons of *Holochilus* and *Lundomys* versus *Noronhomys*. The most conspicuous, as observed in *Noronhomys*, are the weak definition of the superior and inferior gluteal fossae and nondescript femoral tubercle; the stout construction of the whole pelvic limb, especially the diameter of the femoral head, neck, and shaft; the less-rounded contours of the femoral condyles and the short, wide patellar fossa; and the shallow tibial fossae and medial placement of the tibial crest. Although hind-limb structure and shape in *Holochilus* and *Lundomys* can be intelligibly related to their amphibious behavior and paddling locomotion, these same attributes in *Noronhomys* depict a limb subject to quite different working loads and biomechanical stresses, none of which clearly indicates semiaquatic habits. (The pronounced scar on its lower tibial crest alone intimates as much, but the functional context of this difference is obscure.) Instead, *N. vespuccii* appears to have been a stout-limbed, terrestrial rodent, largely ambulatory or perhaps clambering in its movement.

Such a conclusion seems to contradict the close phyletic relationship otherwise inferred for *Holochilus* and *Noronhomys* (fig. 22) and forces a choice between two ad hoc explanations. One, the two genera are only distantly related, the unmodified hind-limb structure suggesting origination of *Noronhomys* from a generalized terrestrial form prior to the differentiation of the (*Pseudoryzomys–Lundomys–Holochilus*) clade. According to this view, the numerous craniodental similarities that link *Noronhomys* and *Holochilus* evolved in parallel; failure to detect this remarkable homoplasy must be owed to the absence of other characters unobtainable from fossil material. Or two, the progenitor of *Noronhomys* was indeed semiaquatic like *Holochilus* and *Lundomys*, but such skeletal adaptations were lost (reversed) following isolation on a small oceanic island where palustrine and riparian habitats are uncommon or absent.

The latter scenario is more compelling for several reasons. Mammalian long bones are remarkably plastic and individually variable, their shape and thickness adaptively responding, within certain morphogenetic constraints, to unusual activities, forces, and loads (for example, see Lanyon and Rubin, 1985). While capable of ontogenetic change over the lifetime of individuals, limb bones also display considerable evolutionary lability in the descent of populations and species. Such modifications are exemplified by the several instances of Pleistocene dwarfing of proboscideans isolated on islands (Roth, 1992) and by the many occurrences of wing atrophy and flightlessness among birds in insular settings devoid of terrestrial predators (Roff, 1994; Fong et al., 1995). The latter analogy seems especially instructive with regard to Vespucci's rat, in light of the numerous losses of flight documented among rails, ibises, ducks, and geese, groups that have independently and repeatly given rise to terrestrial descendants from semiaquatic or aquatic relatives (Olson, 1973; Olson and James, 1991; Roff, 1994). Self-propelled flight is a complex adaptation, dependent upon finely integrated skeletomuscular, physiological, and neural specializations, yet under favorable circumstances of phylogenetic history and environment, such as encountered in insular settings, reversal to terrestrial locomotion has occurred readily, albeit infrequently, over evolutionary time. The loss of skeletomuscular adaptations for paddle swimming in a population of once semiaquatic rodents stranded on an oceanic island

would seem as probable, if not more easily realized.

Biogeography of Fernando de Noronha

The indigenous vertebrate fauna thus far documented for Fernando de Noronha is, like other oceanic islands, depauperate and unbalanced in comparison with a continental landmass like South America. Absent are freshwater fish, amphibians, bats, and, except for the extinct rodent reported herein, native land mammals (Branner, 1888; Ridley, 1890b); marine birds are dominant, landbirds few (Oren, 1982, 1984). The assortment of species endemic to the island is an odd subset of the mainland fauna: a large sigmodontine rodent (*Noronhomys vespuccii*), a worm-lizard (*Amphisbaenia ridleyi*), a skink (*Mabuya maculata*), and three landbirds—a vireo (*Vireo gracilirostris*, Vireonidae), a flycatcher (*Elaenia ridleyana*, Tyrannidae), and an undescribed flightless rail (*Rallus*, Rallidae). Such disharmony by itself suggests chance dispersal across great overwater distances.

Where systematic evidence has been critically marshalled, the ancestral source of the terrestrial vertebrates on Fernando de Noronha appears to be eastern South America, as would be expected simply on the basis of geographic proximity. This conclusion is certainly true of Vespucci's rat, *Noronhomys*, whose nearest kin *Holochilus* occurs in lowland habitats from northern Venezuela, throughout Amazonia, to southeastern Brazil and northern Argentina. The endemic vireo is thought to be a derivative, albeit a highly specialized one, of the *chivi* group of the redeyed vireo (*V. olivaceus*), which is widespread in South America (Olson, 1994). The endemic flycatcher was long considered to be a subspecies of *E. spectabilis*, an austral migrant that breeds in Brazil south of Amazonia and flies northward through eastern South America, a flight path conducive to island colonization. Although the closest specific relatives of *E. ridleyana* have been recently regarded as obscure (Ridgely and Tudor, 1994), the genus *Elaenia* reaches its greatest species diversity in South America, whence the Noronha bird was certainly derived. The dove of Fernando de Noronha, *Zenaida auriculata* (Columbidae), does not differ from populations on the nearby Brazilian mainland, where this species is migratory and at times extremely abundant. Oren (1982) previously identified a close biogeographic affinity between the Noronhan avifauna and that of the Caribbean, but this general interpretation is biased by the island's ten breeding marine species, which roam widely over tropical oceans and seas. The resident landbirds offer a different picture.

The continental origin of the two endemic reptiles, *Mabuya maculata* (Scincidae) and *Amphisbaenia ridleyi* (Amphisbaenidae), is uncertain, for their relationships have not been rigorously evaluated to date. Both belong to families and genera that occur widely in the New and Old World tropics of South America and Africa, including the West Indies and Mediterranean littoral, a pattern that corresponds to a West Gondwanan distribution (see review and references cited by Bauer, 1993). Ridley (1890b) believed that the endemic skink and worm-lizard are allied to West Indian, not Brazilian, forms. *Amphisbaenia ridleyi* possesses a uniquely derived molariform dentition for feeding on snails (Pregill, 1984), but other than underscoring the form's distinctiveness, the trait offers little clue to the species' nearest relatives. *Mabuya maculata*, on the other hand, has been linked phenetically to certain West African taxa (see Bauer, 1993). Until illuminated by explicit character analyses and defensible phylogenies, biogeographic comment on these two interesting endemics remains largely speculative.

Ridley (1890a) presented a well-reasoned account, which for the era was a very thorough one, on the origins of the biota of Fernando de Noronha. For the reptiles and perhaps certain mollusks, he favored dispersal upon floating trees that drifted to the island, an explanation that seems most plausible for the ancestor of *N. vespuccii*. The infrequent yet recurrent instances of small and large sea-going mats of vegetation, far away from the mainland and bearing a living terrestrial cargo, are well documented (King, 1962; Heatwole and Levins, 1972; Hardy, 1982). The semiaquatic habits and riparian distributions of *Lundomys* and *Holochilus*, as reviewed above, would place these rodents in a prime ecological circumstance for just such

a stranding on a platform of vegetation, eroded from a river's edge and rafted out to sea, and may even have enhanced their survival prospects during oceanic transit. In the case of a progenitor to *Noronhomys*, special pleading for the proverbial single gravid female need not be indulged. The tendency of marsh rats to construct their nests, often in clusters (Barlow, 1969), in trees and grasses growing along streams makes possible the isolation of a small population sample on a raft of any appreciable size, not just a single individual. Winds and currents may have been more favorable for such passive dispersion and sea drift toward Fernando de Noronha during the late Pliocene or early Pleistocene.

REFERENCES

Aguilera, A., and A. Pérez-Zapata
1989. Cariologia de *Holochilus venezuelae* (Rodentia, Cricetidae). Acta Cient. Venez. Genet. 40: 198–207.

Anemone, R. L.
1993. The functional anatomy of the hip and thigh in primates. *In* D. L. Gebo (ed.), Postcranial adaptation in nonhuman primates: 150–174. Dekalb: Northern Illinois Univ. Press, x + 281 pp.

Baird, S. F.
1858. General report upon the zoology of the several Pacific railroad routes. Part I, Mammals. Reports of explorations and surveys for a railroad route from the Mississippi River to the Pacific Ocean, Vol. 8. Washington, D.C.: Beverly Tucker Printer, xlviii + 757 pp.

Baker, R. J., B. F. Koop, and M. W. Haiduk
1983. Resolving systematic relationships with G-bands: a study of five genera of South American cricetine rodents. Syst. Zool. 32: 403–416.

Bandini, A. M.
1745. Vita e lettere di Amerigo Vespucci. Firenze: Stamperia all' Insegna di Apollo, lxxvi + 129 pp.

Barlow, J. C.
1969. Observations on the biology of rodents in Uruguay. R. Ontario Mus. Life Sci. Contr. 75: 59 pp.

Bauer, A. M.
1993. African-South American relationships: a perspective from the reptilia. *In* P. Goldblatt (ed.), Biological relationships between Africa and South America: 244–288. New Haven, CT: Yale University Press, ix + 630 pp.

Boye, P., R. Hutterer, N. López-Martínez, and J. Michaux
1992. A reconstruction of the Lava mouse (*Malpaisomys insularis*), and extinct rodent of the Canary Islands. Z. Säugetierk. 57: 29–38.

Branner, J. C.
1888. Notes on the fauna of the islands of Fernando de Noronha. Am. Nat. 262: 861–871.
1889. The geology of Fernando de Noronha. Part I. Am. J. Sci., Third Ser., New Haven, 37: 145–161.
1890. The aeolian sandstones of Fernando de Noronha. Ibid 39: 247–257.

Braun, J. C.
1993. Systematic relationships of the Tribe Phyllotini (Muridae: Sigmodontinae) of South America. Oklahoma Mus. Nat. Hist. Spec. Publ. No. 2: 50 pp.

Bugge, J.
1970. The contribution of the stapedial artery to the cephalic stapedial supply in muroid rodents. Acta Anat. 76: 313–336.

Carleton, M. D.
1980. Phylogenetic relationships in neotomine-peromyscine rodents (Muroidea) and a reappraisal of the dichotomy within New World Cricetinae. Univ. Michigan Mus. Zool. Misc. Publ. 157: 146 pp.

Carleton, M. D., and R. E. Eshelman
1979. A synopsis of fossil grasshopper mice, genus *Onychomys*, and their relationships to recent species. Univ. Michigan Pap. Paleontol. 21: 63 pp.

Carleton, M. D., and G. G. Musser
1989. Systematic studies of oryzomyine rodents (Muridae, Sigmodontinae): a synopsis of *Microryzomys*. Bull. Am. Mus. Nat. Hist. 191: 83 pp.
1995. Systematic studies of oryzomyine rodents (Muridae: Sigmodontinae): definition and distribution of *Oligoryzomys vegetus* (Bangs, 1902). Proc. Biol. Soc. Washington 108: 338–369.

Cordani, U. G.
1967. K:Ar ages from Fernando de Noroñha. *In* Proceedings of the Symposium on

Continental Drift in the Southern Hemisphere, Montevideo: 85.

Darton, M., and J. Clark
1994. The Macmillan dictionary of measurement. New York: Macmillan Int., vi + 538 pp.

De Almeida, F. F. M.
1958. Geologia e petrologia do Arquipélago de Fernando de Noronha. Serv. Gráfico Inst. Bras. Geogr. Estat. 13: xi + 181 pp.

Dickerman, A. W., and T. L. Yates
1995. Systematics of *Oligoryzomys*: protein-electrophoretic analyses. J. Mammal. 76: 172–188.

Fish, F. E.
1984. Mechanics, power output and efficiency of the swimming muskrat. J. Exp. Biol. 110: 183–201.

Fong, D. W., T. C. Kane, and D. C. Culver
1995. Vestigialization and loss of nonfunctional characters. Ann. Rev. Ecol. Syst. 26: 249–268.

Formisano, L. (ed.)
1992. Letters from a New World. Amerigo Vespucci's discovery of America. New York: Marsilio, xli + 214 pp.

Gebo, D. L. (ed.)
1993. Postcranial adaptation in nonhuman primates. Dekalb: Northern Illinois Univ. Press, x + 281 pp.

Gunn, B. M., and N. D. Watkins
1976. Geochemistry of the Cape Verde Islands and Fernando de Noroñha. Geol. Soc. Am. Bull. 87: 1089–1100.

Handley, C. O., Jr.
1976. Mammals of the Smithsonian Venezuelan Project. Brigham Young Univ. Sci. Bull. Biol. Ser. 20: 91 pp.

Hardy, J. D., Jr.
1982. Biogeography of Tobago, West Indies, with special reference to amphibians and reptiles: a review. Bull. Maryland Herpetol. Soc. 18: 37–142.

Heatwole, H., and R. Levins
1972. Biogeography of the Puerto Rican Bank: flotsam transport of terrestrial animals. Ecology (New York) 53: 112–117.

Hershkovitz, P.
1944. Systematic review of the Neotropical water rats of the genus *Nectomys* (Cricetinae). Univ. Michigan Mus. Zool. Misc. Publ. 58: 101 pp.
1955. South American marsh rats, genus *Holochilus*, with a summary of sigmodont rodents. Fieldiana Zool. 37: 639–673.
1960. Mammals of northern Colombia, preliminary report no. 8: Arboreal rice rats, a systematic revision of the subgenus *Oecomys*, genus *Oryzomys*. Proc. U.S. Natl. Mus. 110: 513–568.
1962. Evolution of Neotropical cricetine rodents (Muridae) with special reference to the phyllotine group. Fieldiana Zool. 46: 524 pp.
1993. A new central Brazilian genus and species of sigmodontine rodent (Sigmodontinae) transitional between akodonts and oryzomyines, with a discussion of murid molar morphology and evolution. Ibid. n. ser. 75: 1–18.

Howell, A. B.
1926. Anatomy of the wood rat. Monogr. Am. Soc. Mammal. 1. Baltimore: Williams and Wilkins, x + 225 pp.

Kesner, M. H.
1980. Functional morphology of the masticatory musculature of the rodent subfamily Microtinae. J. Morphol. 165: 205–222.

King, W.
1962. The occurrence of rafts for dispersal of land animals into the West Indies. Q. J. Florida Acad. Sci. 25: 45–52.

Koenigswald, W. von
1980. Schmelzstruktur und morphologie in den molaren der Arvicolidae (Rodentia). Abh. Senckenb. Naturforsch. Ges. 539: 129 pp.

Lanyon, L. E., and C. T. Rubin
1985. Functional adaptation in skeletal structures. *In* M. Hildebrand, D. M. Bramble, K. F. Liem, and D. B. Wake (eds.), Functional vertebrate morphology: 1–25. Cambridge, MA: Harvard Univ. Press, 430 pp.

Lavocat, R.
1973. Les rongeurs du Miocene d'Afrique Orientale–I. Miocene inferieur. Mem. Trav. Inst. Ec. Pratique des Hautes Etudes, Inst. de Montpellier 1: 284 pp.

Mares, M. A., J. K. Braun, and D. Gettinger
1989. Observations on the distribution and ecology of the mammals of the cerrado grasslands of central Brazil. Ann. Carnegie Mus. 58: 1–60.

Martino, A. M. G., and M. Aguilera M.
1989. Food habits of *Holochilus venezuelae* in rice fields. Mammalia 53: 545–561.

Massoia, E.
1974. Ataques graves de *Holochilus* y otros roedores a cultivos de caña de azúcar. Inst. Nac. Tecnol. Agropecu. IDIA, 321/24: 12 pp.

1981. El estado sistemático y zoogeografía de *Mus brasiliensis* Desmarest y *Holochilus sciureus* Wagner (Mammalia, Rodentia, Cricetidae). Physis Secc. C 39(97): 31–34.

Mitchell-Thomé, R. C.
1970. Geology of the South Atlantic Islands. Beitr. Reg. Geol. Erde 10: vi + 367 pp.

Musser, G. G., and M. D. Carleton
1993. Family Muridae. *In* D. E. Wilson and D. M. Reeder (eds.), Mammal species of the world, a taxonomic and geographic reference, 2nd ed.: 501–755. Washington, D. C.: Smithson. Inst. Press, 1206 pp.

Musser, G. G., M. D. Carleton, E. M. Brothers, and A. L. Gardner
1998. Systematic studies of oryzomyine rodents (Muridae: Sigmodontinae): diagnoses and distributions of species formerly assigned to *Oryzomys "capito."* Bull. Am. Mus. Nat. Hist. 236: 376 pp.

Musser, G. G., and C. Newcomb
1983. Malayasian murids and the giant rat of Sumatra. Bull. Am. Mus. Nat. Hist. 174: 327–598.

Myers, P., B. Lundrigan, and P. K. Tucker
1995. Molecular phylogenetics of oryzomyine rodents: the genus *Oligoryzomys*. Mol. Phylogenet. Evol. 4: 372–382.

Olds, N., and S. Anderson
1987. Notes on Bolivian mammals 2. Taxonomy and distribution of rice rats of the subgenus *Oligoryzomys*. Fieldiana Zoology n. ser. 39: 261–281.

Olson, S. L.
1973. Evolution of the rails of the South Atlantic islands (Aves: Rallidae). Smithson. Contrib. Zool. 152: 53 pp.
1975. Paleornithology of St. Helena Island, South Atlantic Ocean. Smithson. Contrib. Paleobiol. 23: 49 pp.
1981. Natural history of vertebrates on the Brazilian islands of the mid South Atlantic. Natl. Geogr. Soc. Res. Rep. 13: 481–492.
1994. The endemic vireo of Fernando de Noronha (*Vireo gracilirostris*). Wilson Bull. 106: 1–17.

Olson, S. L., and H. F. James
1982. Prodromus of the fossil avifauna of the Hawaiian Islands. Smithson. Contrib. Zool. 365: 59 pp.
1991. Descriptions of thirty-two new species of birds from the Hawaiian Islands. Part I. Non-passeriformes. Ornithol. Monogr. 45: 1–88.

Oren, D. C.
1982. A avifauna do Arquipélago de Fernando de Noronha. Bol. Mus. Para. Emílio Goeldi, Nova Sér.: Zool. (Belém) 118: 1–22.
1984. Resultados de uma nova expedico zoológica a Fernando de Noronha. Bol. Mus. Para. Emílio Goeldi, Sér. Zool. (Belém) 1: 19–44.

Oxnard, C. E., R. H. Crompton, and S. S. Lieberman
1990. Animal lifestyles and anatomies. The case of the prosimian primates. Seattle: Univ. Washington Press, ix + 174 pp.

Patton, J. L., and M. N. F. da Silva
1995. A review of the spiny mouse genus *Scolomys* (Rodentia: Muridae: Sigmodontinae) with the description of a new species from the western Amazon of Brazil. Proc. Biol. Soc. Washington 108: 319–337.

Pereira da Costa, F. A.
1887. A Ilha de Fernando de Noronha, notica historica geographica e economica. Pernambuco: Manoel Figueroa de Faria & Filhos, 52 pp.

Pohl, F. J.
1944. Amerigo Vespucci, pilot major. New York: Columbia Univ. Press, x + 249 pp.

Pregill, G.
1984. Durophagous feeding adaptations in an amphisbaenid. J. Herpetol. 18: 186–191.

Redford, K. H., and G. A. B. da Fonseca
1986. The role of gallery forests in the zoogeography of the cerrado's nonvolant mammalian fauna. Biotropica 18: 126–135.

Reig, O. A.
1977. A proposed unified nomenclature for the enamelled components of the molar teeth of the Cricetidae (Rodentia). J. Zool. (London) 181: 227–241.
1980. A new fossil genus of South American cricetid allied to *Wiedomys*, with an assessment of the Sigmodontinae. Ibid. 192: 257–281.

Repenning, C. A.
1968. Mandibular musculature and the origin of the subfamily Arvicolinae (Rodentia). Acta Zool. Cracov. 13: 1–72.

Ridgely, R. S., and G. Tudor
1994. The Birds of South America. II. The Suboscine Passerines. Austin: Univ. Texas Press, 814 pp.

Ridley, H. N.
1888. A visit to Fernando do Noronha. Zoologist, ser. 3, 12: 41–49.
1890a. Notes on the botany of Fernando de Noronha. J. Linnean Soc. London, Bot. 27: 1–95.
1890b. Notes on the zoology of Fernando Noronha. J. Linnean Soc. London, Zool. 20: 473–570.
Rinker, G. C.
1954. The comparative myology of the mammalian genera *Sigmodon*, *Oryzomys*, *Neotoma*, and *Peromyscus* (Cricetinae), with remarks on their intergeneric relationships. Univ. Michigan Mus. Zool. Misc. Publ. 83: 124 pp.
Roff, D. A.
1994. The evolution of flightlessness: Is history important? Evol. Ecol. 8: 639–657.
Roth, V. L.
1992. Inferences from allometry and fossils: dwarfing of elephants on islands. *In* D. Futuyma and J. Antonovics (eds.), Oxford surveys in evolutionary biology 8: 260–288. New York: Oxford Univ. Press.
Sierra de Soriano, B.
1965. Algunas estructuras externas relacionadas con la vida anfibia en dos especies del genero *Holochilus* Brandt, 1835 (Muridae, Cricetinae). Rev. Fac. Human. Cienc., Montevideo 22: 209–220.
1969. Algunos caracteres externos de cricétinos y su relación con el grado de adaptación a la vida acuática (Rodentia). Physis 28: 471–486.
Stein, B. R.
1981. Comparative limb myology of two opossums, *Didelphis* and *Chironectes*. J. Morphol. 169: 113–140.
1988. Morphology and allometry in several genera of semiaquatic rodents (*Ondatra*, *Nectomys*, and *Oryzomys*). J. Mammal. 69: 500–511.
Steppan, S. J.
1995. Revision of the Tribe Phyllotini (Rodentia: Sigmodontinae), with a phylogenetic hypothesis for the Sigmodontinae. Fieldiana Zool. n. ser. 80: 112 pp.
1996. A new species of *Holochilus* (Rodentia: Sigmodontinae) from the Middle Pleistocene of Bolivia and its phylogenetic significance. J. Vertebr. Paleontol. 16: 522–530.
Swofford, D. L.
1993. Phylogenetic analysis using parsimony (PAUP), version 3.1. Computer program distributed by the Illinois Natural History Survey, Champaign, IL.
Thomas, M. R. O.
1906. Notes on South American rodents. II. On the allocation of certain species hitherto referred respectively to *Oryzomys*, *Thomasomys*, and *Rhipidomys*. Ann. Mag. Nat. Hist., ser. 7, 18: 442–448.
1917. On the arrangement of South American rats allied to *Oryzomys* and *Rhipidomys*. Ann. Mag. Nat. Hist., ser. 8, 20: 192–198.
Twigg, G. I.
1965. Studies on *Holochilus sciureus berbicensis*, a cricetine rodent from the coastal region of British Guiana. Proc. Zool. Soc. London 145: 263–283.
Voss, R. S.
1988. Systematics and ecology of ichthyomyine rodents (Muroidea): patterns of morphological evolution in a small adaptive radiation. Bull. Am. Mus. Nat. Hist. 188: 259–493.
1991. An introduction to the Neotropical muroid rodent genus *Zygodontomys*. Ibid. 210: 113 pp.
1993. A revision of the Brazilian muroid rodent genus *Delomys* with remarks on "thomasomyine" characters. Am. Mus. Novitates 3073: 44 pp.
Voss, R. S., and M. D. Carleton
1993. A new genus for *Hesperomys molitor* Winge and *Holochilus magnus* Hershkovitz (Mammalia, Muridae) with an analysis of its phylogenetic relationships. Am. Mus. Novitates 3085: 39 pp.
Voss, R. S., L. F. Marcus, and P. Escalante P.
1990. Morphological evolution in muroid rodents I. Conservative patterns of craniometric covariance and their ontogenetic basis. Evolution 44: 1568–1587.
Voss, R. S., and P. Myers
1991. *Pseudoryzomys simplex* (Rodentia: Muridae) and the significance of Lund's collections from the caves of Lagoa Santa, Brazil. Bull. Am. Mus. Nat. Hist. 206: 414–432.
Webb, P. W., and R. W. Blake
1985. Swimming. *In* M. Hildebrand, D. M. Bramble, K. F. Liem, and D. B. Wake (eds.), Functional vertebrate morphology: 110–128. Cambridge, MA: Harvard Univ. Press, 430 pp.

Recent issues of the *Novitates* may be purchased from the Museum. Lists of back issues of the *Novitates* and *Bulletin* published during the last five years are available at World Wide Web site http://nimidi.amnh.org. Or address mail orders to: American Museum of Natural History Library, Central Park West at 79th St., New York, NY 10024. TEL: (212) 769-5545. FAX: (212) 769-5009. E-MAIL: scipubs@amnh.org